LHC Higgs Physics beyond the Standard Model

Michael Spannowsky

München 2007

LHC Higgs Physics beyond the Standard Model

Michael Spannowsky

Dissertation
an der Fakultät für Physik
der Ludwig–Maximilians–Universität
München

vorgelegt von
Michael Spannowsky
aus Nürtingen

München, den 22.09.2007

Erstgutachter: Prof. Dr. Harald Fritzsch
Zweitgutachter: Dr. Tilman Plehn
Tag der mündlichen Prüfung: 30.11.2007

Contents

Zusammenfassung

Mit der Inbetriebnahme des Large Hadron Colliders (LHCs) am CERN wird es möglich sein, Protonkollissionen bei weit höherer Schwerpunktsenergie und Luminosität als bisher durchzuführen. Dies ermöglicht die Erfüllung des vordringlichsten Ziels des LHC: die Entdeckung des Higgs-Teilchens, das bis heute einzige unbeobachtete Teilchen im Standard-Modell und die Erklärung zur Herkunft der Masse der Elementarteilchen. Im Rahmen des Standard-Modells gibt es über den gesamten experimentell und theoretisch erlaubten Bereich der Higgs-Masse Prozesse, die die Detektion des Higgs-Teilchens ermöglichen. Allerdings kann das Standard-Modell keine Theorie sein, die alle fundamentalen physikalischen Phänomene erklärt, sondern kann höchstens als effektive Theorie verstanden werden, die bis zu einer bisher noch unbekannten Energieskala Gültigkeit beansprucht. Deshalb sind Erweiterungen des Standard-Modells nötig, die eventuell wiederum Auswirkungen auf Nachweisprozesse des Higgs-Teilchens haben. Ob solche Auswirkungen auftreten wird in der vorliegenden Arbeit in Bezug auf ausgewählte Prozesse unter Berücksichtigung zweier populärer Erweiterungen des Standard-Modells untersucht. Ausgegangen wird von dem Minimalen Supersymmetrischen Standard-Modell (MSSM) und dem Standard-Modell mit vier Generationen (SM4G).
Freie Parameter dieser Modelle sind durch Prozesse der „Flavor Physik“ und elektroschwache Präzisionsmessungen beschränkt. In dieser Untersuchung wird gezeigt, dass das gemeinhin als ausgeschlossen angenommene SM4G nicht ausgeschlossen werden darf. Ausserdem führt die Untersuchung zu dem Ergebnis, dass eine vierte Generation die Erzeugungs- und Zerfallsprozesse des Higgs-Teilchens stark modifiziert.
Im MSSM wird das geladene Higgs-Teilchen untersucht, dessen Entdeckung ein eindeutiger Hinweis auf Physik jenseits des Standard-Modells ist. Für kleines $\tan\beta$ sind, soweit minimale „Flavor-Verletzung“ (MFV) angenommen wird, auch am LHC keine Nachweisprozesse für ein solches Teilchen bekannt. MFV ist motiviert durch die sehr gute Übereinstimmung der experimentellen Resultate aus der „Flavor Physik“ mit den Standard-Modell-Vorhersagen, beruht aber nicht auf fundamentalen theoretischen Überlegungen. Im Rahmen dieser Arbeit wird das MSSM nicht durch die Annahme von MFV eingeschränkt. Dies führt zu einer sehr großen Anzahl freier Parameter. Es werden die Parameter identifiziert, die die Produktion des geladenen Higgs-Teilchens verstärken und außerdem Beschränkungen, z.B. durch seltene B-Zerfälle, untersucht, denen diese Parameter unterworfen sind. Dabei wird deutlich, dass gerade diese freien Parameter nur sehr schwach beschränkt sind und den Wirkungsquerschnitt für die Erzeugung eines geladenen Higgs-Teilchens stark vergrößern können. Ob jedoch das geladene Higgs-Teilchen jenseits von MFV bei kleinen Werten von $\tan\beta$ in den in dieser Arbeit diskutierten Prozessen über dem großen Hintergrund des W-Bosons am LHC zu messen sein wird, kann letztlich nur nach einer detaillierten Detektorstudie beurteilt werden.

Abstract

The Large Hadron Collider (LHC) at CERN will be able to perform proton collisions at a much higher center-of-mass energy and luminosity than any other collider. Its main purpose is to detect the Higgs boson, the last unobserved particle of the Standard Model, explaining the riddle of the origin of mass. Studies have shown, that for the whole allowed region of the Higgs mass processes exist to detect the Higgs at the LHC. However, the Standard Model cannot be a theory of everything and is not able to provide a complete understanding of physics. It is at most an effective theory up to a presently unknown energy scale. Hence, extensions of the Standard Model are necessary which can affect the Higgs–boson signals. We discuss these effects in two popular extensions of the Standard Model: the Minimal Supersymmetric Standard Model (MSSM) and the Standard Model with four generations (SM4G).
Constraints on these models come predominantly from flavor physics and electroweak precision measurements. We show, that the SM4G is still viable and that a fourth generation has strong impact on decay and production processes of the Higgs boson.
Furthermore, we study the charged Higgs boson in the MSSM, yielding a clear signal for physics beyond the Standard Model. For small $\tan\beta$ in minimal flavor violation (MFV) no processes for the detection of a charged Higgs boson do exist at the LHC. However, MFV is just motivated by the experimental agreement of results from flavor physics with Standard Model predictions, but not by any basic theoretical consideration. In this thesis, we calculate charged Higgs boson production cross sections beyond the assumption of MFV, where a large number of free parameters is present in the MSSM. We find that the soft-breaking parameters which enhance the charged–Higgs boson production most are just bound to large values, e.g. by rare B-meson decays. Although the charged–Higgs boson cross sections beyond MFV turn out to be sizeable, only a detailed detector analysis can decide if a charged Higgs boson is detectable against the large W-boson background for small $\tan\beta$.

List of Figures

List of Tables

Chapter 1

Introduction

The Standard Model (SM) of particle physics has been extremely successful for more than three decades and is able to describe the experimental results in high-energy physics up to the maximum energies of all the actually working colliders. It is a gauge theory which combines the electroweak interaction with the theory of quantum chromodynamics to the symmetry group $SU(3) \times SU(2) \times U(1)$. To generate mass terms in the Lagrangian without breaking the gauge invariance explicitly this symmetry group has to be broken spontaneously to $SU(3) \times U(1)$. This breaking mechanism is called 'Higgs Mechanism'. The masses of the SM particles are parametrized by the vacuum expectation value of a complex scalar field, the Higgs field. It is the only particle included in the SM which could not be found so far. Being a basic corner stone of the SM and its extensions, the search for the Higgs particle is one of the most important tasks in today's high-energy physics.

The SM matter fields are grouped in three generations. Each generation consists of an up-type quark, a down-type quark, a down-type lepton and its neutrino. The corresponding particles among the three generations are identical to each other, except for their mass and flavor. For a long time in theoretical studies even a fourth generation has been considered, a straightforward extension of the SM.

But despite its big success in explaining most of the experimental results, the Standard Model cannot be a complete theory of fundamental physics - not just because gravitation has to be incorporated. It contains 19 free parameters which must be determined experimentally and it does not explain the recently measured neutrino mixing [1] which could result in another 7 free parameters, 3 neutrino masses, 3 lepton-mixing angles and a CP-violating phase.

To explain anomalous astronomical observations like the rotation speed of galaxies, which is known as the galaxy rotation problem [3], and the 'Bullet cluster (1E 0657-56)' [2], the assumption of the existence of dark matter, massive stable particles which do not emit or reflect enough electromagnetic radiation to be detected, seems to be necessary in cosmological models. In the SM there is no cold-dark-matter candidate.

A conceptual problem in the SM, which is called hierarchy problem comes from the mass instability of the only fundamental scalar particle, the Higgs boson, under quantum fluctuations. Loop contributions to the Higgs mass become quadratically divergent with cutoff scale and have to be absorbed into the counter terms for the physical Higgs mass. This leads to the fine tuning problem of the parameters in the Higgs potential. In consequence, extensions of the Standard

Model are necessary to find a more fundamental theory of nature.

Supersymmetric models are extensions to the Standard Model which are able to solve most of these problems. Coleman and Mandula [4] showed that if there is only a finite number of particles below any given mass and if the S-matrix is nontrivial and analytic, the most general Lie algebra of symmetry operators which commute with the S-matrix is a direct product of some internal symmetry group and the Poincaré group. This 'no-go' theorem states that it is impossible to mix internal and Lorentz space-time symmetries in a nontrivial way. Supersymmetric models circumvent this Coleman-Mandula theorem by replacing the Lie algebra by a graded Lie algebra.
In the Minimal Supersymmetric Standard Model (MSSM) - one of the most popular models in physics beyond the Standard Model - which is essentially a straightforward supersymmetrization of the SM, one introduces only the couplings and fields that are necessary for consistency. Supersymmetry ensures the desired cancellation of quadratic divergences for the scalar masses by relating bosonic and fermionic degrees of freedom. The hierarchy problem does therefore not occur in the Higgs sector of the MSSM. Assuming an intermediate supersymmetry breaking scale - between the weak scale and a TeV scale - the three Standard Model couplings unify at a scale $M_U \simeq 3 \times 10^{16}\ \mathrm{GeV}$ being compatible with grand-desert unification scenarios.
In the R-parity conserving MSSM the lightest supersymmetric particle (LSP) is stable[1] and therefore a promising candidate for cold dark matter. In many models R-parity is imposed to explain the stability of the proton.
If supersymmetry is a local symmetry, then even gravity can be incorporated in the called supergravity. In supergravity there are particles with higher spin states: the massless spin-2 gravitino has a spin-3/2 fermion superpartner called the gravitino.
All these circumstances make the MSSM a serious candidate for the next step in a deeper understanding of nature beyond present knowledge. With the Large Hadron Collider[2] (LHC) there is going to be a facility to test this model extensively.
Beside these nice features of the MSSM there are theoretical and phenomenological setbacks as well. Supersymmetry cannot be an exact and unbroken symmetry in nature. Otherwise the Standard Model particles and their superpartners have to have the same mass, which is experimentally excluded. A large amount of theoretical work has been done trying to understand the mechanism of spontaneous supersymmetry breaking. The three most extensively studied mechanisms are the Gravity-, the Gauge- (GMSB) and the Anomaly-Mediated Supersymmetry Breaking (AMSB). All of these models involve extensions of the MSSM to include new particles and interactions at very high mass scales but they differ in how this should be done. From a phenomenological point of view it seems to be acceptable to parametrize our ignorance by just introducing extra terms that break supersymmetry explicitly in the Lagrangian, without assuming a specific breaking scenario. To maintain a hierarchy between the electroweak scale and the Planck mass scale the supersymmetry-breaking couplings should be soft (positive mass dimension). Compared to the MSSM with unbroken supersymmetry the number of free parameters is greatly enlarged - up to 124 allowing all phases. Although still huge, large regions of the

[1] In many scenarios the lightest neutralino turns out to be the LSP.

[2] The construction of the LHC at CERN in Geneva is going to be finished in 2008.

parameter space are ruled out experimentally. Sever constraints come from lepton number conservation, the suppression of FCNCs and bounds on CP violation by electric dipole moments.
To generate mass for both up-type and down-type quarks in a way consistent with supersymmetry a second Higgs doublet is needed. After breaking the weak gauge symmetry the model contains five physical Higgs particles: a charged Higgs boson pair $(H^{\pm})$, two CP-even neutral Higgs bosons (h^0 and H^0 with $m_{h^0} \leq m_{H^0}$) and one CP-odd neutral Higgs boson (A^0). The Higgs sector is extended compared to the SM and thus shows different phenomenological patterns. In various analyses the detectability of the 5 Higgs bosons have been studied. Especially the charged Higgs - an unquestionable signal for new physics - was shown to be a difficult to detect at the LHC.

In this thesis we consider effects in Higgs physics for extensions of the Standard Model.
The outline is as following: First a short introduction to Higgs physics in the SM is given, including the most promising production and decay processes, as well as theoretical bounds to the Higgs mass. For later reference the two Higgs-doublet model is discussed, followed by a 'fermiophobic Higgs' which does not interact via the theoretically poorly motivated Yukawa couplings.
Chapter 3 is dedicated to the question if a fourth generation is a possible extension of the Standard Model. We consider bounds from electroweak precision measurements, flavor physics and direct searches by experiment. It appears that a fourth generation is a possible scenario and not ruled out by any observable. A fourth generation would affect Higgs signatures which might be observed at the LHC.
In Chapter 4 we give a brief introduction to supersymmetric theories, whereas we focus on the Minimal Supersymmetric Standard Model. We discuss the minimal-flavor violation assumption, crucial for the following part.
The non-trivial task of producing a charged Higgs for small $\tan\beta$ with a measurable cross section is the main topic of Chapter 5. Giving up the assumption of minimal-flavor violation might provide a possible solution. Beyond MFV prohibited large flavor-changing neutral currents may occur. To respect constraints we consider rare B-meson decays and theoretical arguments. After presenting the single-Higgs cross sections in minimal flavor violation and beyond, we show the results for a charged Higgs in association with a hard jet.

Chapter 2

Higgs Physics

The Standard Model predicts that not all gauge bosons are massless [5], which was experimentally shown in 1983 [6]. But for renormalizable quantum field theories it is not possible to simply add an explicit mass term for these gauge bosons to the Lagrangian. Theories with massive gauge bosons are either not renormalizable (σ-model) or not gauge invariant. The Higgs mechanism may solve this problem.
In the Standard Model the problem of finding a mechanism to generate mass terms for the gauge bosons, W and Z, without spoiling the renormalizability of the theory is solved by the Higgs mechanism. The $SU(2)_W \times U(1)_Y$ symmetry is broken in such a way that the electromagnetic symmetry $U(1)_Q$ is remaining. The origin of this mechanism is subject to present research [7].

2.1 Standard-Model Higgs

The SM incorporates the two concepts of local gauge invariance and spontaneous symmetry breaking (SSB) to implement a Higgs mechanism. The idea of spontaneous symmetry breaking is realized by introducing at least one new complex scalar field, the so called Higgs field Φ, which behaves like a doublet under $SU(2)_L$ gauge transformations and has hypercharge $Y = +1$. With I_3, the quantum number of the third component of the weak isospin operator, the electromagnetic charge is defined as $Q = I_3 + \frac{Y}{2}$. Assigning a vacuum expectation value (VEV) to the upper component would break the $U(1)_Q$ symmetry. Thus, only the lower component of the doublet can obtain a vacuum expectation value. After SSB the Higgs field can be parametrized as

$$\Phi(x) = \begin{pmatrix} \phi^+(x) \\ \phi^0(x) \end{pmatrix} = \begin{pmatrix} G^+(x) \\ \frac{1}{\sqrt{2}}(v + H(x) + iG^0(x)) \end{pmatrix}, \tag{2.1}$$

where G^+ is a complex and H and G^0 are two real scalar fields. This choice of a weak-isospin doublet also allows for Yukawa couplings. The Higgs part of the Lagrangian reads

$$\mathcal{L}_H = \mathcal{L}_{kin} - \mathcal{L}_{yuk} - V(\Phi) \tag{2.2}$$

with

$$\Phi^c = i\sigma_2\Phi^* = \begin{pmatrix} \phi^{0^*} \\ -\phi^{+^*} \end{pmatrix}, \tag{2.3}$$

which is also an $SU(2)_L$ doublet but has hypercharge $Y = -1$. The Higgs-doublet field allows for Yukawa interactions to up-type *and* down-type right-handed fermion fields with the strength of the Yukawa couplings y_f^{ij}:

$$\mathcal{L}_{yuk} = y_e^{ij}\bar{L}_i^R\Phi e_{R,j} + y_u^{ij}\bar{Q}_i\Phi^c u_{R,j} + y_d^{ij}\bar{Q}_i\Phi d_{R,j} + h.c.. \tag{2.4}$$

The non-kinematic part of the SM Lagrangian containing only Higgs fields is called Higgs potential

$$V(\Phi) = -\mu^2\left(\Phi^\dagger\Phi\right) + \frac{\lambda}{4}\left(\Phi^\dagger\Phi\right)^2, \qquad \mu^2, \lambda > 0. \tag{2.5}$$

It generates the SSB as well as the self interaction terms of the scalar boson.
$V(\Phi)$ has a minimum for

$$|\langle\Phi\rangle|^2 = \frac{2\mu^2}{\lambda} \equiv \frac{v^2}{2} \neq 0. \tag{2.6}$$

Breaking a continuous global symmetry leads to the appearance of massless scalar particles, the Goldstone bosons [8], here $G^\pm$ and G^0. One boson occurs for each broken generator of the symmetry group. In case of a broken continuous local symmetry, like a gauge symmetry, these degrees of freedom are unphysical and can be eliminated by transition to the unitary gauge. The kinetic part of $\mathcal{L}_H$ is given by

$$\mathcal{L}_{kin} = (D_\mu\Phi)(D^\mu\Phi)^\dagger \quad ; \quad D_\mu \equiv \partial_\mu - \frac{ig'}{2}YB_\mu - ig\tau_i W_\mu^i \tag{2.7}$$

where W_μ^i with $i = 1,2,3$ are the vector fields (gauge eigenstates), associated to the three generators $\tau_i \equiv \sigma_i/2$ of the $SU(2)_L$ symmetry. B_μ is the vector field associated to the Y generator of the $U(1)_Y$ symmetry.
After fully expanding the term $|D_\mu\Phi|^2$ of the Lagrangian $\mathcal{L}_H$ and diagonalizing the mass matrix of the gauge bosons, the three Goldstone bosons have been absorbed by the $W^\pm$ and Z bosons to form their longitudinal components and to get their masses. The photon remains massless. We obtain the following mass eigenstates

$$W_\mu^\pm = \frac{W_\mu^1 \mp iW_\mu^2}{\sqrt{2}}, \quad M_W = \frac{e}{2\sin\theta_W}v, \tag{2.8}$$

$$M_Z = \frac{e}{2\sin\theta_W\cos\theta_W}v = \frac{M_W}{\cos\theta_W}, \tag{2.9}$$

$$\begin{pmatrix} Z_\mu \\ A_\mu \end{pmatrix} = \begin{pmatrix} \cos\theta_W & -\sin\theta_W \\ \sin\theta_W & \cos\theta_W \end{pmatrix}\begin{pmatrix} W_\mu^3 \\ B_\mu \end{pmatrix}. \tag{2.10}$$

The heavy gauge bosons receive a mass proportional to the vacuum expectation value of the Higgs field. The parameter e is the electromagnetic charge. The Weinberg angle θ_W and the scale of electroweak symmetry breaking $v \simeq 246\ \mathrm{GeV}$ are determined by the experimentally known W and Z boson masses [9, 10].

In (2.1) only the Higgs field H is physical, with its mass $m_H = \sqrt{2}\mu$ being a free parameter of the theory. Experimental searches give a lower bound for the Higgs mass $m_H > 114.4\ \mathrm{GeV}$ at 95% C.L. [11], while a fit from electroweak precision data indicates a mass in the narrow region of $m_H = 129^{+74}_{-49}$ [12].

2.1.1 Theoretical constraints on the Higgs mass

Several theoretical considerations constrain the Higgs mass to the sub-TeV region [13]. This region is favored by analyses of unitarity, triviality and vacuum stability.

- **Unitarity**[1]**:** If in the process $W^+W^- \to ZZ$ all diagrams involving the Higgs boson are omitted, the amplitude of this process grows with the center-of-mass energy $\sqrt{s}$, in violation of unitarity [13, 14]. The bad high-energy behavior occurs when the external bosons are longitudinal[2]. After decomposing the amplitude into partial waves and imposing partial wave unitarity, it is possible to deduce a bound on the Higgs mass.

  $$a_J(s) = \frac{1}{32\pi}\int d(\cos\theta)\, P_J(\cos\theta)\, \mathcal{M}(s,\theta) \tag{2.11}$$

  is the expansion of the J-th partial wave, with P_J the J-th Legendre polynomial and the scattering matrix element $\mathcal{M}$. Partial wave unitarity requires that

  $$|a_J|^2 \leq |\mathrm{Im}\, a_J|\,, \tag{2.12}$$

  implying $|a_J| \leq 1$ and

  $$|\mathrm{Re}\, a_J| \leq \frac{1}{2}. \tag{2.13}$$

  For $J = 0$ the amplitude for $W_L^+W_L^- \to Z_LZ_L$ scattering in the limit $s \gg m_H$ is given by [15]

  $$a_{J=0} \to -\frac{5m_H^2}{64\pi v^2}. \tag{2.14}$$

  From (2.13) and (2.14) the Higgs mass bound

  $$m_H < 780\ \mathrm{GeV}$$

  can be derived.

[1] More precisely 'tree-level unitarity'.

[2] In the large-energy limit the polarization vector of W_L can be approximated by

$$\varepsilon_L^\mu(p) \simeq \frac{p^\mu}{m_W}.$$

- **Triviality:** In a ϕ^4-theory the quartic self-coupling λ increases monotonically as a function of the momentum scale Q, which might lead to a coupling of infinite strength, called a Landau pole. In the Higgs sector a similar observation can be made, except from the fact, that λ receives contributions with both signs. Here, just showing the dominant terms, the renormalization group equation (RGE) for $\lambda(Q)$ is given by [16]

$$16\pi^2 \frac{d\lambda}{d\log Q} \simeq 12\lambda^2 - 3\lambda g_2^2 - 9\lambda g_1^2 + 4\lambda \sum N_f y_f^2 - 4 \sum N_f y_t^4. \tag{2.15}$$

  The last two terms encode the Higgs wave function and quartic terms induced by fermions, whereas the sum is over all identical fermions with degeneracy N_f. The first term dominates for $\lambda \to \infty$, while the last term dominates for $\lambda \to 0$. With m_H as input, together with the RGE for g_1, g_2 and y_t (2.15) can be solved. For large m_H we obtain

$$\Lambda \simeq Q \exp\left[\frac{4\pi^2}{3\lambda(Q)}\right] \tag{2.16}$$

  for any $Q < \Lambda$. Thus, large Higgs masses may lead to a Landau pole at lower energy scales. For any value of Λ, there is a corresponding maximum value of m_H, for which the theory remains perturbative. Simulations on the lattice [17], taking non-perturbative effects into account, find a Higgs mass bound of

$$m_H < 640 \text{ GeV}. \tag{2.17}$$

- **Vacuum Stability:** If m_H is very small, the top Yukawa contribution in Eq.(2.15) dominates, driving λ negative [18]. Hence, the Higgs potential may become unbounded from below and the Higgs vacuum expectation value can go to infinity. Depending on the validity region of the SM a lower Higgs mass bound can be gained. With the cut-off scale $\Lambda_C \sim 10^3$ GeV the lower Higgs mass is [19]

$$m_H \geq 70 \text{ GeV}. \tag{2.18}$$

  Assuming a global minimum for the VEV is not necessary, if the probability of tunneling into another vacuum over the age of the Universe is much less than 1 [20]. Allowing a metastable vacuum can weaken the bound on m_H.

2.1.2 SM Higgs decay and production channels

There are four favorable production channels for a Higgs boson at the LHC (Fig 2.1). Due to high gluon luminosity the dominant Higgs production mechanism at the LHC will be the gluon-fusion process (GF)

$$pp \to gg \to H.$$

This process, mediated by top and bottom quark loops, provides the largest production cross-section for the whole Higgs mass range of interest. QCD corrections to this process increase the

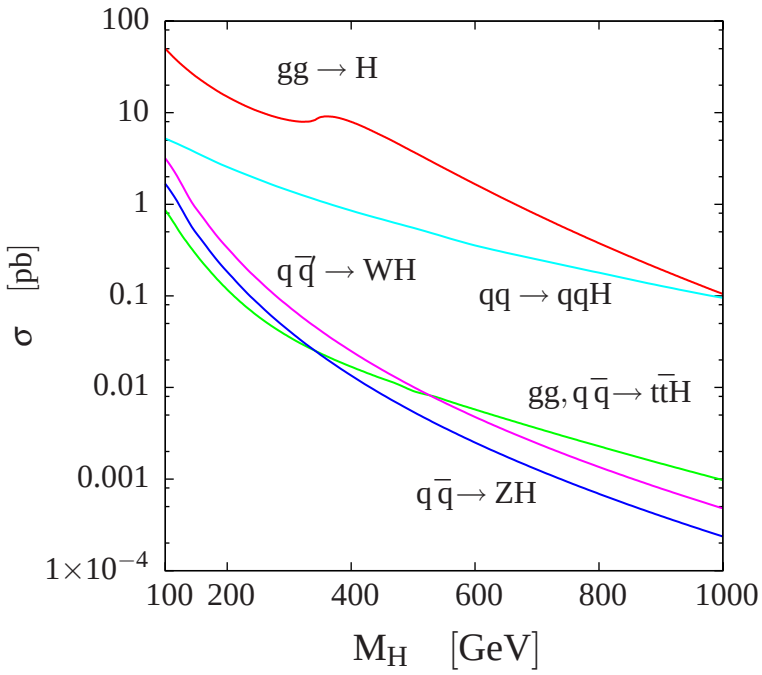

Figure 2.1: Most important NLO cross sections for the production of a Standard-Model Higgs at the LHC.

total cross section by $50 - 100\%$ [21]. At LO the Higgs boson does not acquire any transverse momentum p_T. For large Higgs masses the gluon fusion production process decreases faster than the W- and Z-boson fusion process (WBF) [22]

$$pp \to qq + W^*W^*/Z^*Z^* \to qqH.$$

Thus, in this mass region WBF can compete with GF. Even in the intermediate Higgs mass range these processes are relevant, since the additional forward jets offer the opportunity to reduce the background significantly. Suppressed compared to the former two, but still sizeable, especially in the intermediate mass range $m_H \lesssim 2m_Z$, is the Higgs-radiation off W or Z gauge bosons

$$pp \to q\bar{q} \to Z^*/W^* \to H + Z/W.$$

The NLO QCD corrections, which can be inferred from the Drell-Yan process, increase the total cross section by $\mathcal{O}(30\%)$ [23]. The radiation off top quarks [24]

$$pp \to q\bar{q}/gg \to Ht\bar{t}$$

with $H \to b\bar{b}$ cannot be used for a direct Higgs boson detection because of an overwhelming QCD background for $b\bar{b}$ and the inability to reconstruct the Higgs mass very precisely.
The cross sections are calculated with the programs HIGLU, VV2H, V2HV and HQQ [25] and for the branching ratios we used Hdecay [26] with slight modifications - if necessary, e.g. in Section 2.3.

Once the Higgs mass is fixed, its decay pattern is completely determined. The Higgs couplings to gauge bosons and fermions are proportional to the masses of the particles, hence preference is given to decays into the heaviest particles allowed by phase space. In general, the decay processes can be separated in three classes:

- **Fermionic Decays:** The Higgs couples directly to all fermions with the strength of the according Yukawa coupling. Thus, for a light Higgs the preferred fermionic decay channel is $H \to b\bar{b}$, and for a heavy one ($m_H \gtrsim 340$ GeV) $H \to t\bar{t}$.

- **Decays to massive gauge bosons:** Above the WW and ZZ kinematical thresholds, the Higgs boson will decay mainly into pairs of massive gauge bosons, with a decay width of the W bosons two times larger than the one of the Z bosons. Even below the kinematical thresholds decays to one or two off-shell vector bosons are important, the more so as $H \to Z^*Z^* \to 4l$ and $H \to W^*W^* \to l^{\pm}\nu l'^{\pm}\nu'$ will give clear signals.

- **Loop induced decays:** Since massless gauge bosons, e.g. γ and g, do not couple to the Higgs boson directly, these decays are mediated by loops involving massive particles. These decays are particularly interesting because of two reasons. On the one hand they receive sizeable branching ratios for a light Higgs ($m_H \lesssim 150$ GeV) with a rather clear signal, at least for $H \to \gamma\gamma$ and $H \to Z\gamma$. On the other hand new physics may affect these decays and thus can open a window to extensions of the SM. For later reference we give the leading order formula for $H \to \gamma\gamma$ and $H \to gg$ [27]:

$$\begin{aligned}\Gamma_{H\to\gamma\gamma} &= \frac{G_\mu \alpha^2 m_H^3}{128\sqrt{2}\pi^3}\left|\sum_f N_c Q_f^2 A_f(\tau_f) + A_W(\tau_W)\right|^2 \\ \Gamma_{H\to gg} &= \frac{G_\mu \alpha_s^2 m_H^3}{36\sqrt{2}\pi^3}\left|\frac{3}{4}\sum_f A_f(\tau_f)\right|^2 ,\end{aligned} \tag{2.19}$$

where A_f and A_W are the form factors for the spin-$\frac{1}{2}$ and spin-1 particles respectively. These form factors are

$$\begin{aligned}A_f(\tau) &= 2\left[\tau + (\tau-1)f(\tau)\right]\tau^{-2} \\ A_W(\tau) &= -\left[2\tau^2 + 3\tau + 3(2\tau-1)f(\tau)\right]\tau^{-2}\end{aligned} \tag{2.20}$$

with $\tau_i = m_H^2/4m_i^2$, $(i = f, W)$ and $f(\tau)$ defined as the three–point integral

$$f(\tau) = \begin{cases} \arcsin^2\sqrt{\tau} & \tau \le 1 \\ -\frac{1}{4}\left[\ln\frac{1+\sqrt{1-\tau^{-1}}}{1-\sqrt{1-\tau^{-1}}} - i\pi\right]^2 & \tau > 1. \end{cases} \tag{2.21}$$

The $H\gamma\gamma$ and $HZ\gamma$ couplings are mediated by W boson and charged fermion loops, while the Hgg coupling is mediated only by quark loops.

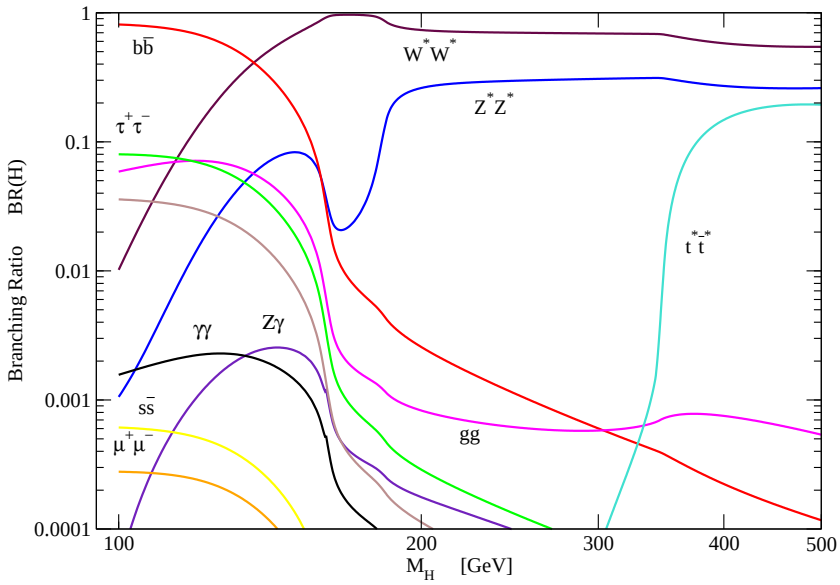

Figure 2.2: Branching ratios for a Standard-Model Higgs.

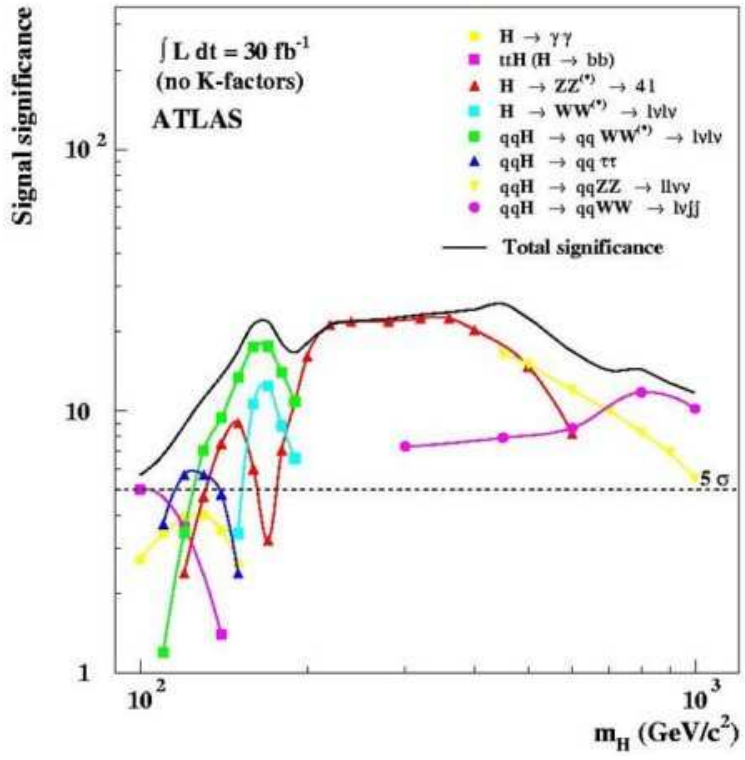

Figure 2.3: ATLAS significance analysis [28].

Detector analyses at ATLAS [28] and CMS [29] have shown that the SM Higgs can be detected with at least 5σ significance over the whole theoretically allowed mass region after collecting an integrated luminosity of $\mathcal{L}$ =30 fb^{-1}.
For a light Higgs boson ($m_H \lesssim 135$ GeV) there are two promising processes: The 'silver' detection channel, $gg \to H \to \gamma\gamma$ and the channel with vector boson fusion and decay into τ lepton pair. The latter is the first channel to detect a Higgs boson with $m_H = 120\,\mathrm{GeV}$. In the intermediate region, between 120 GeV $\lesssim m_H \lesssim 2\,m_Z$, the process $H \to W^*W^* \to ll\nu\nu$ is very promising. $BR\,(H \to WW)$ is already quite large, if not even dominating, and the clean leptonic decays attain 4% of the WW sample. Finally, the so-called 'gold plated' mode for $m_H \gtrsim 2m_Z$ is given by $gg \to H \to Z^*Z^* \to 4l$. It allows the detection of a Higgs boson up to the mass of $\mathcal{O}\,(1\,\mathrm{TeV})$.

2.2 Two-Higgs-doublet model

Although the SM is very successful in describing most of the Elementary Particles phenomenology, the Higgs sector remains unknown so far. Thus, there is no fundamental reason to assume that the Higgs sector must be minimal (i.e. only one Higgs doublet), and we could wonder about a next-to-minimal extension. The simplest extension of the SM Higg sector is called Two Higgs Doublet Model (2HDM), which consists of adding a second Higgs doublet with the same quantum numbers as the first one. This approach is also motivated by the fact that the ratio between the masses of the top and bottom quarks is of the order of $m_t/m_b \approx 171/4 \approx 43$. In the SM both quark masses come from the same Higgs doublet, which implies a non natural hierarchy between their corresponding Yukawa couplings. However, if the bottom quark received its mass from one doublet and the top from another doublet, the hierarchy of their Yukawa couplings could be more natural if the free parameters of the theory acquired the appropriate values.
The 2HDM contains two Higgs doublets with the same quantum numbers and hypercharges $Y_1 = Y_2 = 1$. In general, both doublets could acquire a VEV

$$\Phi_1\,(x) = \begin{pmatrix} \phi_1^+\,(x) \\ \frac{1}{\sqrt{2}}\,(v_1 + h_1\,(x) + ig_1\,(x)) \end{pmatrix} \tag{2.22}$$

$$\Phi_2\,(x) = \begin{pmatrix} \phi_2^+\,(x) \\ \frac{1}{\sqrt{2}}\,(v_2 + h_2\,(x) + ig_2\,(x)) \end{pmatrix}, \tag{2.23}$$

where we assumed that there is no spontaneous CP violation, i.e. both VEVs could be taken real. In fact, unlike to the SM Higgs potential, the potential of the 2HDM is not unique and can lead to different Feynman rules. But for this thesis we impose the assumptions consistent with the Minimal Supersymmetric Standard Model (MSSM) [30], i.e. no explicit or spontaneous CP violation and no flavor-changing neutral currents at tree level. With these assumptions, the

Higgs potential which spontaneously breaks $SU(2)_L \times U(1)_Y$ down to $U(1)_Q$ is

$$\begin{aligned} V(\Phi_1,\Phi_2) &= \lambda_1\left(\Phi_1^\dagger\Phi_1 - v_1^2\right)^2 + \lambda_2\left(\Phi_2^\dagger\Phi_2 - v_2^2\right)^2 \\ &+\lambda_3\left[\left(\Phi_1^\dagger\Phi_1 - v_1^2\right) + \left(\Phi_2^\dagger\Phi_2 - v_2^2\right)\right]^2 \\ &+\lambda_4\left[\left(\Phi_1^\dagger\Phi_1\right)\left(\Phi_2^\dagger\Phi_2\right) - \left(\Phi_1^\dagger\Phi_2\right)\left(\Phi_2^\dagger\Phi_1\right)\right] \\ &+\lambda_5\left|\Phi_1^\dagger\Phi_2 - v_1v_2\right|^2. \end{aligned} \tag{2.24}$$

The λ_i are real non-negative parameters. The Lagrangian for the Higgs sector can be cast into the form

$$\mathcal{L}_H = \mathcal{L}_{kin} + \mathcal{L}_Y - V(\Phi_1,\Phi_2), \tag{2.25}$$

$$\mathcal{L}_{kin} = \sum_{i=1,2}\left(D_\mu\Phi_i\right)^\dagger\left(D^\mu\Phi_i\right). \tag{2.26}$$

From the Lagrangian (2.25) with the kinetic part (2.26), the scalar potential (2.24) and the Yukawa terms we can obtain the full 2HDM spectrum, as well as the scalar-gauge-boson interactions, the scalar-fermion interactions and the pure scalar-scalar interactions.
For the Yukawa sector there are three different choices which are widely studied.
In the 2HDM type I, only one Higgs doublet couples to the fermions, thus the Yukawa Lagrangian becomes

$$\mathcal{L}_{Y,I} = -\left(y_e^{ij}\bar{L}_i^R\Phi_1 e_{R,j} + y_u^{ij}\bar{Q}_i\Phi_1^c u_{R,j} + y_d^{ij}\bar{Q}_i\Phi_1 d_{R,j} + h.c.\right). \tag{2.27}$$

In case of type II models one doublet couples to the down sector of fermions while the other Higgs doublet couples to the up sector. This is a natural scenario in the MSSM and leads to

$$\mathcal{L}_{Y,II} = -\left(y_e^{ij}\bar{L}_i^R\Phi_1 e_{R,j} + y_u^{ij}\bar{Q}_i\Phi_2^c u_{R,j} + y_d^{ij}\bar{Q}_i\Phi_1 d_{R,j} + h.c.\right). \tag{2.28}$$

The 2HDM type III allows couplings between both Higgs doublets and up and down quarks:

$$\begin{aligned} \mathcal{L}_{Y,III} &= -\left(y_{e,1}^{ij}\bar{L}_i^R\Phi_1 e_{R,j} + y_{u,1}^{ij}\bar{Q}_i\Phi_1^c u_{R,j} + y_{d,1}^{ij}\bar{Q}_i\Phi_1 d_{R,j}\right. \\ &\left. + y_{e,2}^{ij}\bar{L}_i^R\Phi_2 e_{R,j} + y_{u,2}^{ij}\bar{Q}_i\Phi_2^c u_{R,j} + y_{d,2}^{ij}\bar{Q}_i\Phi_2 d_{R,j} + h.c.\right). \end{aligned} \tag{2.29}$$

There are 8 degrees of freedom from the two Higgs doublets. All the bilinear scalar terms can be collected in a Higgs mass matrix. After diagonalizing this matrix we obtain the mass eigenstates, which are defined from (2.22) and (2.23) by the following relations:

$$\begin{aligned} G^\pm &= \phi_1^\pm\cos\beta + \phi_2^\pm\sin\beta, \\ H^\pm &= -\phi_1^\pm\sin\beta + \phi_2^\pm\cos\beta, \\ G^0 &= g_1\cos\beta + g_2\sin\beta, \\ A^0 &= -g_1\sin\beta + g_2\cos\beta, \\ H^0 &= h_1\cos\alpha + h_2\sin\alpha, \\ h^0 &= -h_1\sin\alpha + h_2\cos\alpha. \end{aligned} \tag{2.30}$$

The spectrum consists of two CP-even Higgs scalars (H^0, h^0), one CP-odd scalar (A^0), two charged Higgs bosons $(H^\pm)$ and the Goldstone bosons $(G^\pm, G^0)$. Together with the masses, the important parameters describing 2HDMs are the mixing angle in the neutral CP-even sector α and the ratio of the vacuum expectation values of the two Higgs doublets

$$\tan\beta \equiv \frac{v_2}{v_1} \qquad \text{with} \qquad 0 < \beta < \frac{\pi}{2}. \tag{2.31}$$

It can be shown that in the 2HDM the $H^\pm W^\mp Z$ vertex is absent at tree level, which is a general feature for models with only Higgs doublets and singlets [31]. The $H^\pm W^\mp \gamma$ tree-level vertex is zero as consequence of the conservation of the electromagnetic current. Due to the absence of these interactions between two gauge bosons and just one charged Higgs its detectability suffers a lot.

2.3 Higgs without couplings to fermions

In the SM, the huge imbalance between the number of free parameters, introduced by the Higgs mechanism for the gauge fields and the fermion fields is striking. The interaction strength between the weak bosons and the scalar field is dictated by gauge invariance and completely governed by just 4 free parameters. But to describe the Yukawa sector it is necessary to introduce at least 13 free parameters (9 fermion masses and 4 CKM mixing angles). Thus the appraisal of these two mechanisms is very different and it is perfectly possible that not both of them derive their origin from the same scalar field.
In the type I 2HDM set ups with a light CP-even 'fermiophobic Higgs[3]' appear naturally for $\alpha = \pi/2$ [32]. But extending the Higgs sector always necessitates the incorporation of new free parameters and possibly new production and decay channels for the Higgses to the model. Without allowing more assumptions than imposed on the SM, and from a purely phenomenological point of view, it might be acceptable to leave the explanation of the fermion masses disregarded and just consider the implications on Higgs physics in doing so. Hence, we discuss a Higgs boson with SM couplings to gauge bosons, but without tree-level couplings to fermions. In this scenario, there are several major changes compared to the purely SM Higgs boson (Sec.2.1.2) – from the phenomenological point of view. Especially for $m_H \lesssim 160$ GeV the decay channels change completely: direct fermionic decays are absent, and thus the dominating decay over the whole mass region is the decay to off-shell and on-shell W bosons. The absence of fermionic decays also promotes the loop-induced decay modes $H \to \gamma\gamma$ and $H \to Z\gamma$, because of the fact that there are less competing decays and no negative interference between the quark and W-boson form factors (2.19). A lower mass bound, comparable to the SM Higgs mass bound, was established by LEP: $m_H > 109.7\,\mathrm{GeV}$ at 95% C.L. [33]. For larger values of m_H the branching ratio of the loop-induced decay to photons drops quite fast below the 0.01% level. If m_H is havier than 200 GeV the branching ratio to W^*W^* is two times larger than to Z^*Z^* – as in the SM.

[3] Sometimes they are called 'bosonic Higgs'

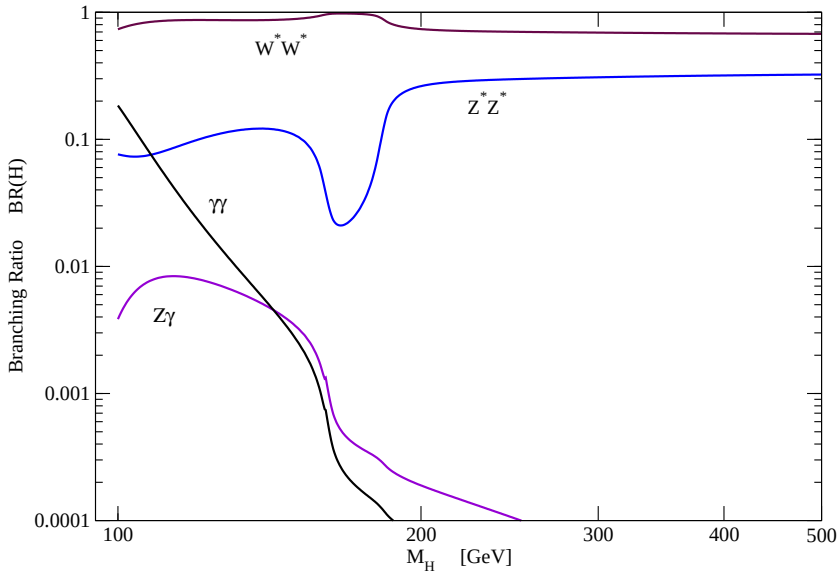

Figure 2.4: Branching Ratios for a fermiophobic Higgs

While the changes for the Higgs decays will not affect its detectability negatively, this cannot be stated about the production processes. Here, the dominant one over the whole region of parameter space, $gg \to H$, is not possible and the production process in association with heavy quarks has a smaller cross section. The $t\bar{t}H$ final state can only be produced with quarks in the initial state at leading order, and not with gluons. Hence, just Higgs production by weak-boson fusion or in association with a heavy gauge boson are the relevant mechanisms.

The question remains: is a fermiophobic Higgs a serious challenge for the LHC? The collaborations at ATLAS and CMS are aware of this possibility. Several studies have been performed. As in the SM, in the region of $m_H \lesssim 2\ m_Z$, one of the viable promising processes is $q\bar{q} \to HW \to l^{\pm}\nu l^{\pm}\nu jj$ or $3l$. The necessary integrated luminosity to exclude a fermiophobic Higgs at 95% C.L. is below $30\ \mathrm{fb}^{-1}$, whereas an exclusion at 5σ needs up to $70\ \mathrm{fb}^{-1}$ [29]. The same was done for the Tevatron with similar results [34]. For $m_H \gtrsim 2\ m_Z$ the two WBF processes $qq \to qqH$ with $H \to WW/ZZ \to l\nu jj/\nu\nu ll$ are useful [35]. They may cover the whole region with a signal significance larger than 5σ for a luminosity of $30\ \mathrm{fb}^{-1}$. Thus, although a higher luminosity is needed to detect a fermiophobic Higgs compared to a SM Higgs, it is no real challenge for the LHC. There are processes to cover the region from its experimental bound ($m_H \gtrsim 105$ GeV) up to the theoretical one ($m_H \lesssim 700$ GeV).

A modification to the fermiophobic Higgs, widely called 'topcolor Higgs', is also considered in several studies at the Tevatron [36, 37]. Topcolor Higgses do couple SM-like to bosons and the top quark, but no other fermions . The gluon-fusion production process is allowed and in magnitude comparable to the SM one. Although the negatively interfering W and top form factors reappear in the decay $H \to \gamma\gamma$ and $H \to Z\gamma$, all the dominant Higgs detection channel mentioned in Section 2.1.2 are restored to a large extent, except for $qq \to t\bar{t}H$ with $H \to b\bar{b}$,

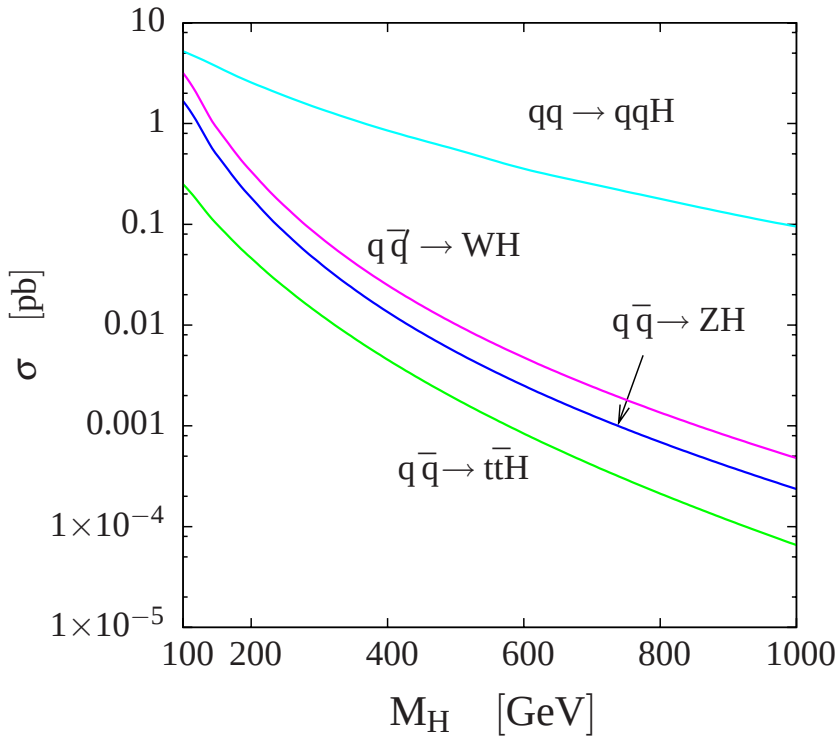

Figure 2.5: Cross sections for a fermiophobic Higgs

and cover the whole mass region. Within this model it seems to be possible to explain the top-quark mass and the masses of the heavy gauge bosons by the usual Higgs mechanism while the light fermions might receive their masses from a further interaction, e.g. Technicolor [38].

Chapter 3

Four generations and Higgs physics

3.1 Introduction

A straightforward extension of the SM is the inclusion of a fourth generation of chiral matter, which can be done in a conceptionally easy way. The idea of a fourth generation of matter fields, incorporated in the usual SM gauge group, has been considered and discarded many times, wrongly leaving the impression that it is either ruled out or highly disfavored by experimental data [39].
Although a wide literature regarding a possible fourth generation exists, its status remains subtle [40]. A serious constraint on new physics are the oblique parameters [41] (Sec. 3.3.2), which were taken into account in Ref. [42] for one (and more) extra generations. It was shown, that one generation can be perfectly consistent with a heavy (500 GeV) Higgs. Older analyses were performed using a global (numerical) fit to 2001 electroweak data or relied on a light neutrino (50 GeV) to minimize the contributions to the oblique parameters [43, 44, 45]. Because of the fact that this neutrino mass region is ruled out by LEP II, if the neutrino is unstable, and electroweak data has since been refined (in particular M_W), it is hard to determine how to compare their results with present experimental bounds.
A fourth generation could also affect Higgs signatures and thus might change the favored detection channels at the LHC [46, 47, 48, 49]. The LHC is even able to probe heavy quarks throughout their mass range, providing the possibility to search for the quarks of the fourth generation themselves [50, 51].
For a phenomenological relevant analysis a viable parameter region has to be found, for which it is necessary to consider bounds from flavor physics, electroweak data and direct experimental searches. We then use typical spectra to compute the consequences for fourth-generation particle production and decay, as well as the effects on the Higgs sector of the Standard Model.

3.2 Lagrangian with four Generations

Within this model of a chiral fourth family we enlarge the SM to include a complete sequential fourth generation of chiral matter (Q_4, u_4, d_4, L_4, e_4), as well as a single right-handed neutrino

ν_4. Structurally the gauge interactions remain the same

$$\mathcal{L}_{gauge} = i\overline{Q}_p \not{D} Q_p + i\overline{u}_p \not{D} u_p + i\overline{d}_p \not{D} d_p + i\overline{L}_p \not{D} L_p + i\overline{e}_p \not{D} e_p + i\overline{\nu}_p \not{\partial} \nu_p, \tag{3.1}$$

where the covariant derivatives contain,

$$\begin{aligned} D_\mu Q_p &= \left[\partial_\mu - ig_3\lambda^a G^a_\mu - ig_2\tau^i W^i_\mu - ig_Y Y_Q B_\mu\right] Q_p, \\ D_\mu u_p &= \left[\partial_\mu - ig_3\lambda^a G^a_\mu - ig_Y Y_u B_\mu\right] u_p, \\ D_\mu d_p &= \left[\partial_\mu - ig_3\lambda^a G^a_\mu - ig_Y Y_d B_\mu\right] d_p, \\ D_\mu L_p &= \left[\partial_\mu - ig_2\tau^i W^i_\mu - ig_Y Y_L B_\mu\right] L_p, \\ D_\mu e_p &= \left[\partial_\mu - ig_Y Y_e B_\mu\right] e_p, \end{aligned} \tag{3.2}$$

with G^a_μ, W^i_μ and B_μ the gauge bosons of $SU(3)$, $SU(2)$ and $U(1)$, respectively with generators λ^a, τ^i and $Y_{\{Q,u,d,L,e\}} = \{1/3, 4/3, -2/3, -1, 2\}$. The Yukawa couplings and right-handed neutrino masses are given by

$$\begin{aligned} \mathcal{L}_{yuk} &= y_u^{pq}\overline{Q}_p \Phi^c u_{R,q} + y_d^{pq}\overline{Q}_p \Phi d_{R,q} + y_e^{pq}\overline{L}_p \Phi e_{R,q} \\ &\quad + y_\nu^{pq}\overline{L}_p \Phi^c \nu_{R,q} + \frac{1}{2} M_{pq}\overline{\nu}^c_{R,p}\nu_{R,q} + \text{h.c.}\,. \end{aligned} \tag{3.3}$$

The generation indices are $p, q = 1, 2, 3, 4$ while we reserve $i, j = 1, 2, 3$ for the Standard Model. SU(2) contractions are implicit. Light neutrino masses can arise from either a hierarchy in neutrino Yukawa couplings $y^\nu_{ij} \ll y_{44}$ or right-handed neutrino masses $M_{ij} \gg M_{44}$ or some combination. We mainly consider two possibilities for the fourth–generation neutrino mass: purely Dirac ($M_{44} = 0$) and mixed ($M_{44} \sim y^\nu_{44} v$).

3.3 Constraints on a fourth generation

There are four obvious restrictions on a fourth generation: (1) The decay width of the Z boson; (2) Oblique electroweak effects; (3) Generational mixing; (4) Direct search bounds. We discuss them one-by-one.

3.3.1 The invisible width of the Z

The Z boson couples gauge-like to all fermions, including neutrinos. Therefore, the total decay width, Γ_Z, has contributions from all fermions with $m_f < M_Z/2$:

$$\Gamma_Z = \Gamma_{ee} + \Gamma_{\mu\mu} + \Gamma_{\tau\tau} + \Gamma_{q\bar{q}} + N\Gamma_{\nu\bar{\nu}}, \tag{3.4}$$

where N is the number of neutrinos in which the Z boson can decay. A further decay channel to a fourth neutrino would not be observed directly, but it would increase the Z decay rate and thus increase Γ_Z, resulting in a decrease in the measured peak cross-sections for the visible final states. At LEP, the number of light neutrinos was found to be $N = 2.98 \pm 0.05 \pm 0.04$ [52]. Once a fourth–generation neutrino has a mass $m_\nu \gtrsim M_Z/2$, the constraint from the invisible Z width becomes irrelevant.

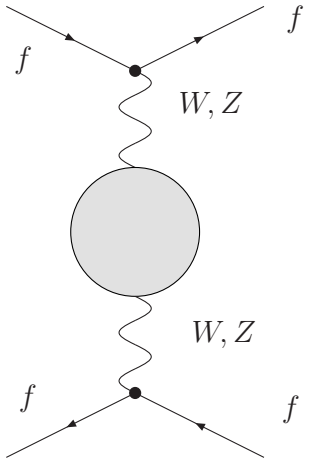

Figure 3.1: Electroweak corrections in $f\bar{f} \to f\bar{f}$ scattering.

3.3.2 Oblique electroweak effects

Most of the present and future collider experiments can be interpreted as two-particle scattering of light fermions, either because they actually involve the scattering of two fermions, or an initial fermion decays into three lighter ones. There is a large class of models, i.e. SM with four generations, which contribute dominantly to precision measurements by modifying the propagation of gauge bosons which are exchanged by the fermions (Fig. 3.1). These contributions alter the gauge boson vacuum polarizations

$$\Pi_{ab}^{\mu\nu}(q) = \left[\Pi_{ab}^{\mathrm{SM}}\left(q^2\right) + \Pi_{ab}^{\mathrm{new}}\left(q^2\right)\right] g^{\mu\nu} + q^\mu q^\nu \Delta\left(q^2\right), \tag{3.5}$$

with $a, b = \gamma, W, Z$. For light fermions the form factors Δ can be neglected.

The parameters S, T and U are suitable combinations of self-energies (called oblique parameters [53]) that describe such effects at the one-loop level of electroweak corrections [41][54]:

$$\begin{aligned}
\alpha(M_Z)\,\Delta T &\equiv \frac{\Pi_{WW}^{\mathrm{new}}(0)}{M_W^2} - \frac{\Pi_{ZZ}^{\mathrm{new}}(0)}{M_Z^2}, \\
\frac{\alpha(M_Z)}{4 s_Z^2 c_Z^2}\Delta S &\equiv \frac{\Pi_{ZZ}^{\mathrm{new}}(M_Z^2) - \Pi_{ZZ}^{\mathrm{new}}(0)}{M_Z^2} \\
&\quad - \frac{s_Z^2 - s_Z^2}{c_Z s_Z}\frac{\Pi_{Z\gamma}^{\mathrm{new}}(M_Z^2)}{M_Z^2} - \frac{\Pi_{\gamma\gamma}^{\mathrm{new}}(M_Z^2)}{M_Z^2}, \\
\frac{\alpha(M_Z)}{4 s_Z^2}(\Delta S + \Delta U) &\equiv \frac{\Pi_{WW}^{\mathrm{new}}(M_W^2) - \Pi_{WW}^{\mathrm{new}}(0)}{M_W^2} \\
&\quad - \frac{c_Z}{s_Z}\frac{\Pi_{Z\gamma}^{\mathrm{new}}(M_Z^2)}{M_Z^2} - \frac{\Pi_{\gamma\gamma}^{\mathrm{new}}(M_Z^2)}{M_Z^2},
\end{aligned} \tag{3.6}$$

where $c_Z = \cos\theta_W\,(M_Z)$ and $s_Z = \sin\theta_W\,(M_Z)$. To calculate ΔS (and ΔT and ΔU) we use exact one-loop expressions [55]. Using these parameters, the effect of new physics on measured quantities, i.e. $\sin^2\theta_W$, M_Z, Γ_Z, can be parameterized, giving severe constraints on S, T and U themselves.

Splitting the up-type from down-type fermion masses in the same electroweak doublet can result in a negative contribution to S. In the large mass limit $m_{u,d} \gg M_Z$, the contribution to S depends logarithmically on the ratio m_u/m_d [41, 42]:

$$\Delta S = \frac{N_c}{6\pi}\left(1 - Y \ln\frac{m_u^2}{m_d^2}\right), \tag{3.7}$$

where Y is the hypercharge of the left-handed doublet of fermions with degeneracy (color factor) N_c. (3.7) is a very good approximation and agrees to an accuracy of ± 0.01 with the full calculation. Clearly the fourth–generation contributions to S are reduced if $m_{u_4}/m_{d_4} > 1$ for quarks ($Y = 1/3$) and $m_\nu/m_\ell < 1$ for leptons ($Y = -1$).

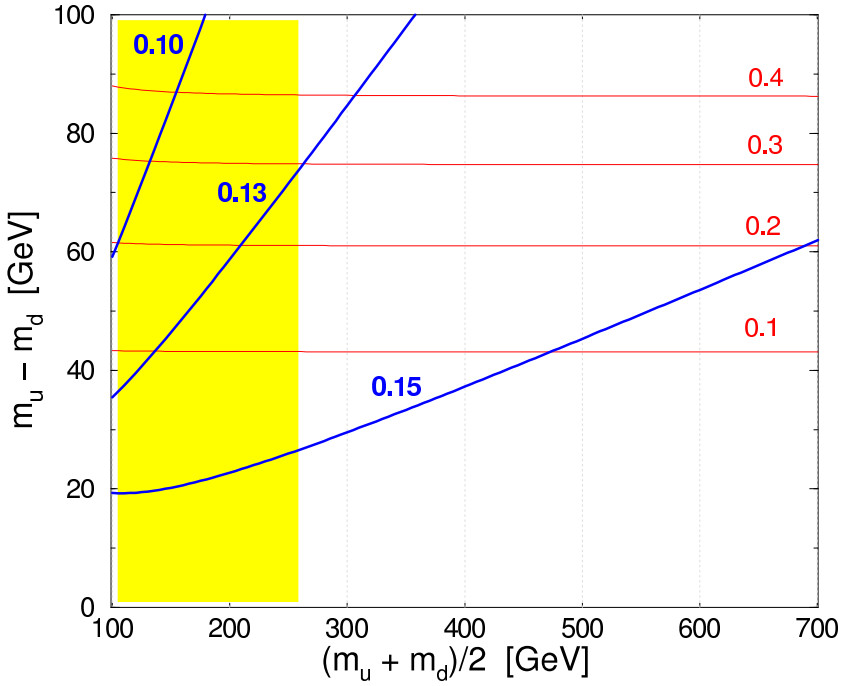

Figure 3.2: The blue lines show the contours of constant ΔS_q, whereas the red ones show ΔT_q for the fourth–generation quarks. The yellow region is excluded by Tevatron searches ($m_{u_4,d_4} > 258$ GeV).

In Figure 3.2 we show the size of the contribution from the (u_4, d_4) doublet as a function of the masses of the quarks. The effect of using the exact one–loop expressions is modest. The typical size of U is smaller than 0.02 everywhere, and so we set $U = 0$ throughout.

An appropriate split between the masses of the neutral and charged lepton of the fourth generation may minimize the contributions to the S parameter: $m_{\nu,\ell} \simeq 100, 135$ GeV implies

parameter set	m_{u_4}	m_{d_4}	m_H	$\Delta S_{\rm tot}$	$\Delta T_{\rm tot}$
(a)	310	260	115	0.15	0.19
(b)	320	260	200	0.19	0.20
(c)	330	260	300	0.21	0.22
(d)	400	350	115	0.15	0.19
(e)	400	340	200	0.19	0.20
(f)	400	325	300	0.21	0.25

Table 3.1: Contributions to ΔS and ΔT from a fourth generation. For the lepton masses we choose $m_{\nu_4} = 100$ GeV and $m_{\ell_4} = 155$ GeV, giving $\Delta S_{\nu\ell} = 0.00$ and $\Delta T_{\nu\ell} = 0.05$. All points are within the 68% CL contour defined by the LEP EWWG.

$(\Delta S_\nu, \Delta T_\nu) \simeq (0.02, 0.02)$, and the slightly larger values $m_{\nu,\ell} \simeq 100, 155$ GeV give $(\Delta S_\nu, \Delta T_\nu)$ $\simeq (0.00, 0.05)$.
We define $(S, T) = (0, 0)$ for the Standard Model with $m_t = 170.9$ GeV [1] and $m_H = 115$ GeV. This is within 1σ of the central value of recent fits of combined electroweak data from LEP Electroweak Working Group (LEP EWWG) [56] and the PDG [39]. Both groups use the most precise constraints on S and T: $\sin^2\theta^{\rm eff}_{\rm lept}$ and M_W. Due to the fact that the S-T plot generated by the LEP EWWG is newer and just uses the leptonic decay width Γ_ℓ, which is not α_s-sensitive instead of the decay width of the Z boson Γ_Z, the peak hadronic cross section σ_h, and $R_q = \sigma_{q\bar{q}}/\sigma_h$, we use the LEP EWWG results when quoting levels of confidence in the following. However, we do not expect to obtain significant differences by using the PDG data.

In Table 3.1 we provide several examples of fourth–generation fermion masses which yield contributions to the oblique parameters that are within the 68% C.L. ellipse of the electroweak precision constraints. We illustrate the effect of increasing Higgs mass with compensating contributions from a fourth generation in Figure 3.3.
More precisely, the fit to electroweak data is in agreement with the existence of a fourth generation and a light Higgs comparable to the fit to the Standard Model alone with $m_H = 115$ GeV. Using suitable contributions from the fourth-generation quarks, heavier Higgs masses up to 315 GeV remain in agreement with the 68% C.L. limits derived from electroweak data. Heavier Higgs masses up to 750 GeV are permitted if the agreement with data is relaxed to the 95% C.L. limits.

It is by no means necessary to restrict our analysis to purely Dirac neutrinos. There is also a possible reduction of $S_{\rm tot}$ when the fourth-generation neutrino has a Majorana mass comparable to the Dirac mass [58, 59]. Using the exact one-loop expressions of Ref. [59], we calculate the contribution to the electroweak parameters with a Majorana mass. However, it is not easy

[1] The measured top quark mass changed slightly over the last years. A combined analysis from CDF and D0 [57] yields:

$$m_t = 170.9 \pm 1.1 \pm 1.5 \text{ GeV}.$$

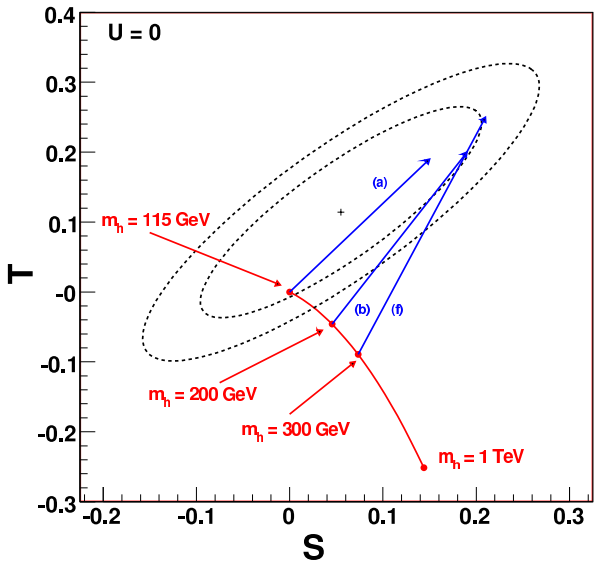

Figure 3.3: The 68% and 95% C.L. constraints on the (S, T) parameters obtained by the LEP Electroweak Working Group [56]. The red line shows the shift in the (S, T) plane, resulting from increasing the Higgs mass, whereas the blue arrows indicate the the shifts in ΔS and ΔT from a fourth generation with the parameter sets given in Table 3.1.

to find parameter regions where the S parameter is lowered by ΔS_ℓ, without contributing to $\Delta U_\ell \simeq -\Delta S_\ell$ and ΔT_ℓ or violating current direct-search bounds from LEP II (Sec.3.3.4). This does not mean that we exclude Majorana-type neutrinos, for which we find regions of $\Delta S_\ell \simeq 0$. For example, the lepton Dirac and Majorana masses $(m_D, M_{44}) = (141, 100)$ GeV give the lepton mass eigenstates $(m_{\nu_1}, m_{\nu_2}, m_\ell) = (100, 200, 200)$ GeV, contributing to the oblique parameters of $(\Delta S_\ell, \Delta T_\ell) = (0.01, 0.04)$.

3.3.3 Bounds from flavor physics

Flavor physics can constrain the off-diagonal elements $V_{u_4 i}, V_{j d_4}$ of the 4×4 CKM matrix. As in the Standard Model, tree-level flavor-changing neutral currents are absent. Rough constraints on the mixing between the first/second and fourth generation can be extracted requiring unitarity of the enlarged 4×4 CKM matrix. The SM 3×3 sub-matrix is well tested by a variety of SM processes [39]. The unitarity of the CKM matrix provides the relation

$$\sum_{l=1}^{4} V_{pl} V_{ql}^* = \delta_{pq}. \tag{3.8}$$

From (3.8) it is possible to deduce the absolute values of CKM matrix entries for the fourth generation. Using combined measurements [39] gives the following numbers:

$$\begin{aligned} |V_{ud_4}|^2 &= 1-|V_{ud}|^2-|V_{us}|^2-|V_{ub}|^2 \simeq 0.0008 \pm 0.0011, \\ |V_{cd_4}|^2 &= 1-|V_{cd}|^2-|V_{cs}|^2-|V_{cb}|^2 \simeq -0.03 \pm 0.027, \\ |V_{u_4d}|^2 &= 1-|V_{ud}|^2-|V_{cd}|^2-|V_{td}|^2 \simeq -0.001 \pm 0.005\ . \end{aligned} \tag{3.9}$$

If we require all of these constraints[2] on the additional CKM elements be satisfied to 1σ, we find

$$|V_{ud_4}| \lesssim 0.04, \quad |V_{u_4d}| \lesssim 0.08, \quad |V_{cd_4}| \lesssim 0.17.$$

As all CKM elements suffer from uncertainties unitarity considerations can just be conservative. The size is of $|V_{ud_4}| \lesssim 0.04$ is still significantly larger than the smallest elements in the CKM matrix $|V_{ub}|$,$|V_{td}|$. Four CKM elements are left (V_{td_4}, V_{u_4s}, V_{u_4b}, and $V_{u_4d_4}$) but could be constrained through a global fit to the 4×4 CKM matrix, including the contributions of the fourth-generation quarks to specific observables in loops [61, 62]. Comparable to the SM, the elements connecting the heaviest and second heaviest generation are much less constrained than the others. To extend the approach of considering unitarity to constrain some of the remaining elements V_{tb} has to be known from experiment. Single top production processes can be used to obtain a lower limit $V_{tb} > 0.68$ at 95% C.L. [63]. Hence, if the mass difference between the fourth and third generation is large enough, a fourth generation will decay predominantly into the third.
There are two additional CP-violating phases in the 4×4 CKM matrix, but since their effects are proportional to the unknown real parts of the off-diagonal CKM mixings, we ignore their effects.

A fourth generation does not only introduce new sources of flavor violation in the quark sector but also in the lepton sector, where the analogon to the CKM matrix is the Pontecorvo-Maki-Nakagawa-Sakate (PMNS) matrix, defined as

$$U_{PMNS} \equiv U_{e_L} U_{\nu_L}^\dagger = \begin{pmatrix} U_{e\nu_e} & U_{e\nu_\mu} & U_{e\nu_\tau} & U_{e\nu_4} \\ U_{\mu\nu_e} & U_{\mu\nu_\mu} & U_{\mu\nu_\tau} & U_{\mu\nu_4} \\ U_{\tau\nu_e} & U_{\tau\nu_\mu} & U_{\tau\nu_\tau} & U_{\tau\nu_4} \\ U_{e_4\nu_e} & U_{e_4\nu_\mu} & U_{e_4\nu_\tau} & U_{e_4\nu_4} \end{pmatrix}. \tag{3.10}$$

The unitary matrices $U_{e_L}^\dagger$ and $U_{\nu_L}^\dagger$ perform the rotation from gauge to mass eigenstates for the left-handed leptons. In this model the PMNS matrix is a 4×4 matrix, receiving constraints from lepton flavor violation in the charged and neutral sectors. One rather stringent constraint comes from the non-observation of the FCNC process $\mu \to e\gamma$. For weak-scale purely Dirac neutrinos this constraint is straightforward to estimate using [64]. We obtain $|U_{e4}U_{\mu4}| \lesssim 4 \times 10^{-4}$. This suggests that first/second-generation mixings with the fourth generation need to be a bit smaller than about 0.01 to satisfy all constraints. Other generational mixings can also be constrained

[2] More stringent constraints can be obtained with specific processes. For example, in [60] it is mentioned that the recent observation of D^0-$\overline{D}^0$ mixing leads to the constraint $|V_{ud_4}V_{cd_4}| \lesssim 0.002$ which is an order of magnitude stronger than those obtained from unitarity considerations.

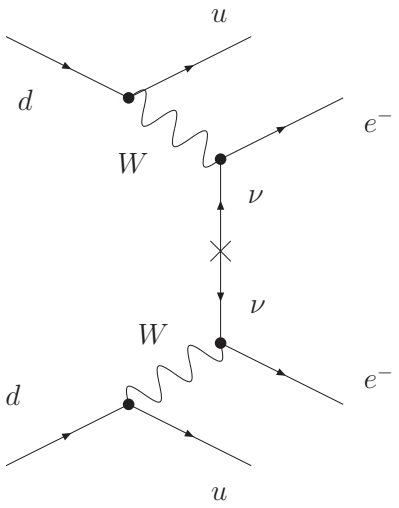

Figure 3.4: Neutrinoless double beta decay

from the absence of lepton-flavor violating effects, where again third/fourth-generation mixings are the most weakly constrained.

Processes with neutrinoless double beta decay provide the best experimental test whether neutrinos are Dirac or Majorana particles (Fig.3.4).
Further, assuming a weak-scale Majorana mass M_{44} they can provide significant constraints on $|U_{i4}|$. Such a process can be mediated by a very light neutrino mixing with a weak–scale Majorana neutrino. Assuming only mixing between the first and fourth generation [65], we obtain

$$\frac{|U_{e4}|^2 p_F^2 M_{44}}{3m_D^2} \lesssim \mathrm{eV}\,, \tag{3.11}$$

where $m_D = y^\nu_{44} v$ and PMNS phases are ignored. This expression is valid as long as the fourth-generation neutrino masses exceed the characteristic energy scale of the double-beta nuclear process, $m_{\nu_{1,2}} \gg p_F \simeq 60$ MeV. Inserting characteristic values, we obtain

$$|U_{e4}| \lesssim 0.9 \times 10^{-2}\, \frac{m_D}{M_{44}^{1/2} (100\ \mathrm{GeV})^{1/2}} \tag{3.12}$$

This bound is just relevant for Majorana masses which are not below a certain value, $M_{44} \lesssim 10$ MeV.

3.3.4 Direct search limits

Mass bounds on the particles of the fourth generation were gained from searches at LEP II and Tevatron. Bounds from LEP II are more severe for the leptonic sector, while the experiments

at Tevatron constrain the quark sector more severely. This leads to a lower mass bound at LEP II for a charged lepton of 101 GeV [66] and a bound on unstable neutral Dirac neutrinos are $(101, 102, 90)$ GeV for the decay modes $\nu_4 \to (e, \mu, \tau) + W$. Assuming a Majorana mass just weakens these limits by about 10 GeV. There is little difference between bounds for different flavors, charged versus neutral leptons, and Majorana versus Dirac mass. Hence, to be conservative, we apply the LEP II bounds, $m_{\nu_4,\ell_4,u_4,d_4} \gtrsim 100$ GeV, throughout.

The CDF search at Tevatron gains the strongest bounds on the up-type quark mass from the channel $u_4\overline{u}_4 \to q\overline{q}W^+W^-$, obtaining for the lower bound $m_{u_4} > 258$ GeV to 95% C.L. [67]. In this analysis no b-tag was used, so there is no dependence on the final-state jet flavor, and hence this limit applies independent of the CKM elements $V_{u_4 i}$. There is no analogous limit on the mass of d_4 beyond the LEP II bound [68]. If $m_{d_4} > m_t + m_W$ and $|V_{td_4}| \gg |V_{ud_4}|, |V_{cd_4}|$, then $d_4\overline{d}_4 \to t\bar{t}WW$ is the dominant decay channel. The $t\bar{t}$ final state is very instable and receives huge QCD backgrounds, hence the reconstruction of m_{d_4} is not possible. If the decay proceeds through a lighter generation, then the production rate and signal are the same as for u_4, and so we expect a bound on the mass of d_4 similar to that on u_4. If $m_{d_4} < m_t + m_W$, then d_4 decay could proceed through a 'doubly-CKM' suppressed tree-level process $d_4 \to cW$ or through the one-loop process $d_4 \to bZ$ [69, 70]. In particular, taking $\mathrm{BR}(d_4 \to bZ) = 1$, CDF obtains the bound $m_{d_4} > 268$ GeV at 95% C.L. [71]. Again, for a conservative estimation we choose to adopt the largely CKM-independent bound $m_{u_4,d_4} > 258$ GeV.

3.3.5 Results from Constraints

The results from Sections 3.3.2-3.3.4 do constrain the parameter space of the SM with an additional fourth generation but still leave enough freedom to conclude, that such a model is perfectly possible and by far not excluded. A Majorana mass for the neutrinos of the fourth generation is not even necessary, although it might weaken the constraints further. The region which is in agreement with all experimental constraints and with minimal contributions to the electroweak precision oblique parameters is characterized by

$$\begin{aligned} m_{\ell_4} - m_{\nu_4} &\simeq 30 - 60 \text{ GeV}, \\ m_{u_4} - m_{d_4} &\simeq \left(1 + \frac{1}{5}\ln\frac{m_H}{115\,\text{GeV}}\right) \times 50 \text{ GeV}, \\ |V_{ud_4}|, |V_{u_4 d}| &\lesssim 0.04, \\ |U_{e4}|, |U_{\mu 4}| &\lesssim 0.01, \\ m_{\nu_4,\ell_4} &> 100 \text{ GeV} \quad \text{and} \quad m_{u_4,d_4} > 258 \text{ GeV}. \end{aligned} \tag{3.13}$$

The other elements of the CKM and PMNS matrix are not strongly constrained. The smallest contribution to the oblique parameters occurs for small Higgs masses. Splitting between the lepton and quark masses is small, hence the two–body decays $\ell_4 \to \nu_4 W$ and $d_4 \to u_4 W$ generally do not occur. Finally, while there are strong restrictions on the mass *differences* between the up-type and down-type fields, there are much milder restrictions on the *scale* of the mass.

3.4 Higgs Searches

After concluding, that a fourth generation is in agreement with all measurable observables we have at hand, we want to analyze the impact of this SM extension on Higgs physics. Expecting a change in the branching-ratio, production cross section and significance pattern we consider all of them, to make comparison with Sections 2.1.2 and 2.3 easy.

3.4.1 Theoretical constraints on the Higgs sector

As discussed in Section 2.1.1 the Higgs mass is subject to theoretical constraints, limiting it to the sub-TeV region: (1) the possibility that the quartic coupling is driven negative, destabilizing the electroweak scale, and (2) large Yukawa couplings driving the Higgs quartic and/or the Yukawas themselves to a Landau pole (2.16), *i.e.* entering a strong-coupling regime.
In both cases the problematic coupling is the Higgs quartic, since it receives much larger new contributions to its renormalization group running from the fourth-generation quark Yukawas couplings. The renormalization group equation for the quartic coupling λ is given in (2.15).
Adopting again the conservative approach we do not impose a stable vacuum, but a meta-stable: The possibility of the transition into a different vacuum during the age of the universe due to quantum fluctuations has to be smaller than 1. It can be shown that the probability that the electroweak vacuum has survived quantum fluctuations until today is given, in semi-classical approximation by [20]

$$p \approx \left(\frac{\mu}{H}\right)^4 e^{-S} \ll 1, \tag{3.14}$$

where S is the Euclidean action, the solution of the classical field equations interpolating between the two sides of the barrier. μ is the cut-off scale, where new physics enters and where the calculation is not valid any more. Hence, the scale at which this inequality is saturated is a minimum scale, requiring new physics. $H = 1.4\ 10^{-42}\ \mathrm{GeV}$ is the Hubble scale. S can be approximated by

$$S \simeq \frac{16\pi^2}{3\left|\lambda\left(\mu\right)\right|}. \tag{3.15}$$

Thus, the critical region where the transition probability is close to 1 is

$$\lambda\left(\mu\right) \lesssim \frac{4\pi^2}{3\ln\left(H/\mu\right)}. \tag{3.16}$$

From the second constraint we can deduce an upper bound for the Higgs mass. Demanding that the quartic coupling remains perturbative, $\lambda(\mu) \lesssim 4\pi$, we find that the bound of the Higgs on the cut-off scale of the theory rapidly becomes small as the Higgs mass is increased. Both of the constraints were taken into account in Figure 3.5.
We find the maximal cut-off scale, before new physics of any kind enters, occurs for Higgs masses in the neighborhood of 300 GeV. Much lower Higgs masses, in particular $m_H < 2M_W$, imply other new physics must enter to prevent developing a deeper minimum away from the electroweak-breaking vacuum.

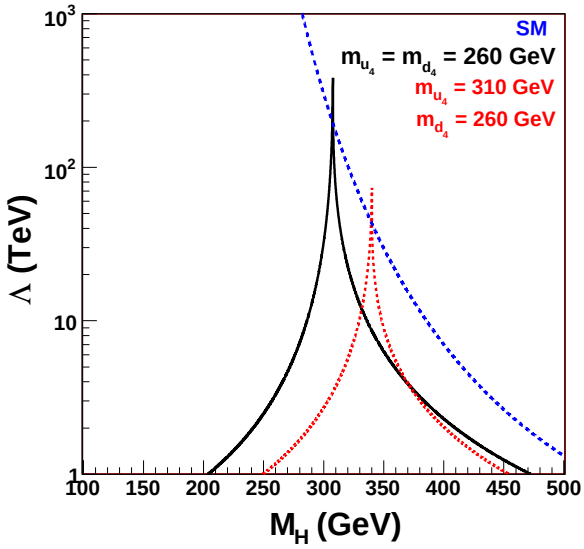

Figure 3.5: The maximum scale at which new physics enters into the Higgs potential to avoid either a too short–lived vacuum or to avoid a Landau pole in λ. These two constraints are qualitatively distinct: meta–stability can be restored by *weakly* coupled physics below a TeV scale, whereas the Landau pole signals a strongly interacting Higgs sector. The dashed curve reproduces the SM triviality bound.

3.4.2 Phenomenological implications on the Higgs search

The set of mixing elements and mass hierarchies shown in (3.13) has significant effects on Higgs searches at the LHC. One clear observation is that Higgs decays into fourth–generation particles, if possible at all, are expected only into leptons, unless the Higgs is exceptionally heavy which is disfavored by precision data.

As discussed in Section 2.1.2, a loop-induced decay and production processes are especially sensitive to new physics. In the SM the top is the only colored particle with sizeable coupling to the Higgs. A fourth generation with two additional heavy quarks increases the effective ggH coupling by roughly a factor of 3, and hence increases the production cross section $\sigma_{gg\to H}$ by a factor of 9 [72]. The Yukawa coupling exactly compensates for the large decoupling quark masses in the denominator of the loop integral [27]. This result is nearly independent of the mass of the heavy quarks, once they are heavier than the top. This enhancement allowed CDF and D0 to very recently rule out a Higgs in a four generation model within the mass window of roughly $145 < m_H < 185$ GeV to 95% C.L. using the process $gg \to h \to W^+W^-$ [73, 74].

A fourth generation induces important changes in the branching ratios of the Higgs. Due to their large Yukawa couplings, the effective ggH coupling strength is dramatically increased and thus the decay rate of $H \to gg$ as well. It even becomes the dominant decay mode for a Higgs mass lighter than about 140 GeV, if in this region no decays into fourth-generation fermions

m_H	115	200
A_W	-8.0321	$-9.187 - 5.646i$
A_t	1.370	1.458
A_{u_4}	1.344	1.367
A_{d_4}	1.349	1.382
A_{ℓ_4}	1.379	1.491

Table 3.2: The dominant form factors for the decay $H \to \gamma\gamma$ and $H \to gg$ according to (2.19) for the parameter points (a) and (b). For $H \to gg$ just the quark loops contribute.

occur. Unfortunately it is probably impossible to extract from the two-jet background at the LHC. The presence of this decay effectively suppresses all other two-body-decays branching ratios, including the light-Higgs discovery mode $H \to \tau\tau$, by roughly a factor 0.6. In the mass region above $140\ \mathrm{GeV}$ bosonic decays dominate over the fermionic ones.
More subtle effects occur for the loop-induced decay $H \to \gamma\gamma$. In Table 3.2 we show numbers of the form factors (2.19). Whereas the form factors for $H \to gg$, which are induced by quarks, interfere constructively, the interference between heavy quarks and spin W bosons is destructively. Hence, the branching ratio $BR(H \to \gamma\gamma)$ is suppressed by roughly a factor $1/9$ compared to the SM. The numbers are almost independent from the exact fermion masses, as long as they are large enough. In particular, the contributions from the fermions in our reference parameters points (a) and (b) can be described by the decoupling limit. The enhancement factor of 9 in σ_{gg} breaks down if the Higgs mass is around the top thresh-old region and subsequent heavy-quark thresholds. Here, absorptive imaginary parts appear (Table 3.2).
We show the complete set of branching ratios in Figure 3.6. All predictions for Higgs decays are computed with a modified version of Hdecay [26] which includes radiative corrections also to the fourth–generation decays, but no off-shell effects for these decays. Due to the color factor N_c decays into tops are prefer into the leptons of the fourth generation ℓ_4 and ν_4, but all of them are smaller than the decays to the massive gauge bosons. In general, there are decays into fourth-generation quarks as well - if the Higgs is heavy enough.
For a light Higgs below 200 GeV the effects on different gluon–fusion channels are roughly summarized by

$$\begin{aligned}
\sigma_{gg}\mathrm{BR}(\gamma\gamma)\big|_{\mathrm{G4}} &\simeq \sigma_{gg}\mathrm{BR}(\gamma\gamma)\big|_{\mathrm{SM}} \\
\sigma_{gg}\mathrm{BR}(ZZ)\big|_{\mathrm{G4}} &\simeq (5\cdots 8)\,\sigma_{gg}\mathrm{BR}(ZZ)\big|_{\mathrm{SM}} \\
\sigma_{gg}\mathrm{BR}(f\overline{f})\big|_{\mathrm{G4}} &\simeq 5\,\sigma_{gg}\mathrm{BR}(f\overline{f})\big|_{\mathrm{SM}}\,.
\end{aligned} \tag{3.17}$$

In Figure 3.7 we show a set of naively scaled discovery contours for a generic compact LHC detector, modifying all known discovery channels according to fourth-generation effects [29]. The enhancement of the production cross section implies, that the 'gold-plated mode'. $H \to ZZ \to 4\mu$ can be used throughout the Higgs mass range, from the LEP II bound to beyond 500 GeV. Both WW channels [75, 76] are still relevant, but again the gluon–fusion channel[3]. As mentioned above, the weak–boson–fusion discovery decay $H \to \tau\bar{\tau}$ becomes relatively less

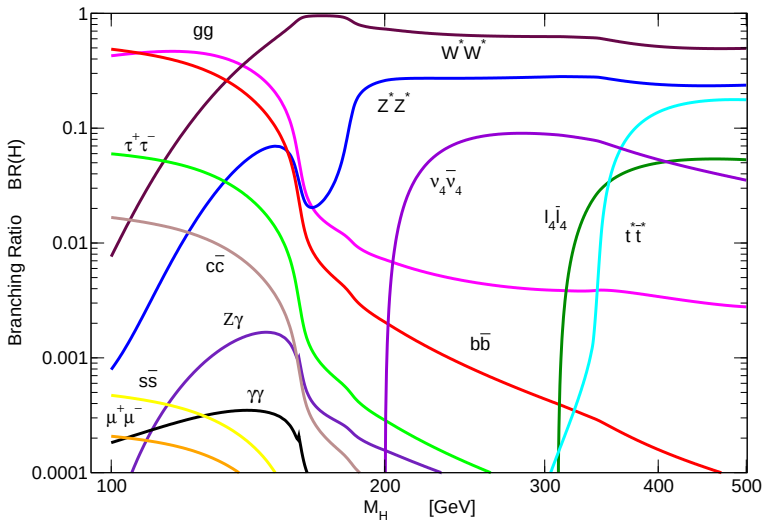

Figure 3.6: Branching ratio of the Higgs with fourth–generation effects assuming $m_\nu = 100$ GeV and $m_\ell = 155$ GeV. For the fourth–generation masses we follow the reference point (b).

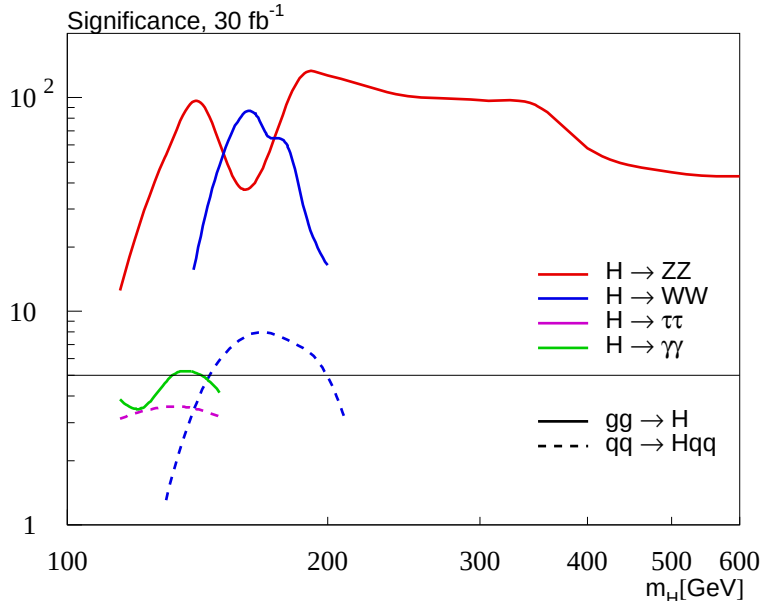

Figure 3.7: Scaled LHC discovery contours for the fourth–generation model. All channels studies by CMS are included. The significances have naively been scaled to the modified production rates and branching rations using the fourth–generation parameters of reference point (b).

important, even though its significance is only slightly suppressed. Weak-boson-fusion production with a subsequent decay to photons is suppressed by one order of magnitude compared to the Standard Model and not shown anymore, while for the gluon-fusion channel with a decay to photons the corrections to the production rate and the decay width accidentally cancel.
Measuring the relative sizes of the different production and decay modes would allow an interesting study of Higgs properties that should be easily distinguishable from other scenarios (two Higgs doublet model, Supersymmetry, etc.). Moreover, there may be novel search strategies for the Tevatron that would be otherwise impossible given just the SM Higgs production rate.

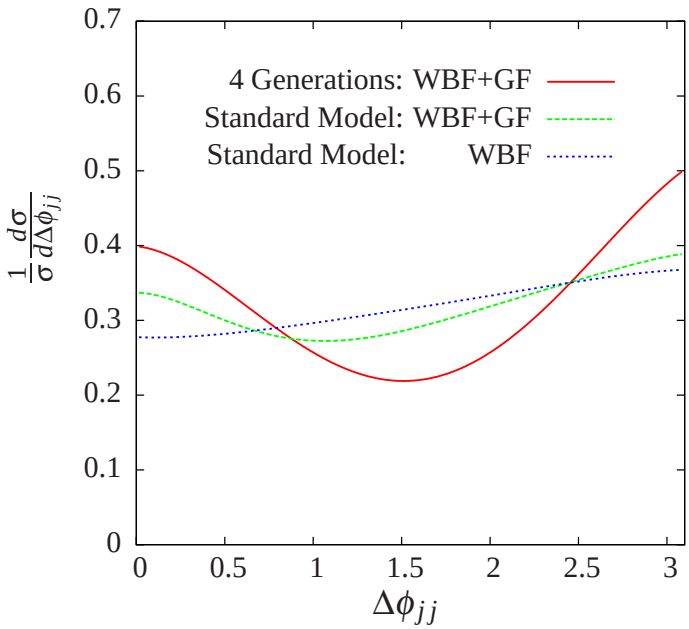

Figure 3.8: Angular distribution of vector-boson fusion channel at LHC assuming reference point (b) with the Higgs mass $m_H = 200$ GeV and cuts from (3.23).

Weak–boson–fusion Higgs production has interesting features beyond its total rate. It has the advantage of allowing us to extract a Higgs sample only based on cuts on the two forward tagging jets, allowing us to observe Higgs decays to taus and even invisible Higgs decays [77, 78].
Apart from the Weak–boson–fusion a Higgs + two jets can be produced by gluon-gluon fusion. The calculation of this process is quite involved at leading order in α_s, where triangle, box and pentagon quark loops occur. However, if the Higgs mass is below the threshold for the creation of the heavy quarks, $m_H \leq 2m_f$, the coupling of the Higgs to the gluons via a fermion loop can be replaced by an effective coupling [27]. The effective Hgg vertex in the large fermion-mass limit is given by a dimension 5 operator [79]

$$\mathcal{L}_{eff} = a_1 H G^{\alpha}_{\mu\nu} G^{\mu\nu,\alpha}, \tag{3.18}$$

[3] The gluon–fusion tends to be more promising at CMS analyses for a SM Higgs, whereas the weak-boson-channel is prefer fourth-generation enhancement.

whereas the coupling HVV, with $V = H, Z$ is

$$\mathcal{L}_{HVV} = a_2 H V_\mu V^\mu, \tag{3.19}$$

with Lorentz-invariant form factors a_1, a_2. This reveals the tensor structure

$$T^{\mu\nu}(q_1, q_2) = a_2(q_1, q_2)\, g^{\mu\nu} + a_1(q_1, q_2)\,[q_1 \cdot q_2 g^{\mu\nu} - q_2^\mu q_1^\nu]\,. \tag{3.20}$$

Here q_1 and q_2 are the four-momentums of the bosons. The form factors a_2 and a_1 can affect the shape of $\Delta\phi_{jj}$, the angle between the two jets transverse momentum. The difference in the azimuthal angle is defined by

$$\Delta\phi_{jj} = \arccos \frac{\vec{p}_{T,1} \cdot \vec{p}_{T,2}}{\|\vec{p}_{T,1}\|\,\|\vec{p}_{T,2}\|}, \tag{3.21}$$

with the outgoing jet momentums p_1 and p_2.
We employ the following common WBF cuts, which are usually used to discriminate the contributions from weak boson fusion and gluon fusion:

$$|n_{j_1} - n_{j_2}| > 4.2, \qquad n_{j_1} \cdot n_{j_2} < 0, \qquad m_{ij} > 600\text{GeV}, \tag{3.22}$$

$$p_{T,j} > 20\ \text{GeV}, \qquad |n_j| < 5, \qquad R_{ij} > 0.6. \tag{3.23}$$

η_{j_1} is the pseudo-rapidity of the jet j_1:

$$\eta_{j_1} = \frac{1}{2} \ln \frac{1 + \cos\theta}{1 - \cos\theta}, \tag{3.24}$$

where θ is the angle between the particles momentum and the beam axis. The jet separation ΔR_{ij} is defined as

$$\Delta R_{ij} = \sqrt{\Delta n_{ij}^2 + \Delta\phi_{ij}^2}, \tag{3.25}$$

with the pseudo-rapidity difference between the two jets Δn_{ij}.
After applying the cuts in (3.23), the WBF dominate the gluon-fusion contributions in the SM with just three generations, hence the differential cross section remains almost insensitive against a variation of $\Delta\phi_{jj}$. But the modification to the ggH coupling from a fourth generation leads to a larger relative size of the gluon–fusion process in the H+2 jets sample. For $\Delta\phi_{jj} = \pi/2$ the gluon-fusion differential cross section has a minimum, yielding peaks around $\Delta\phi_{jj} = (0, \pi)$. This causes a modification in the angular correlation, shown in Figure 3.8. We did the analysis using Madevent [80], and used the HEFT model [27]. Measuring this distribution would provide an interesting probe of the relative sizes of the weak–vector–boson fusion over gluon fusion, which provides a distinctive differentiation between three and four generations.

3.5 Summary

The results of this chapter have been published in [81]. We investigated the possibility of the existence of a fourth generation in the Standard Model and its effects on Higgs physics. A fourth generation is in perfect agreement with present measurements of electroweak precision data and is not ruled out by quark-flavor or lepton-flavor physics. The new parameters introduced in this way, e.g. the masses and mixing matrices, are just weakly constrained. The LHC with its high center-of-mass energy should be able to produce and find the fourth generation quarks. Even easier than in the SM, the Higgs can be found using the 'golden mode' $pp \to H \to ZZ$ for a wide range of mass even with small integrated luminosity. Given measures of the cross section for Higgs production as well as branching ratios of Higgs into subdominant modes, the LHC will find the fourth generation, if it exists.

Chapter 4

Supersymmetry

Supersymmetric models are one of the most popular candidates for the SM extension. One reason is the fact, that in the SM no internal symmetry protects scalar mass terms from receiving quadratically–divergent renormalization corrections. If the SM is assumed to be the correct theory up to a possible GUT scale or even to the Planck scale ($\tilde{}10^{19}$ GeV), the smallness of the electroweak scale, or equivalently of the parameter μ^2, is technically unnatural [82] (*hierarchy problem*). In order to generate the observed masses of the weak gauge bosons, μ^2 has to be of the order of $(100 \text{ GeV})^2$. To keep the renormalized Higgs mass at the order of the electroweak scale, its bare mass has to be fine-tuned in each order of perturbation theory to cancel the radiative corrections almost exactly. By noticing that the loop corrections from bosons and fermions have opposite sign, in supersymmetric theories the hierarchy problem may be solved technically by relating bosonic and fermionic degrees of freedom. In ordinary gauge theories space-time and internal symmetries are independent of each other. Coleman and Mandula proofed that this is necessarily the case in any four-dimensional quantum field theory with non-zero scattering amplitudes [4]. To circumvent this No-Go theorem, aiming to extend a Poincaré invariant theory by global supersymmetry, an N-extended super-Poincaré Algebra containing central charges can be introduced (Haag-Lopuszanski-Sohnius theorem [83]). The supersymmetry generators Q^i $[i = 1, ..., N]$ and their complex conjugate $\bar{Q}^i$ transform fermionic into bosonic fields and vice versa, therefore obeying an anticommutation relation which leads to a Z_2 graded Lie algebra. N determines the maximum spin present in the particle spectrum of the theory. Renormalizability requires a maximum spin of one for global supersymmetry, which is equivalent to $N \leq 4$. The most interesting case for our work seems to be $N = 1,$ where the central charges vanish and the generators $Q, \bar{Q}$ anticommute with themselves. This is the only global supersymmetric algebra which is compatible with observed low energy particle spectrum and CP violation.

4.1 R Parity

The most general superpotential (4.7) can give rise to lepton and baryon number violating interactions and can mediate proton decay at tree level through the exchange of the scalar partner

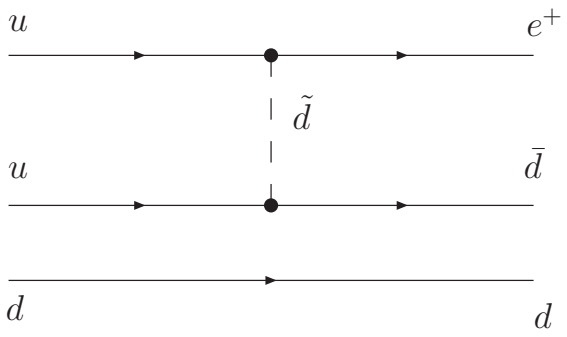

Figure 4.1: Proton decay in theories with R-parity violation.

of the down quark. The MSSM either needs to suppress the different couplings in order not to violate experimental bounds, or remove the possible B and L violating terms assuming a new Z_2 symmetry. This new symmetry is called 'R parity' [84]. R parity can be defined as a multiplicative quantum number such that all particles of the SM have R parity +1, while their SUSY partners have R parity -1. All of the Higgs particles in the two–Higgs–doublet model are described by $R = +1$. The conserved charge is defined as

$$R = (-1)^{3B+L+2S},$$

where B is the baryon number, L the lepton number and S the spin of the particle.

The conservation of R parity has phenomenologically a crucial impact on scattering and decay processes. For example, starting from an initial state involving ordinary SM particles (R-even), the supersymmetric particles must be produced in pairs. Furthermore, the lightest SUSY particle ('LSP') is absolutely stable, which makes it a popular candidate for cold dark matter.

4.2 Supersymmetry breaking

If supersymmetry was an exact symmetry of nature, particles and their superpartners would have the same mass. Since no superpartners have been observed yet, supersymmetry must be broken at energies accessible to present experiments. From a theoretical perspective, it is expected that it should be an exact symmetry that is broken spontaneously. This means that the Lagrangian remains invariant under the supersymmetry transformations, but it receives a vacuum state which is not invariant [85].
Many different models of spontaneous supersymmetry breaking have been proposed. Typically the breaking takes place at very high energies in a so-called 'hidden' sector. Thereafter it is transmitted to a visible sector, e.g. gravity-mediated [86] and gauge-mediated [87] supersymmetry breaking models. In the absence of knowledge about the SUSY breaking mechanism, it seems to be phenomenologically acceptable to parametrize the effects of SUSY breaking by

adding to the Lagrangian all possible SUSY breaking terms, consistent with all desired symmetries at the SUSY breaking scale, that do not lead to the re-appearance of quadratic divergences [88] (called soft breaking terms). Only the following terms are soft supersymmetry breaking up to all orders in perturbation theory:

$$\begin{array}{ll} \bullet \text{ scalar mass terms} & m_{ij}^2 A_i^* A_j \\ \bullet \text{ trilinear scalar interactions} & t_{ijk} A_i A_j A_k + h.c. \\ \bullet \text{ mass terms for gauge particles} & \frac{1}{2} m_l \bar{\lambda}_l \lambda_l \\ \bullet \text{ bilinear terms} & b_{ij} A_i A_j + h.c. \\ \bullet \text{ linear terms} & l_i A_i \end{array} \tag{4.1}$$

The Lagrangian consists of two parts, one which is invariant under supersymmetry transformations and one which is not:

$$\mathcal{L} = \mathcal{L}_{SUSY} + \mathcal{L}_{soft}. \tag{4.2}$$

4.3 The Minimal Supersymmetric Standard Model

The MSSM is the most widely studied realistic SUSY model. It is essentially a straightforward supersymmetrization of the Standard Model, where one introduces only those couplings and fields that are necessary for consistency. Its basic structure is well-known and has been thoroughly discussed in the literature [89].

The single particle states live in irreducible representations of the corresponding algebra which are called supermultiplets. Each supermultiplet contains both fermion and boson states with the same electric charge, weak isospin, and color degrees of freedom, commonly known as superpartners. The matter fields, e.g. the quarks and leptons, are represented through chiral superfields where each of the fermions gains a complex scalar partner. To distinguish the spin-0 superpartners from the SM particles they are prefixed with an 's' (short for scalar). The SM gauge fields, i. e. the gluons, the $W^{\pm}$, the Z^0 and γ, become parts of vector superfields and get fermionic partners called gluinos, winos and photino respectively. The $SU\,(3)$ ghost fields are defined by re-writing the Fadeev-Popov determinant; therefore they do not have supersymmetric partners.

To ensure anomaly cancellation and because of the fact that the product of a chiral superfield and a conjugate one is not chiral but a vector multiplet, it is necessary to introduce at least two Higgs doublets H_1 and H_2 which give masses to down- and up-type quarks respectively. In supersymmetric models, in contrast to Section 2.2, one employs two Higgs doublet fields of opposite hypercharge: H_1 with $Y = -1$ and H_2 with $Y = 1$. The relation between these fields and the ϕ_i of Section 2.2 are:

$$\begin{aligned} \phi_1^j &= \varepsilon_{ij} H_1^{i*} \\ \phi_2^j &= H_2^j \end{aligned} \tag{4.3}$$

where i, j are $SU(2)$ indices and $\epsilon_{12} = -\epsilon_{21} = 1,\ \epsilon_{11} = \epsilon_{22} = 0$. The doublet is

$$H_1 = \begin{pmatrix} H_1^1 \\ H_1^2 \end{pmatrix} = \begin{pmatrix} \frac{1}{\sqrt{2}} (v_1 + h_1 - i g_1) \\ -\phi_1^- \end{pmatrix} \tag{4.4}$$

where $\phi_1^- = \left(\phi_1^+\right)^*$.
After breaking $SU\left(2\right) \times U\left(1\right)$ invariance they form five physical Higgs particles which have to develop supersymmetric partner fields. This yields neutral and charged Majorana/Dirac fermions with the same quantum numbers as the $SU\left(2\right)$ gauginos. The renormalizable MSSM Lagrangian is constructed by including all possible interaction terms of dimension four or less that satisfy the spacetime supersymmetry algebra, $SU\left(3\right) \times SU\left(2\right) \times U\left(1\right)$ gauge invariance and $B - L$ conservation[1].
The particle content of the MSSM is summarized in (4.5).

	superfields	fermion fields	boson fields	$SU\left(3\right)_C$	$SU\left(2\right)_L$	$U\left(1\right)_Y$
matter sector						
squarks, quarks	$\hat{Q}_i$	$\begin{pmatrix} u_{L,i} \\ d_{L,i} \end{pmatrix}$	$\begin{pmatrix} \tilde{u}_{L,i} \\ \tilde{d}_{L,i} \end{pmatrix}$	$\mathbf{3}$	$\mathbf{2}$	$\frac{1}{3}$
	$\hat{U}_i$	$u^c_{R,i}$	$\tilde{u}^+_{R,i}$	$\mathbf{3}^*$	$\mathbf{1}$	$-\frac{4}{3}$
	$\hat{D}_i$	$d^c_{R,i}$	$\tilde{d}^+_{R,i}$	$\mathbf{3}^*$	$\mathbf{1}$	$\frac{2}{3}$
sleptons, leptons	$\hat{L}_i$	$\begin{pmatrix} \nu_{L,i} \\ e_{L,i} \end{pmatrix}$	$\begin{pmatrix} \tilde{\nu}_{L,i} \\ \tilde{e}_{L,i} \end{pmatrix}$	$\mathbf{1}$	$\mathbf{2}$	-1
	$\hat{E}_i$	$e^c_{R,i}$	$\tilde{e}^+_{R,i}$	$\mathbf{1}$	$\mathbf{1}$	2
Higgs sector						
Higgs, Higgsinos	H_1	$\begin{pmatrix} \tilde{H}^1_1 \\ \tilde{H}^2_1 \end{pmatrix}$	$\begin{pmatrix} H^1_1 \\ H^2_1 \end{pmatrix}$	$\mathbf{1}$	$\mathbf{2}$	-1
	H_2	$\begin{pmatrix} \tilde{H}^1_2 \\ \tilde{H}^2_2 \end{pmatrix}$	$\begin{pmatrix} H^1_2 \\ H^2_2 \end{pmatrix}$	$\mathbf{1}$	$\mathbf{2}$	1

(4.5)

	superfields	fermion field	boson field	$SU\left(3\right)_C$	$SU\left(2\right)_L$	$U\left(1\right)_Y$
gluino, gluon	$\hat{G}^a$	$\tilde{\lambda}^a_G$	G^a_μ	8^{adj}	1	0
winos, W bosons	$\hat{W}^i$	$\tilde{\lambda}^i_W$	W^i_μ	1	3^{adj}	0
bino, B boson	$\hat{B}$	$\tilde{\lambda}_B$	B_μ	1	1	0

(4.6)

A convenient way to handle supermultiplets in non-abelian supersymmetric theories is the superspace formalism [90]. As Lorentz invariance is inherently manifest in the 4-dimensional Minkowski space, supersymmetry is inherently manifest in the superspace formalism. Elements of superspace are specified by supercoordinates $\left(x_\mu, \theta, \bar{\theta}\right)$, with θ and $\bar{\theta}$ being anti-commuting Grassmann coordinates. All superfields can be written as a finite power series in these Grassmann variables, containing the component fields in the coefficients. Just two elements enter the supersymmetric Lagrangian:

[1] B =baryon number and L =lepton number

- the so-called F term of a chiral supermultiplet, denoted as Φ_{θ^2} in the expansion of the superfield in the Grassmann variable θ,
- the so-called D-term of a vector multiplet $V_{\theta^2\bar{\theta}^2}$.

The kinetic real vector supermultiplet is defined as the product of a chiral supermultiplet and its conjugate $\bar{\Phi}_j\Phi_j$. Its D-terms contain the F components of the chiral multiplets $F_j^*F_j$, which is absorbed into the scalar potential. Knowing the gauge groups, the particle content and the gauge transformation properties, the only freedom is in the choice of the superpotential $W(\{\Phi\})$. Using the fact that the product of two chiral superfields is again chiral and restricting the mass dimension to be not bigger than four, one obtains for the superpotential:

$$W(\{\Phi\}) = m_{ij}\Phi_i\Phi_j + \lambda_{ijk}\Phi_i\Phi_j\Phi_k. \tag{4.7}$$

In the Lagrangian, the superpotential occurs as $\left(W + \bar{W}\right)$, whereas the scalar potential is defined as

$$V = -\left(F_j^*F_j + \frac{\partial W(A)}{\partial A_j}F_j + \frac{\partial \bar{W}(\bar{A})}{\partial \bar{A}_j}F_j^*\right) \tag{4.8}$$

The scalar potential contains the non-Yukawa terms arising from the superpotential W. Using the Euler-Lagrange equation yields

$$F_j^* = -\frac{\partial W(A)}{\partial A_j}, \tag{4.9}$$

where A_j are the sfermion fields in the supermultiplet. Adding the D auxiliary component field for vector multiplets of non-abelian gauge groups, the scalar potential is then readily derived to be

$$V = \sum_j |F_j|^2 + \frac{1}{2}\sum_a (D^a)^2 = \sum_j |F_j|^2 + \frac{g^2}{2}\sum_a \left(S^*T^aS\right)^2, \tag{4.10}$$

where S are scalar fields transforming under the fundamental representation of the corresponding gauge group and T^a are the generators of the underlying gauge group.
The most general renormalizable R-parity conserving superpotential, compatible with gauge invariance, is

$$W_{MSSM} = \varepsilon_{IJ}\left[y_e^{ij}\hat{H}_1^I\hat{L}^{Ji}\hat{E}^j - y_u^{ij}\hat{H}_2^I\hat{Q}^{Ji}\hat{U}^j + y_d^{ij}\hat{H}_1^I\hat{Q}^{Ji}\hat{D}^j - \mu\hat{H}_1^I\hat{H}_2^J\right], \tag{4.11}$$

where $\varepsilon_{12} = -\varepsilon_{21} = 1$, μ is the Higgs mass parameter, the y_e, y_u and y_d are the same 3×3 Yukawa-coupling matrices as in the Standard Model and i and j denote the generation index. Using (4.11) the Lagrangian of the MSSM consists of kinetic, mass and interactions terms for all fermions, Higgs and gauge bosons of the MSSM. It can be cast into the form

$$\mathcal{L}_{SUSY} = \mathcal{L}_{chiral} + \mathcal{L}_{vec,1} + \mathcal{L}_{vec,2}. \tag{4.12}$$

The chiral part of the Lagrangian is governed by (4.11),

$$\mathcal{L}_{chiral} = \left(\varepsilon_{IJ}\left[y_e^{ij}\hat{H}_1^I\hat{L}^{Ji}\hat{E}^j - y_u^{ij}\hat{H}_2^I\hat{Q}^{Ji}\hat{U}^j + y_d^{ij}\hat{H}_1^I\hat{Q}^{Ji}\hat{D}^j - \mu\hat{H}_1^I\hat{H}_2^J\right]\Big|_F + \text{h.c.}\right). \tag{4.13}$$

$\mathcal{L}_{vec,1}$ contains the kinetic terms of fermions as well as the interaction terms of scalar, spinor and vector fields:

$$\begin{aligned}\mathcal{L}_{vec,1} &= \Big[\hat{Q}^\dagger e^{2g'V'+2gV+2g_sV_s}\hat{Q} + \hat{U}^\dagger e^{2g'V'-2g_sV_s^T}U + \hat{D}^\dagger e^{2g'V'-2g_sV_s^T}\hat{D} \\ &\quad +\hat{L}^\dagger e^{2g'V'+2gV}\hat{L} + \hat{E}^\dagger e^{2g'V'}\hat{E} \\ &\quad +\hat{H}_1^\dagger e^{2g'V'+2gV}\hat{H}_1 + \hat{H}_2^\dagger e^{2g'V'+2gV}\hat{H}_2\Big]\Big|_D .\end{aligned} \tag{4.14}$$

The following notation has been used:

$$V_s = T_s^a V_s^a, \quad V = T^a V^a, \quad V' = \frac{Y}{2}v', \tag{4.15}$$

where T_s^a, T^a and Y are the generators of $SU(3)_C$, $SU(2)_L$, and $U(1)_Y$ respectively.
The second vector part consists of the kinetic terms of gauge bosons,

$$\mathcal{L}_{vec,2} = \left(\left[\frac{1}{16g^2}W^{a\alpha}W^a_\alpha + \frac{1}{16g'^2}W'^\alpha W'_\alpha + \frac{1}{16g_s^2}W_s^{a\alpha}W^a_{s\alpha}\right]\right) \tag{4.16}$$

with the field-strength tensors

$$W^a_{s\alpha} = -\frac{1}{4}\bar{D}\bar{D}\left(e^{-2g_sV_s}D_\alpha e^{2g_sV_s}\right), \tag{4.17}$$

$$W^a_\alpha = -\frac{1}{4}\bar{D}\bar{D}\left(e^{-2gV}D_\alpha e^{2gV}\right), \tag{4.18}$$

$$W'_\alpha = -\frac{1}{4}\bar{D}\bar{D}\left(e^{-2g'V'}D_\alpha e^{2g'V'}\right) = -\frac{g'}{4}\bar{D}\bar{D}D_\alpha V'. \tag{4.19}$$

The covariant derivatives are defined to be

$$\bar{D}_{\dot\alpha} = \partial_\alpha - i_\alpha\left(\sigma_\mu\bar\theta\right)\partial^\mu \quad \text{or} \quad D_\alpha = \bar\partial_{\dot\alpha} + i\left(\theta\sigma_\mu\right)_{\dot\alpha}\partial^\mu. \tag{4.20}$$

As indicated in (4.2), in the MSSM explicit supersymmetry breaking is realized by adding soft breaking terms to (4.12). Respecting the criteria for soft breaking terms from Section 4.2, the soft breaking Lagrangian can be cast into the form

$$\begin{aligned}\mathcal{L}_{soft} &= \frac{1}{2}\left(M_3\overline{\tilde\lambda_s^a}\tilde\lambda_s^a + M_2\overline{\tilde\lambda_W^a}\tilde\lambda_W^a + M_1\overline{\tilde\lambda_B}\tilde\lambda_B + h.c.\right) \\ &\quad -M^2_{\tilde Q,ij}\left(\tilde u^*_{L,i}\tilde u_{L,j} + \tilde d^*_{L,i}\tilde d_{L,j}\right) - M^2_{\tilde U,ij}\tilde u^*_{R,i}\tilde u_{R,j} - M^2_{\tilde D,ij}\tilde d^*_{R,i}\tilde d_{R,j} \\ &\quad -M^2_{\tilde L,ij}\left(\tilde v^*_{L,i}\tilde v_{L,j} + \tilde e^*_{L,i}\tilde e_{L,j}\right) - M^2_{\tilde E}\tilde e^*_{R,i}\tilde e_{R,j} - m_1^2|H_1|^2 - m_2^2|H_2|^2 \\ &\quad +m_{12}^2\left(\varepsilon_{ij}H_1^iH_2^j + h.c.\right) - \Big(\varepsilon_{IJ}\Big(A^e_{ij}H_1^I\tilde L^{Ji}\tilde E^j - A^u_{ij}H_2^I\tilde Q^{Ji}\tilde U^j \\ &\quad + A^d_{ij}H_1^I\tilde Q^{Ji}\tilde D^j\Big) + h.c.\Big).\end{aligned} \tag{4.21}$$

Again the indices i and j denote the three generations. The trilinear couplings A^e_{ij}, A^u_{ij} and A^d_{ij}, the gaugino mass parameters M_1, M_2 and M_3, the bilinear Higgs coupling m_{12}, as well as the

scalar mass parameters $M^2_{\tilde{Q},ij},\ M^2_{\tilde{U},ij},\ M^2_{\tilde{D},ij},\ M^2_{\tilde{L},ij}$ and $M^2_{\tilde{E},ij}$ can be complex. The Higgs mass parameters m_1 and m_2 are real numbers.
Analogously to the SM it is necessary to include gauge-fixing and ghost terms for consistent quantization of the MSSM Lagrangian. They are selected in an identical way compared to the SM. Hence, the full expression of the MSSM Lagrangian reads

$$\mathcal{L}_{MSSM} = \mathcal{L}_{SUSY} + \mathcal{L}_{soft} + \mathcal{L}_{gauge-fixing} + \mathcal{L}_{ghost}. \tag{4.22}$$

4.3.1 Mass spectrum of the MSSM

4.3.1.1 Quarks, Leptons and gauge bosons

The identification of quark, lepton and gauge boson eigenstates and the corresponding masses follows the usual Standard Model analysis. Using (4.11) one constructs the quark mass matrix. According to Appendix A the weak eigenstates are rotated to the mass eigenstates using the CKM matrix. The diagonalized Yukawa matrices $y'_e,\ y'_u$ and y'_d determine the fermion masses:

$$m_e = y'_e v_1, \quad m_d = y'_d v_1, \quad m_u = y'_u v_2. \tag{4.23}$$

Neutrino mixing is not considered in the MSSM, hence the charged lepton interaction eigenstates and mass eigenstates coincide.
Electroweak symmetry breaking turns the W^i and B gauge bosons into the mass eigenstates $W^{\pm},\ Z$ and the photon γ.

4.3.1.2 Higgs Masses

The Higgs spectrum of the MSSM can be constructed in complete analogy to Section 2.2. The scalar potential is calculated according to (4.10). It appears that because of the assumed CP invariance of the Higgs sector the real and imaginary components of the neutral Higgs bosons do not mix, so that the 4×4 mass matrix in the neutral sector decomposes into two 2×2 blocks. After diagonalizing the mass matrices for the charged Higgs, the CP-odd and CP-even Higgs,

$$\begin{aligned}
M_{h_1h_2} &= \begin{pmatrix} m_1^2+\mu^2+M_Z^2\left(\frac{1}{2}+c2\beta\right) & -m_{12}^2-M_Z^2\, c\beta\, s\beta \\ -m_{12}^2-M_Z^2\, c\beta\, s\beta & m_2^2+\mu^2+M_Z^2\left(\frac{1}{2}-c2\beta\right) \end{pmatrix}, \\
M_{g1g2} &= \begin{pmatrix} m_1^2+\mu^2+\frac{1}{2}M_Z^2 c2\beta & -m_{12}^2 \\ -m_{12}^2 & m_2^2+\mu^2-\frac{1}{2}M_Z^2 c2\beta \end{pmatrix}, \\
M_{\phi_1^-\phi_2^+} &= \begin{pmatrix} m_1^2+\mu^2+\frac{1}{2}M_Z^2\left(c^2\beta+c2\theta_W\, s^2\beta\right) & -m_{12}^2-M_W^2 c\beta\, s\beta \\ -m_{12}^2-M_W^2 c\beta\, s\beta & m_2^2+\mu^2+\frac{1}{2}M_Z^2\left(c^2\beta\, c2\theta_W+s^2\beta\right), \end{pmatrix}
\end{aligned}$$

with $c\beta = \cos\beta$ and $s\beta = \sin\beta$ one obtains (2.30) for the mass eigenstates with the Higgs masses at tree-level

$$\begin{aligned} m^2_{H,h} &= \frac{1}{2}\left[M_A^2 + M_Z^2 \pm \sqrt{\left(M_A^2 + M_Z^2\right)^2 - 4M_Z^2 M_A^2 \cos^2 2\beta}\right] \\ m^2_{H^\pm} &= M_A^2 + M_W^2. \end{aligned} \tag{4.24}$$

Relations and constraints resulting from (4.24),

$$m_h < M_Z, \quad m_H > M_A, \quad m_{H^\pm} > M_A, M_W, \quad m_h^2 + m_H^2 = M_A^2 + M_Z^2,$$

are just valid at lowest order of perturbation theory. The light neutral Higgs corrections have been calculated at one loop [91] and at two-loop [92].

4.3.1.3 Chargino and Neutralino Masses

After the breakdown of $SU(2)_L \times U(1)_Y$ the states with the same electric charge, color and spin mix. Hence, gauginos and higgsinos cannot be physical particles with definite mass. In the non-colored charged sector there are two candidate pairs, the Winos $\tilde{W}^\pm$ and the charged Higgsinos $\tilde{H}_1^+$ and $\tilde{H}_2^+$ with

$$\tilde{W}^\pm = \begin{pmatrix} -i\tilde{\lambda}_W^\pm \\ \overline{i\tilde{\lambda}_W^\pm} \end{pmatrix}, \qquad \tilde{H}_1^+ = \begin{pmatrix} \tilde{H}_2^1 \\ \overline{\tilde{H}_1^2} \end{pmatrix} \quad \text{and} \quad \tilde{H}_2^+ = \begin{pmatrix} \tilde{H}_1^2 \\ \overline{\tilde{H}_2^1} \end{pmatrix} \tag{4.25}$$

Analogously to the W boson, we have the relation

$$\tilde{\lambda}_W^\pm = \frac{1}{\sqrt{2}}\left(\tilde{\lambda}_W^1 \mp i\tilde{\lambda}_W^2\right). \tag{4.26}$$

The four two-component Weyl spinors combine to two four-component Dirac fermions $\tilde{\chi}_1^+, \tilde{\chi}_2^+$ called charginos. The charginos are no Majorana particles, hence their mass matrix is not symmetric,

$$M_{\tilde{\chi}^+} = \begin{pmatrix} M_2 & \sqrt{2}M_W \sin\beta \\ \sqrt{2}M_W \cos\beta & \mu \end{pmatrix}. \tag{4.27}$$

(4.27) is diagonalized by two unitary matrices, U and V, which are chosen such, that $m_{\tilde{\chi}_{1,2}^+}$ are both positive and $m_{\tilde{\chi}_1^+} \leq m_{\tilde{\chi}_2^+}$, which gives the mass eigenstates

$$\tilde{\chi}_i^+ = \begin{pmatrix} V\begin{pmatrix} -i\tilde{\lambda}_W^+ \\ \tilde{H}_2^1 \end{pmatrix} \\ U\begin{pmatrix} -i\tilde{\lambda}_W^- \\ \tilde{H}_1^2 \end{pmatrix} \end{pmatrix}, \qquad i = 1, 2. \tag{4.28}$$

Not only the charged gauginos and higgsinos mix with each other. Also the neutral ones, the two neutral Higgsinos $\tilde{H}_1^0$ and $\tilde{H}_2^0$, the Zino $\tilde{Z}$ and the Photino $\tilde{A}$,

$$\tilde{H}_1^0 = \begin{pmatrix} \tilde{H}_1^1 \\ \overline{\tilde{H}_1^1} \end{pmatrix}, \quad \tilde{H}_2^0 = \begin{pmatrix} \tilde{H}_2^2 \\ \overline{\tilde{H}_2^2} \end{pmatrix}, \quad \tilde{Z} = \begin{pmatrix} -i\tilde{\lambda}_Z \\ \overline{i\tilde{\lambda}_Z} \end{pmatrix}, \quad \tilde{A} = \begin{pmatrix} -i\tilde{\lambda}_A \\ \overline{i\tilde{\lambda}_A} \end{pmatrix}, \tag{4.29}$$

combine to mass eigenstates, called neutralinos. Comparable to the SM the latter two are obtained by rotating $\tilde{\lambda}_W^3$ and $\tilde{\lambda}_B$ by the EW mixing angle,

$$\tilde{\lambda}_Z = \tilde{\lambda}_W^3 \cos\theta_W - \tilde{\lambda}_B \sin\theta_W, \qquad \tilde{\lambda}_A = \tilde{\lambda}_W^3 \sin\theta_W + \tilde{\lambda}_B \cos\theta_W. \tag{4.30}$$

The neutralinos are four-component Majorana fermions, whose mass matrix is diagonalized by a unitary matrix N

$$N^* M_{\chi^0} N^\dagger = M_{\chi^0,\text{diag}}, \tag{4.31}$$

with

$$M_{\tilde{\chi}^0} = \begin{pmatrix} M_1 & 0 & -M_Z \cos\beta \sin\theta_W & M_Z \sin\beta \sin\theta_W \\ 0 & M_2 & M_Z c_\beta c_W & M_Z \sin\beta \cos\theta_W \\ -M_Z \cos\beta \sin\theta_W & M_Z \cos\beta \cos\theta_W & 0 & -\mu \\ -M_Z \sin\beta \sin\theta_W & -M_Z \sin\beta \cos\theta_W & -\mu & 0 \end{pmatrix}. \tag{4.32}$$

The neutralino mass eigenstates are given by:

$$\begin{pmatrix} \tilde{\chi}_1^0 \\ \tilde{\chi}_2^0 \\ \tilde{\chi}_3^0 \\ \tilde{\chi}_4^0 \end{pmatrix} = N \begin{pmatrix} -i\tilde{\lambda}_B \\ -i\tilde{\lambda}_W^3 \\ \tilde{H}_1^1 \\ \tilde{H}_2^2 \end{pmatrix}.$$

As the superpartners of the gluons, the gluinos, are the only fermions which possess exclusively strong interactions. They do not mix with other particles. The eight gluinos are Majorana particles with mass $m_{\tilde{g}} = |M_3|$ and have the following form

$$\tilde{g}^a = \begin{pmatrix} -i\tilde{\lambda}_G^a \\ i\tilde{\lambda}_G^a \end{pmatrix}, \qquad a = 1, ..., 8 \quad .$$

4.3.1.4 Squarks and Sleptons

Within the SM, the only source of flavor violation arises through the rotation of the up-type (down-type) fermion interaction eigenstates $f'_{L,R}$ to the basis of physical mass eigenstates $f_{L,R}$, such that

$$f_{L,R} = V_{L,R}^f f'_{L,R}. \tag{4.33}$$

These unitary matrices $V_{L,R}^f$ diagonalize the quark Yukawa matrices. As in the SM, the CKM matrix is $V = V_L^u V_L^{d\dagger}$. In the super-CKM basis [93], as a first step, the squarks and sleptons are rotated 'parallel' to their fermionic superpartners, which means that the squark interaction eigenstates undergo the same rotations at high energy scale as their quark counterparts. Thus, their charged-current interactions are also proportional to the SM CKM-matrix. These field

redefinitions enter the soft-breaking Lagrangian (4.21). The bi-unitary matrices can be absorbed into new couplings:

$$A^q = V^q \bar{A}^q U^{q\dagger}, \quad m^2_{\tilde{U}_R} = U^u m^2_{\tilde{U}} U^{u\dagger}, \quad m^2_{\tilde{D}_R} = U^d m^2_{\tilde{D}} U^{d\dagger}, \tag{4.34}$$

$$m^2_{\tilde{U}_L} = V^u m^2_{\tilde{Q}} V^{u\dagger}, \qquad m^2_{\tilde{D}_L} = V^d m^2_{\tilde{Q}} V^{d\dagger}. \tag{4.35}$$

The sfermion mass spectrum is obtained by diagonalizing the 6×6 sfermion mass matrices, which receive contributions from the D-terms (gauge interactions), the F-terms (superpotential), the M- and A-terms (soft breaking sector), using unitary mixing matrices $Z_{\tilde{f}}$:

$$Z_{\tilde{f}} M \tilde{f} Z^\dagger_{\tilde{f}} = \text{diag}\left(m^2_{\tilde{f}_{1i}}, m^2_{\tilde{f}_{2i}}\right). \tag{4.36}$$

The entries in the mass matrices which determine the mixing among two left-handed (LL), two right-handed (RR) or left- and right-handed sfermions (LR) can be summarized by

$$\begin{aligned} M_{\tilde{f}LLij} &= m^2_{\tilde{f}_L ij} + \left(m^2_{f_i} + \left(T_3^f - Q_f \sin^2\theta_W\right) M_Z^2 \cos 2\beta\right)\delta_{ij}, \\ M_{\tilde{f}RRij} &= m^2_{\tilde{f}_R ij} + \left(m^2_{f_i} + Q_f M_Z \sin^2\theta_W \cos 2\beta\right)\delta_{ij}, \\ M_{\tilde{f}LRij} &= \left\langle H_f^0 \right\rangle A^f_{ij} - m_{f_i}\mu^* \delta_{ij} \begin{cases} \cot\beta & \text{for up-like sfermions} \\ \tan\beta & \text{for down-like sfermions} \end{cases}. \end{aligned} \tag{4.37}$$

Q_f is the fraction of the electromagnetic charge of the sfermion, T_3^f is the third component of weak isospin and $\left\langle H_f^0 \right\rangle$ denotes the VEV for the appropriate Higgs field. Following the quark notation, doublet squarks are labeled as L, as opposed to $SU(2)$ singlets, which are marked as R. Squark mass matrices are given in the basis defined by diagonal quark Yukawas (super-CKM basis). At this point we recall, that the matrices of the M-term contributions, $m_{\tilde{u}_L}$ and $m_{\tilde{d}_L}$, cannot be specified independently. $SU(2)_L$ gauge invariance implies that

$$m_{\tilde{d}_L} = V^\dagger m_{\tilde{u}_L} V. \tag{4.38}$$

The sfermion mass eigenstates are given for the up squarks, down squarks and selectrons respectively

$$Z_u \begin{pmatrix} \tilde{u}_L \\ \tilde{c}_L \\ \tilde{t}_L \\ \tilde{u}_R \\ \tilde{c}_R \\ \tilde{t}_R \end{pmatrix} = \begin{pmatrix} \tilde{u}_1 \\ \tilde{c}_1 \\ \tilde{t}_1 \\ \tilde{u}_2 \\ \tilde{c}_2 \\ \tilde{t}_2 \end{pmatrix}, \quad Z_d \begin{pmatrix} \tilde{d}_L \\ \tilde{s}_L \\ \tilde{b}_L \\ \tilde{d}_R \\ \tilde{s}_R \\ \tilde{b}_R \end{pmatrix} = \begin{pmatrix} \tilde{d}_1 \\ \tilde{s}_1 \\ \tilde{b}_1 \\ \tilde{d}_2 \\ \tilde{s}_2 \\ \tilde{b}_2 \end{pmatrix}, \quad Z_e \begin{pmatrix} \tilde{e}_L \\ \tilde{\mu}_L \\ \tilde{\tau}_L \\ \tilde{e}_R \\ \tilde{\mu}_R \\ \tilde{\tau}_R \end{pmatrix} = \begin{pmatrix} \tilde{e}_1 \\ \tilde{\mu}_1 \\ \tilde{\tau}_1 \\ \tilde{e}_2 \\ \tilde{\mu}_2 \\ \tilde{\tau}_2 \end{pmatrix}. \tag{4.39}$$

In general all entries of the 6×6 mass matrices can be different from zero. But often the assumption of minimal flavor violation (Sec.4.3.2) is imposed which can simplify the pattern of the matrices tremendously.

In the sneutrino sector only left-handed fields exist. Therefore interaction and mass eigenstates are identical with the mass eigenvalues

$$m^2_{\tilde{\nu}_I} = \frac{1}{2} m_Z^2 \cos 2\beta + m^2_{\tilde{\nu}_L}. \tag{4.40}$$

4.3.2 Minimal flavor violation and mass insertion approximation

After supersymmetry breaking using soft terms, the MSSM in its most general form, allowing all phases, has up to 124 free parameters. This is a large number for phenomenological predictions. Many of the free parameters in the SUSY-breaking sector lead to large contributions to flavor-changing neutral currents (FCNCs), which might violate the experimental constraints [94].
As the experimental results from flavor physics are in good agreement with theoretical predictions of the SM, where flavor violation just occurs due to the Yukawa couplings [95, 96], very often the assumption of minimal flavor violation is imposed on the MSSM. A commonly accepted definition of minimal flavor violation was just recently established, stemming from an effective field theory approach [97]. We adopt this definition for our analysis.
In the absence of Yukawa couplings the largest group of unitary field transformations that commutes with the gauge group of the MSSM is $U\left(3\right)^5$, which can be decomposed as

$$G_F \equiv \left[SU\left(3\right) \otimes U\left(1\right)\right]^5 = \bigotimes_{F=Q,U,D,L,E} \left[SU\left(3\right) \otimes U\left(1\right)\right]_F . \tag{4.41}$$

The Yukawa interactions, derived from the superpotential (4.11), break the flavor group G_F, but the flavor symmetry can be recovered by treating the $y_{u,d,e}$ in (4.11) as spurions[2] and requiring them to have indices transforming under $\left[SU\left(3\right)\right]^5$ as

$$\left[\hat{y}_u\right]_{\bar{3}_Q 3_U} , \qquad \left[\hat{y}_d\right]_{\bar{3}_Q 3_D} , \qquad \left[\hat{y}_e\right]_{\bar{3}_L 3_E} . \tag{4.42}$$

Using the flavor group G_F, the fermion superfields can be rotated in such a way, that the spurion fields obtain a pattern proportional to a diagonal matrix y'_i:

$$\hat{y}_u = V^T y'_u, \qquad \hat{y}_d = y'_d, \qquad \hat{y}_e = y'_e. \tag{4.43}$$

For low $\tan\beta$, all FCNC effects can be described by one single off-diagonal structure [97]

$$\left(\lambda_{FC}\right)_{ij} = \begin{cases} \left(\hat{y}_u \hat{y}_u^\dagger\right)_{ij} \approx \lambda_t^2 V_{3i} V_{3j}^* & i \neq j, \\ 0 & i = j, \end{cases} \tag{4.44}$$

with $\lambda_t = \left(y_u\right)_{33}$. Sub–leading effects on the r.h.s. of (4.44) are suppressed by powers of m_c/m_t [98]. In minimal-flavor violation all higher-dimensional operators are invariant under CP and under the flavor group G_F, i.e. flavor violation is completely determined by the structure of the Yukawa couplings. This constraints the higher-dimensional operators which can be constructed from the fields of the MSSM and the spurions $\hat{y}$ in a non-trivial way. All operators allowed by MFV can be expanded in powers of λ_{FC}. In (4.44) we neglect down-quark contributions, which is an acceptable approximation if both μ and $\tan\beta$ are small. According to this assumption in the MFV MSSM, the soft-breaking terms have to be related to the Yukawa couplings in a way which preserves the flavor group G_F formally.

[2] For the definition of the spurion fields we shift the notation in (4.11) by $y_i \to \hat{y}_i$

The hermitian 6×6 squark mass matrices from Section 4.3.1.4 for up and down-type squarks are composed of the left and right-handed blocks $M^2_{q\,AB}$. Each block is a 3×3 matrix in generation space:

$$\mathcal{M}^2_q = \begin{pmatrix} M^2_{q\,LL} & M^2_{q\,LR} \\ M^{2\,\dagger}_{q\,LR} & M^2_{q\,RR} \end{pmatrix} \qquad (q = u, d; A, B = L, R)\ . \tag{4.45}$$

The explicit expressions for the $M^2_{q\,AB}$ are given in (4.38). To derive the MFV relations for the soft-breaking terms, they can be treated as spurion fields, transforming under G_F as follows:

$$\left[m^2_{\tilde{d}_L}\right]_{3_Q\bar{3}_Q}\ , \quad \left[m^2_{\tilde{u}_R}\right]_{\bar{3}_U 3_U}\ , \quad \left[m^2_{\tilde{d}_R}\right]_{\bar{3}_D 3_D}\ , \quad \left[A^d\right]_{\bar{3}_Q 3_U}\ , \quad \left[A^u\right]_{\bar{3}_Q 3_D}\ . \tag{4.46}$$

With (4.42) we obtain the following conditions [97]:

$$\begin{aligned}
m^2_{\tilde{d}_L} &= m_0^2 \left(a_1 \mathbb{1} + b_1 \hat{y}_u \hat{y}_u^\dagger + b_2 \hat{y}_d \hat{y}_d^\dagger \hat{y}_u \hat{y}_u^\dagger + b_3 \hat{y}_d \hat{y}_d^\dagger \hat{y}_u \hat{y}_u^\dagger + b_4 \hat{y}_u \hat{y}_u^\dagger \hat{y}_d \hat{y}_d^\dagger\right), \\
m^2_{u_R} &= m'^2_{0u} \left(a_2 \mathbb{1} + b_5 \hat{y}_u^\dagger \hat{y}_u\right), \\
m^2_{d_R} &= m'^2_{0d} \left(a_3 \mathbb{1} + b_6 \hat{y}_d^\dagger \hat{y}_d\right), \\
A^u &= \hat{y}_u A_0 \left(a_4 \mathbb{1} + b_7 \hat{y}_d \hat{y}_d^\dagger\right), \\
A^d &= \hat{y}_d A_0 \left(a_5 \mathbb{1} + b_8 \hat{y}_u \hat{y}_u^\dagger\right).
\end{aligned}$$

The a_i and b_i are real. Hence, to a very good approximation, whereas we neglect effects from renormalization group running, the SUSY-breaking mass parameters are the generation-universal SUSY-breaking scalar masses m_0^2, m'^2_{0q} and the tri-linear term A_0.

To discuss the sources of new-physics flavor violation, it is useful to define the dimensionless mass insertions [99, 100]

$$\delta^q_{AB,ij} \equiv \frac{M^2_{q\,AB\,ij}}{\tilde{m}^2}. \tag{4.47}$$

The denominator is the geometric mean $\tilde{m}^2 = m_{A\,ii} m_{B\,jj}$ of the squared scalar masses of $\tilde{q}_{Ai}$ and $\tilde{q}_{Bj}$. The off-diagonal entries of δ^q_{AB} are significant only in non-MFV models and can be complex, inducing CP violation. We confine ourselves to real δ^q_{AB} and use the intuitive mass-insertion approximation only for illustration and order-of-magnitude estimates [101].

Chapter 5

Charged Higgs in minimal flavor violation and beyond

The intention of building the LHC at CERN is either to verify the Standard Model as it is proposed or to find new physics. A charged Higgs particle is a signal for physics beyond the Standard Model, at least for an extended Higgs sector. In several models of new physics an extended Higgs sector is proposed, e.g. 2HDM, MSSM, triplet-Higgs models. At a first glance the detection of a heavy charged scalar might look as an easy task but in the 2HDM or MSSM it is not, due to the fact that there is no $H^{\pm}W^{\pm}Z$ Vertex at tree level (Sec. 2.2). In the SM and MSSM the detectability of a neutral Higgs profits a lot from its tree-level Higgs-Gauge-Boson couplings (Sec.2.1) where in the MSSM and 2HDM the production of a single charged Higgs and its decay is only possible via Yukawa couplings. In the most prominent two-Higgs-doublet model type II (Sec. 2.2) there is no doubt that we will see the light neutral scalar Higgs in the usual Standard Model search channels [28]. Unfortunately, to positively identify an extended Higgs sector it might not be sufficient to simply study this light Higgs [102]. An additional heavy charged Higgs is the most distinct signature of a second Higgs doublet. In contrast to, for example, a heavy neutral scalar, it does not get faked by additional scalars that are not linked to the Higgs sector.

Over the years, many charged-Higgs search strategies at the LHC have been proposed and studied. For a pure MSSM-type two-Higgs-doublet model the entire leading-order parameter space is described by the charged-Higgs mass m_{H^+} vs. $\tan\beta$ plane, where $\tan\beta$ is the ratio of the two vacuum expectation values. Almost all of the LHC search strategies make use of a particularity in the type-II two-Higgs-doublet model: the heavy-quark Yukawa couplings to the heavy Higgs states are governed by $y_b \tan\beta$ and by $y_t/\tan\beta$. The most promising strategy for finding a charged Higgs at the LHC will therefore include couplings to incoming or outgoing bottom quarks.
The most promising charged-Higgs production channel is in association with a top quark [103, 104, 105, 106]. The rate can be computed in a 5-flavor or in a 4-flavor scheme, i.e. with or without using bottom parton densities [107]. Because of the complexity of the top-associated final state, a charged-Higgs decay to hadronic $\tau^+\nu$ [108, 109] is easier to extract from the backgrounds than the (likely undetectable) decay to $t\bar{b}$ [110, 111].

Unfortunately, all strategies described above are bound to fail for small $\tan\beta$. The bottom-induced search channels only cover $\tan\beta \gtrsim 20$, leaving a hole $\tan\beta = 2\cdots 20$ in the parameter space. For example in the MSSM in this region we might only see a light SM-like Higgs, unless we are lucky enough to produce light Higgses in pairs coming from a resonant heavy neutral Higgs [112]. There are several ideas how to cover this region searching for a charged Higgs, e.g. the production in association with a W [113] or pair production. The latter occurs at tree-level with incoming bottom quarks $b\bar{b} \to H^+H^-$, it can also be loop mediated $gg \to H^+H^-$, or for low and intermediate $\tan\beta$ we can search for $q\bar{q} \to H^+H^-$ [114]. Unfortunately, none of these strategies are too promising, because the rates without $\tan\beta$ enhancement are small.

Looking beyond bottom-mediated production channels reveals an opportunity linked to charged-Higgs searches: while it is well known how to absorb the leading unflavored supersymmetric loops into an effective bottom Yukawa coupling [115, 106], the production via light-flavor quarks can be heavily affected by the flavor structure of the model embedding the two Higgs doublets. As discussed in Section 4.3.2 in an MFV model there are no other sources of flavor violation other than the Yukawa ineractions. For the case of the MSSM with unbroken R parity, the MFV condition is automatically satisfied for supersymmetric gauge couplings (D terms) and for scalar couplings in the superpotential (F terms). However, general soft SUSY breaking introduces new sources of flavor violation.
According to Section 4.3.2 MFV implies that (i) all soft scalar squark masses need to be diagonal in flavor space and (ii) all tri-scalar A-terms describing the squark-squark-Higgs couplings have to be proportional to the Yukawas. This set of MFV assumptions automatically avoids a large fraction of experimental constraints.

Such a minimal-flavor-violation assumption is not necessary. While some flavor-non-diagonal MSSM couplings are tightly constrained, others can be of order one [99, 100]. In general, constraints on flavor-changing neutral currents (FCNC) in K and B physics with their external down-type quarks are more severe when we consider flavor violation among down squarks. In K and B physics down-squark effects can be mediated by strongly interacting gluino loops, while up-squark effects are mediated by the weak interaction. Currently, we only have upper bounds on charm or top FCNCs with the exception of the recent $D^0\bar{D}^0$-mixing measurements, which mostly constrains mixing between first and second-generation squarks [116]. Stringent limits on the flavor structure including the third generation arise from $b \to s$ and $b \to d$ transitions in B meson mixing and decays. Particularly constraining are the radiative decays $B \to X_s\gamma$ and $B \to \rho\gamma$, the semileptonic decays $B \to X_s\ell^+\ell^-$ and $B \to \pi\ell^+\ell^-$, and the $B_{d,s}-\overline{B}_{d,s}$ mass differences [117, 118, 119, 120, 121, 122, 123, 124, 125, 126].
The analysis proceeds as follows: The multi-dimensional parameter space of the NMFV MSSM is very large. At first, in Section 5.1, we discuss the general constraints on this model. In Section 5.2 we study the single-charged-Higgs production $q\bar{q}' \to H^\pm$ in the MSSM, assuming MFV and allowing for general flavor violation. In Section 5.3 we calculate charged-Higgs production rates in association with a hard jet, within and beyond MFV. A brief background study for the LHC environment is included.

5.1 Constraints on parameter space

To calculate rare B decays the effective Hamiltonian theory combined with renormalization group techniques [127] became a standard tool over the last 25 years [128], accessible if the external momenta p are much smaller than the masses of the internal particles m_i ($m_i^2 \gg p^2$). Particles for which this is true can be 'integrated out', which means that the heavy particles are removed from the theory as dynamical degrees of freedom. Hence an effective low energy theory can be constructed from a full theory using the Operator Product Expansion (OPE) which factorizes QCD and weak effects. In general the transition amplitudes generated by the effective Hamiltonian H_{eff} have the following structure:

$$\langle f \ |H_{eff}| \ i\rangle = \frac{G_F}{\sqrt{2}} \sum_j V_{CKM}^j C_j(\mu) \langle f \ |O_j(\mu)| \ i\rangle . \tag{5.1}$$

G_F is the Fermi constant describing the point-like interaction after 'integrating out' the W boson at the renormalization scale μ. O_j are the local operators which govern the decay. The Cabibbo-Kobayashi-Maskawa (CKM) factors V_{CKM}^j (App. A) and the Wilson Coefficients C_j [129] describe the strength with which a given operator enters the Hamiltonian. The Wilson coefficients are perturbative quantities, while O_j are local operators which govern the decay in question, their matrix elements are non-perturbative elements. Hence, the physics beyond Standard Model affects exceptionally the Wilson coefficients and does not alter physics at the soft scale. A promising way to detect effects of new physics on B decays is to look for deviations of flavor-changing neutral-current processes from their Standard Model predictions. FCNC processes only occur at the loop-level in the SM and MSSM. Hence, it provides a sensitive probe of the flavor sector of these models. The vast number of past and ongoing flavor physics measurements has serious impact on flavor physics at the LHC. From the previous section and the rough estimate in (5.53) it is obvious that without any constraints on squark mixing the charged-Higgs production rates could be arbitrarily large. However, flavor physics strongly constrains the structure of the general squark matrices in (4.45). The important parameters are the LR entries in the A-terms $A^{u,d}$ and the corresponding (LL, RR)-type mass matrices $m^2_{\tilde{U}_L,\tilde{D}_L,\tilde{U}_R,\tilde{D}_R}$.

5.1.1 B-$\bar{B}$ mixing

Weak interactions do not conserve quark flavors and can mix B^0 with $\bar{B}^0$ states, for example by box diagrams like Figure 5.1.
Therefore B^0 and $\bar{B}^0$ has to be considered as a coupled system with the possibility of a transition between them. This phenomenon of B^0-$\bar{B}^0$ oscillation (known as B^0-$\bar{B}^0$ mixing) occurs for other flavors, too[1]. Here, as we are interested in flavor violating parameters between thested in flavor violating parameters between the first/second and third generation the process of interest is B_q^0-$\bar{B}_q^0$ mixing [2].

[1] Such oscillations were first found in the $K^0 - \bar{K}^0$ system [131]. From the calculation of the $K_L - K_S$ mass difference even the charm quark mass could be estimated before its discovery [132].

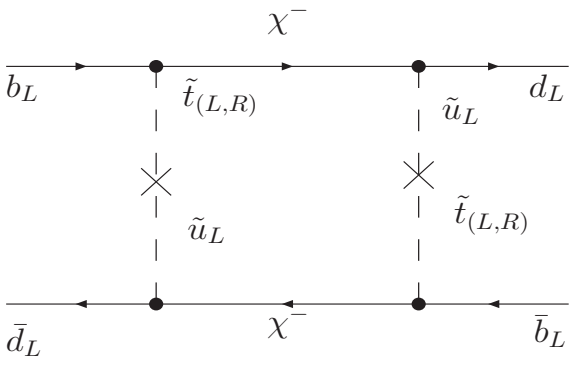

Figure 5.1: Chargino contribution to Operator O_1 in B-$\bar{B}$ mixing.

$B^0 = \left(\bar{b}q\right)$ and $\bar{B}^0 = (b\bar{q})$ are flavor eigenstates. The transition between the two flavor eigenstates are caused by the off-diagonal terms in the effective Hamiltonian (5.6):

$$2m_B \left|M_{12}\right| = \left|\left\langle \bar{B}^0 \left| H_{eff}^{\Delta B=2} \right| B^0 \right\rangle\right|. \tag{5.2}$$

The factor $2m_B$ reflects the normalization of external states.
In supersymmetric theories the effective Hamiltonian for $\Delta B = 2$ transitions can be generated, in addition to the W box diagrams of the SM, through box diagrams mediated by charged Higgs, neutralino, photino, gluino and chargino exchanges [126]. While the Higgs contributions can be neglected because of the smallness of the quark masses, the neutralino and photino exchange diagrams are also suppressed compared to the gluino and chargino ones, due to their electroweak neutral couplings to fermions and sfermions. Thus the dominant contributions for the off-diagonal entry can be expanded by

$$M_{12} = M_{12}^{SM} + M_{12}^{\tilde{g}} + M_{12}^{\tilde{\chi}^+} + M_{12}^{H^+} \tag{5.3}$$

where M_{12}^{SM}, $M_{12}^{\tilde{g}}$, $M_{12}^{\tilde{\chi}^+}$ and $M_{12}^{H^+}$ indicate the SM, gluino, chargino and charged Higgs contributions respectively.
The SM contributions are known at NLO accuracy in QCD and are given by

$$M_{12}^{SM} = \frac{G_F^2}{12\pi^2}\eta_B \hat{B}_{B_q} f_{B_q}^2 m_B M_W^2 \left(V_{tq}V_{tb}^*\right)^2 S_0\left(x_t\right), \tag{5.4}$$

where f_{B_q} is the B-meson decay constant, $\hat{B}_{B_q}$ is a renormalization-group-invariant parameter, $\eta = 0.55 \pm 0.01$ and

$$S\left(x_t\right) = \frac{4x_t - 11x_t^2 + x_t^3}{4\left(1-x_t\right)^2} - \frac{3x_t^3 \ln x_t}{2\left(1-x_t\right)^3}, \tag{5.5}$$

where $x_t = m_t^2/M_W^2$.

[2] $B_d^0 - \bar{B}_d^0$ gave the first indication of a large top quark mass [133].

The most general effective Hamiltonian for $\Delta B = 2$ processes, induced by gluino, charged Higgs boson and chargino exchanges through $\Delta B = 2$ box diagrams, can be expressed as

$$H_{eff}^{\Delta B=2} = \sum_{i=1}^{5} C_i(\mu) Q_i(\mu) + \sum_{i=1}^{3} \widetilde{C}_i(\mu) \widetilde{Q}_i(\mu) + h.c., \tag{5.6}$$

where $C_i(\mu), \widetilde{C}_i(\mu)$ and $Q_i(\mu), \widetilde{Q}_i(\mu)$ are the Wilson coefficients and operators respectively renormalized at the scale μ. The effective operators are defined in the following way:

$$\begin{array}{lll} Q_1 = \bar{q}_L^{\alpha}\gamma_{\mu} b_L^{\alpha} \bar{q}_L^{\beta}\gamma_{\mu} b_L^{\beta}, & Q_2 = \bar{q}_R^{\alpha} b_L^{\alpha}\ \bar{q}_R^{\beta} b_L^{\beta}, & Q_3 = \bar{q}_R^{\alpha} b_L^{\beta}\ \bar{q}_R^{\beta} b_L^{\alpha}, \\ Q_4 = \bar{q}_R^{\alpha} b_L^{\alpha}\ \bar{q}_L^{\beta} b_R^{\beta}, & Q_5 = \bar{q}_R^{\alpha} b_L^{\beta}\ \bar{q}_L^{\beta} b_R^{\alpha}. & \end{array} \tag{5.7}$$

The operators $\widetilde{Q}_{1,2,3}$ are obtained from $Q_{1,2,3}$ by exchanging $L \leftrightarrow R$. In this work we are predominantly interested in mixing in the up-squark sector, which is mediated by charginos or charged Higgs bosons. Due to the smallness of the Yukawa couplings of the light quarks we can safely neglect the contributions to all operators except from $Q_1, \widetilde{Q}_2$ and $\widetilde{Q}_3$. We assume, that mixing in the down-squark sector, giving rise to gluonic contributions, is just induces due to $SU(2)$ invariance (Sec.5.1.4). In good approximation, they are limited to the LL sector and thus to contributions to the Operator Q_1. Analytical expressions for the Wilson Coefficients in full diagonalization can be found in [126, 125].

The Wilson coefficients at the scale M_S, $C_i(M_S)$, are connected to the low energy ones $C_i(\mu)$ (where $\mu \simeq O(m_b)$) via the renormalization group equations by

$$C_r(\mu) = \sum_i \sum_s \left(b_i^{(r,s)} + \eta c_i^{(r,s)} \right) \eta^{a_i} C_s(M_S) \tag{5.8}$$

where $\eta = \alpha_s(M_S)/\alpha_s(\mu)$. Numerical values for $b_i^{(r,s)}, c_i^{(r,s)}$ and a_i are given in [134].
To reduce the numerical uncertainties of the hadronic quantities, i.e. $\sqrt{f_{B_q}^2 B_{B_q}}$, it is possible to consider the impact of 'new physics' compared to the Standard Model.

For $B_d^0 - \overline{B}_d^0$ mixing at 90 % C.L. the 'new physics' contributions can be estimated [123]:

$$0.46 < \frac{\Delta m_d}{\Delta m_d^{\mathrm{SM}}} < 1.54 \tag{5.9}$$

The same can be done for $B_s^0 - \overline{B}_s^0$ mixing . Using CDF data only [124] the latter implies

$$0.56 < \frac{\Delta m_s}{\Delta m_s^{\mathrm{SM}}} < 1.44 \tag{5.10}$$

at 90 % C.L.. In both cases the error is dominated by the theory uncertainty.

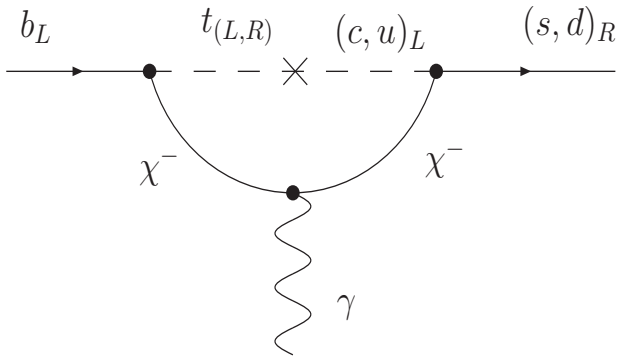

Figure 5.2: Chargino contribution to Operator O_7.

5.1.2 $B \to X_s\gamma$ and $B \to \rho^0\gamma$

The rare inclusive decay process $B \to X_s\gamma$ is one of the most important in B-physics since its experimental observation sets stringent constraints on the parameter space of various extensions of the SM [136][135]. At lowest order this can be described by $b \to s\gamma$. The effective Hamiltonian for this decay is usually expressed as [137]

$$H_{eff} = -\frac{4G_F}{\sqrt{2}} V_{tb}V_{ts}^* \left[\sum_{i=1}^{8} C_i(\mu)\, O_i(\mu) + \sum_{i=1}^{8} \widetilde{C}_i(\mu)\, \widetilde{O}_i(\mu)\right], \tag{5.11}$$

where V_{tb} and V_{ts} are the according elements of the CKM matrix. The operators $\widetilde{O}_i$ are obtained from the operators O_i by interchanging $L \leftrightarrow R$.

$$\begin{aligned}
O_1 &= \left(\bar{s}_{L\alpha}\gamma_\mu b_{L\alpha}\right)\left(\bar{c}_{L\beta}\gamma^\mu c_{L\beta}\right), \\
O_2 &= \left(\bar{s}_{L\alpha}\gamma_\mu b_{L\beta}\right)\left(\bar{c}_{L\beta}\gamma^\mu c_{L\alpha}\right), \\
O_3 &= \left(\bar{s}_{L\alpha}\gamma_\mu b_{L\alpha}\right)\sum_{q=u,d,s,c,b}\left(\bar{q}_{L\beta}\gamma^\mu q_{L\beta}\right), \\
O_4 &= \left(\bar{s}_{L\alpha}\gamma_\mu b_{L\beta}\right)\sum_{q=u,d,s,c,b}\left(\bar{q}_{L\beta}\gamma^\mu q_{L\alpha}\right), \\
O_5 &= \left(\bar{s}_{L\alpha}\gamma_\mu b_{L\alpha}\right)\sum_{q=u,d,s,c,b}\left(\bar{q}_{R\beta}\gamma^\mu q_{R\beta}\right), \\
O_6 &= \left(\bar{s}_{L\alpha}\gamma_\mu b_{L\beta}\right)\sum_{q=u,d,s,c,b}\left(\bar{q}_{R\beta}\gamma^\mu q_{R\alpha}\right), \\
O_7 &= \frac{e}{16\pi^2} m_b \bar{s}_{L\alpha}\sigma_{\mu\nu} b_{R\alpha} F^{\mu\nu}, \\
O_8 &= \frac{g_s}{16\pi^2} m_b \bar{s}_{L\alpha}\sigma_{\mu\nu} T^a_{\alpha\beta} b_{R\beta} G^{\mu\nu}_a.
\end{aligned} \tag{5.12}$$

where $\sigma_{\mu\nu} = \frac{i}{2}\left[\gamma_\mu, \gamma_\nu\right]$ and α, β are $SU(3)$ color indices. $T^a, a = 1...8$ are the generators of QCD. Here $F^{\mu\nu}$ and $G^{a\mu\nu}$ denote the electromagnetic and chromomagnetic field strength tensor, respectively.

To an excellent approximation, the contributions of all operators except from $O_2, O_7, O_8, \widetilde{O}_7$ and $\widetilde{O}_8$ can be neglected [138]. In general, the prediction for the branching ratio $B \to X_s\gamma$ is obtained by normalizing the partial width to the semileptonic one, eliminating a large uncertainty, due to the b-quark mass, m_b^5. The leading order decay rate for the semileptonic process can be expressed by

$$\Gamma\left(B \to X_c e \bar{\nu}_e\right) = \frac{G_F^2 m_b^5}{192\pi^3} f\left(z\right) \left|V_{cb}\right|^2 \tag{5.13}$$

where $f\left(z\right) = 1 - 8z + 8z^3 - z^4 - 12z^2 \ln z$ is a phasespace factor depending on the mass ratio $z = \left(m_c/m_b\right)^2$, while the one for $B \to X_s\gamma$ is given by

$$\Gamma\left(B \to X_s\gamma\right) = \frac{m_b^5 G_F^2 \alpha}{32\pi^4} \left|V_{ts}^* V_{tb}\right|^2 K_{LO}. \tag{5.14}$$

For the ratio we obtain

$$R_{s\gamma} = \frac{\Gamma\left(B \to X_s\gamma\right)}{\Gamma\left(B \to X_c e \bar{\nu}\right)} = \frac{6\alpha}{\pi f\left(z\right)} \left|\frac{V_{ts}^* V_{tb}}{V_{cb}}\right|^2 K_{LO}, \tag{5.15}$$

where the quantity K_{LO} covers the contributions by the Wilson coefficients at the scale m_b. Using the theoretically calculable quantity $R_{s\gamma}$, the branching ratio is given by [139]

$$BR\left(B \to X_s\gamma\right) = R_{s\gamma} \times BR\left(B \to X_c e \bar{\nu}\right) \approx 0.106\, R_{s\gamma}. \tag{5.16}$$

The general structure of $K_{LO} = \left|C^{eff}\left(m_b\right)\right|^2$ is

$$K_{LO} = \sum_{\substack{i,j=7,8 \\ i \leq j}} \sum_{k=L,R} k_{ij} \,\mathrm{Re}\left(C_i^k\left(m_b\right) C_j^{k\,*}\left(m_b\right)\right) + \sum_{i=2,7,8} k_{2i} \,\mathrm{Re}\left(C_i^L\left(m_b\right) C_2 m_b\right) \tag{5.17}$$

where the Wilson coefficients in the NMFV MSSM are decomposed in the following way:

$$\begin{aligned}
C_7^L &= C_{7,SM}^L + C_{7,H^\pm}^L + C_{7,\chi^\pm}^L + C_{7,\chi^0}^L + C_{7,\widetilde{g}}^L \\
C_7^R &= C_{7,\chi^0}^R + C_{7,\widetilde{g}}^R \\
C_8^L &= C_{8,SM}^L + C_{8,H^\pm}^L + C_{8,\chi^\pm}^L + C_{8,\chi^0}^L + C_{8,\widetilde{g}}^L \\
C_8^R &= C_{8,\chi^0}^R + C_{8,\widetilde{g}}^R
\end{aligned} \tag{5.18}$$

Using the renormalization group equations the leading order coefficients at the scale m_b are [140]

$$\begin{aligned}
C_2\left(m_b\right) &= \frac{1}{2}\left(\eta^{-\frac{12}{23}} + \eta^{\frac{6}{23}}\right), \\
C_7^L\left(m_b\right) &= \eta^{\frac{16}{23}} C_7^L\left(M_W\right) + \frac{8}{3}\left(\eta^{\frac{14}{23}} - \eta^{\frac{16}{23}}\right) C_8^L\left(M_W\right) + \sum_{i=1}^{8} h_i \eta^{a_i}, \\
C_7^R\left(m_b\right) &= \eta^{\frac{16}{23}} C_7^R\left(M_W\right) + \frac{8}{3}\left(\eta^{\frac{14}{23}} - \eta^{\frac{16}{23}}\right) C_8^R\left(M_W\right), \\
C_8^L\left(m_b\right) &= \eta^{\frac{14}{23}} C_8^L\left(M_W\right) + \sum_{i=1}^{8} \bar{h}_i \eta^{a_i}, \\
C_8^R\left(m_b\right) &= \eta^{\frac{14}{23}} C_8^R\left(M_W\right),
\end{aligned} \tag{5.19}$$

where $\eta = \alpha_s\left(M_W\right)/\alpha_s\left(m_b\right)$, and

$$\begin{aligned} a_i &= \left(\frac{14}{23}, \frac{16}{23}, \frac{6}{23}, -\frac{12}{23}, 0.4086, -0.4230, -0.8994, 0.1456\right) \\ h_i &= \left(\frac{626126}{272272}, -\frac{56281}{51730}, -\frac{3}{7}, -\frac{1}{14}, -0.6494, -0.0380, -0.0186, -0.0057\right) \\ \bar{h}_i &= \left(\frac{313063}{363036}, 0, 0, 0, 0.9135, 0.0873, 0.0571, 0.0209\right). \end{aligned} \tag{5.20}$$

Finally, the k_{ij} have to be extracted to be able to obtain numerical results for $BR\left(B \to X_s\gamma\right)$. Analytic expressions for the k_{ij} can be found in [138]. These Wilson coefficients $C_{2,7,8}$ and $\widetilde{C}_{7,8}$ have been calculated to one loop order [118] and incorporated into the Feynhiggs library [141]. To include the constraints from $B \to X_s\gamma$ decays we demand at 90% C.L. [117]:

$$2.94 \cdot 10^{-4} < \mathrm{BR}(B \to X_s\gamma) < 4.14 \cdot 10^{-4}. \tag{5.21}$$

The inclusive decay $B \to X_d\gamma$, theoretically favored, is CKM-suppressed compared to $B \to X_s\gamma$ and hence suffers from a large background. Instead, the exclusive decay $B \to \rho^0\gamma$ has been measured recently and can, although theoretically involved, be used to find bounds on the squark mixing parameters, between the first and third generation.
The branching ration for $B \to \rho^0\gamma$ is obtained by just slightly changing the analysis from (5.11)-(5.20). Its decay rate in leading order is given by [142]

$$\Gamma\left(B \to \rho^0\gamma\right) = \frac{G_F^2\alpha}{32\pi^4}\left(1-r\right)^3\left|V_{td}^* V_{tb}\right|^2 m_B^3 m_b^2 \underbrace{\left|C^{eff}\left(\rho^0\gamma\right)\right|^2}_{K_{LO}} c_{\rho^0}^2 F_{\rho^0}^2, \tag{5.22}$$

where $r = m_{\rho^0}^2/m_B^2 \approx 0.021$, $c_{\rho^0} = 1/\sqrt{2}$, $F_{\rho^0} = 0.29$ and the quantity K_{LO}, the contribution from the square of the effective Wilson coefficients, has the same structure as in (5.14). The Wilson coefficients and their running due to the RGE are independent from the external particles. The first signal of $b \to d\gamma$ transitions has recently been seen by BaBar and Belle in $B \to (\rho, \omega)\gamma$ decays [119]. At 90% C.L. we use

$$0.63 \cdot 10^{-6} < \mathrm{BR}(B \to \rho^0\gamma) < 1.24 \cdot 10^{-6}. \tag{5.23}$$

5.1.3 $B \to X_s l^+ l^-$ and $B \to \pi l^+ l^-$

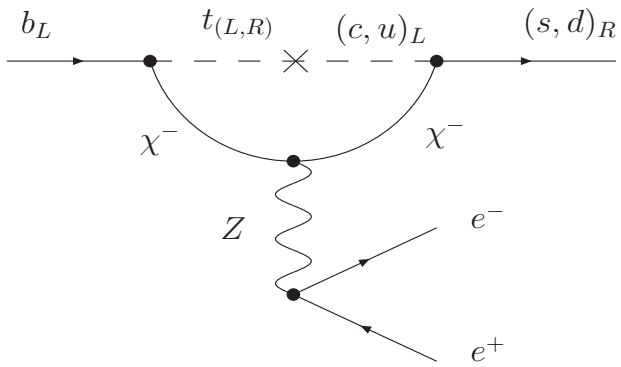

Figure 5.3: Chargino contributions to the Z-Penguin.

To describe the process $b \to s l^+ l^-$, it is necessary to extend the effective Hamiltonian which was used for $b \to s\gamma$, (5.11) by two operators:

$$\mathcal{H}_{eff}\left(b \to s l^+ l^-\right) = \mathcal{H}_{eff}\left(b \to s\gamma\right) - \frac{4G_F}{\sqrt{2}} V_{tb} V_{ts}^* \left[\sum_{i=9}^{10} C_i\left(\mu\right) O_i\left(\mu\right) + \sum_{i=9}^{10} \widetilde{C}_i\left(\mu\right) \widetilde{O}_i\left(\mu\right)\right]. \tag{5.24}$$

Here, to a good approximation, the Wilson Coefficients C_7^{eff}, $\widetilde{C}_7^{eff}$, C_9^{eff}, $\widetilde{C}_9^{eff}$, $\widetilde{C}_{10}$ and C_{10} enter the differential decay width, which are derived by the Wilson Coefficients at the scale M_W using the renormalization group equation [118]:

$$\begin{aligned}
C_7^{eff} &= C_7\left(M_W\right)\eta^{16/23} + \frac{8}{3} C_8\left(M_W\right)\left(\eta^{14/23} - \eta^{16/23}\right) + \sum_{i=1}^{8} h_i \eta^{a_i} \\
C_9^{eff} &= \left(\frac{\pi}{\alpha_s\left(M_W\right)} + \frac{\omega\left(\hat{s}\right)}{\eta}\right)\left(-0.1875 + \sum_{i=1}^{8} p_i \eta^{a_i+1}\right) \\
&\quad + \frac{Y\left(x_t\right) + Y^{SUSY}}{\sin^2\theta} - 4\left(Z\left(x_t\right) + Z^{SUSY}\right) \\
&\quad + \left(E\left(x_t\right) + E^{SUSY}\right)\left(0.1405 + \sum_{i=1}^{8} q_i \eta^{a_i+1}\right) \\
&\quad + 1.2468 + \sum_{i=1}^{8} \eta^{a_i}\left[r_i + s_i\eta + t_i h\left(\frac{m_c}{m_b}, \hat{s}\right) + u_i h\left(1, \hat{s}\right) + v_i h\left(0, \hat{s}\right)\right] \\
C_{10} &= -\frac{Y\left(x_t\right) + Y^{SUSY}}{\sin^2\theta_W}.
\end{aligned} \tag{5.25}$$

With $x_t = (m_t/m_W)^2$ and the magic numbers

$$\begin{aligned}
a_i &= (0.6087, 0.6957, 0.2609, -0.5217, 0.4086, -0.4230, -0.8994, 0.1456)\,, \\
h_i &= (2.2996, -1.0880, -0.4286, -0.0714, -0.6494, -0.0380, -0.0186, 0.0057)\,, \\
p_i &= (0, 0, -0.3941, 0.2424, 0.0433, 0.1384, 0.1648, -0.0073)\,, \\
q_i &= (0, 0, 0, 0, 0.0318, 0.0918, -0.2700, 0.0059)\,, \\
r_i &= (0, 0, 0.8331, -0.1219, -0.1642, 0.0793, -0.0451, -0.1638)\,, \\
s_i &= (0, 0, -0.2009, -0.3579, 0.0490, -0.3616, -0.3554, 0.0072)\,, \\
t_i &= (0, 0, 1.7143, -0.6667, 0.1658, -0.2407, -0.0717, 0.0990)\,, \\
u_i &= (0, 0, 0.2857, 0, -0, 2559, 0.0083, 0.0180, -0.0562)\,, \\
v_i &= (0, 0, 0.1429, 0.1667, -0.1731, -0.1120, -0.0178, -0.0067)\,.
\end{aligned} \tag{5.26}$$

The functions $h\,(z, \hat{s})$ and $\omega\,(\hat{s})$ which appear in (5.26) are given by

$$h\,(z,\hat{s}) = -\frac{8}{9}\log z + \frac{8}{27} + \frac{4}{9}x - \frac{2}{9}\,(2+x)\,\sqrt{|1-x|} \tag{5.27}$$

$$\begin{cases} \log\left|\frac{\sqrt{1-x}+1}{\sqrt{1-x}-1}\right| - i\pi & \text{for } x \equiv 4z^2/\hat{s} < 1 \\ 2\arctan\left(1/\sqrt{x-1}\right) & \text{for } x \equiv 4z^2/\hat{s} > 1 \end{cases} \tag{5.28}$$

$$\begin{aligned}
\omega\,(\hat{s}) = &-\frac{4}{3}\mathrm{Li}_2\,(\hat{s}) - \frac{2}{3}\log(\hat{s})\log(1-\hat{s}) - \frac{2}{9}\pi^2 - \frac{5+4\hat{s}}{3\,(1+2\hat{s})}\log(1-\hat{s}) \\
&-\frac{2\hat{s}\,(1+\hat{s})\,(1-2\hat{s})}{3\,(1-\hat{s})^2\,(1+2\hat{s})}\log(\hat{s}) + \frac{5+9\hat{s}-6\hat{s}^2}{6\,(1-\hat{s})\,(1+2\hat{s})}.
\end{aligned} \tag{5.29}$$

While E^{SUSY} can be safely neglected, the lengthy expressions for Z, Z^{SUSY}, E, Y and Y^{SUSY} can be found in [118]. The Wilson Coefficients $\widetilde{C}_7^{eff}$, $\widetilde{C}_9^{eff}$, $\widetilde{C}_{10}$ can be derived from (5.26) analogously, by changing the chirality structure.
The inclusive $B \to X_s l^+ l^-$ decay width as a function of the invariant mass of the lepton pair $q^2 = m^2_{l^+l^-}$ is given by [120]

$$\frac{d\Gamma\,(\hat{s})}{d\hat{s}} = \frac{G_F^2 m_b^5}{384\pi^3}\lambda^{1/2}\,(1,\hat{s},0)\,\sqrt{1-\frac{4\hat{m}_l^2}{\hat{s}}}\,\sum(\hat{s}) \tag{5.30}$$

where $\hat{s} = q^2/m_b^2$, $\hat{m}_i = m_i/m_b$, $\lambda\,(a,b,c) = a^2+b^2+c^2-2\,(ab+bc+ac)$ and

$$\begin{aligned}
\Sigma\,(\hat{s}) = &\ 4\left(1+\frac{2\hat{m}_l^2}{\hat{s}}\right)\left[\frac{1}{\hat{s}}\left(\left|C_7^{eff}\right|^2 + \left|\widetilde{C}_7^{eff}\right|\right)F_1\,(\hat{s},0)\right. \\
&\left.+3\,\mathrm{Re}\left(C_7^{eff*}C_9^{eff} + \widetilde{C}_7^{eff*}\widetilde{C}_9^{eff}\right)F_2\,(\hat{s},0)\right] \\
&+6\hat{m}_l^2\left(\left|C_9^{eff}\right|^2 + \left|\widetilde{C}_9^{eff}\right|^2 + |C_{10}|^2 + \left|\widetilde{C}_{10}\right|^2\right)F_3\,(\hat{s},0)\,.
\end{aligned} \tag{5.31}$$

The functions F_i read

$$\begin{aligned}
F_1\,(x,y) &= 2\,(1+y)\,(1-y)^2 - x\left(1+14y+y^2\right) - x^2\,(1+y)\,, \\
F_2\,(x,y) &= (1-y)^2 - x\,(1+y)\,, \\
F_3\,(x,y) &= 1-x+y.
\end{aligned} \tag{5.32}$$

For $\mathrm{BR}(B \to X_s \ell^+ \ell^-)$ we use the data averaged over electrons and muons for dilepton masses above 0.2 GeV, leaving us with [123]

$$2.8 \cdot 10^{-6} < \mathrm{BR}(B \to X_s \ell^+ \ell^-) < 6.2 \cdot 10^{-6}. \tag{5.33}$$

A good approximation of the differential decay width for the process $B \to \pi l^+ l^-$, not considering any factorization theorem, can be found in [121]:

$$\begin{aligned} \frac{d\Gamma\left(B \to \pi l^+ l^-\right)}{ds} &= \frac{G_F^2 \alpha^2 m_B^5}{1536\pi^5} \left|V_{tb} V_{ts}\right|^2 \lambda_\pi^{3/2}\left(\hat{s}\right) \left[f_+^2\left(\hat{s}\right) \left(\left| C_9^{eff}\left(\hat{s}\right)\right|^2 + \left| C_{10} + \widetilde{C}_{10}\right|^2 \right) \right. \\ &\left. + \frac{4 m_b^2 f_T^2\left(\hat{s}\right)}{\left(m_B + m_\pi\right)} \left| C_7^{eff}\right|^2 + \frac{4 m_b f_T\left(\hat{s}\right) f_+\left(\hat{s}\right)}{m_B + m_\pi} \mathrm{Re}\left(C_9^{eff}\left(\hat{s}\right) C_7^{eff\,*}\right) \right]. \end{aligned} \tag{5.34}$$

Here, the lepton mass m_l was neglected. The Wilson Coefficients C_7^{eff} and C_{10} can be derived from (5.26) by simply exchanging the strange and down quark. However, C_9^{eff} has to be changed according to [143]:

$$\begin{aligned} C_9^{eff}\left(\hat{s}\right) &= C_9 + 0.124\omega\left(\hat{s}\right) + h\left(\hat{m}_c, \hat{s}\right)\left(3C_1 + C_2 + 3C_3 + C_4 + 3C_5 + C_6\right) \\ &+ \lambda_d \left[h\left(\hat{m}_c, \hat{s}\right) - h\left(\hat{m}_u, \hat{s}\right)\right]\left(3c_1 + c_2\right) - \frac{1}{2} h\left(\hat{m}_d, \hat{s}\right)\left(C_3 + 3C_4\right) \\ &- \frac{1}{2} h\left(\hat{m}_b, \hat{s}\right)\left(4C_3 + 4C_4 + 3C_5 + C_6\right) + \frac{2}{9}\left(3C_3 + C_4 + 3C_5 + C_6\right), \end{aligned} \tag{5.35}$$

including a factor

$$\lambda_q \equiv \frac{V_{ub} V_{uq}^*}{V_{tb} V_{tq}}. \tag{5.36}$$

λ_s was neglected in (5.26). Because of $\lambda_d \gg \lambda_s$ this is not possible in (5.35). The Wilson Coefficients C_1 and C_2 are induced at tree level, hence they do not receive SUSY contributions. The penguin coefficients C_3-C_6 in general receive contributions from new physics but they are $\mathcal{O}\left(10^{-2}\right)$ while the coefficients C_{10} and C_9 are $\mathcal{O}\left(5\right)$. Thus these are neglected, leaving the approximation

$$\begin{aligned} C_1 &= -0.249, \quad C_2 = 1.108, \quad C_3 = 0.011, \\ C_4 &= -0.026, \quad C_5 = 0.007, \quad C_6 = -0.031. \end{aligned} \tag{5.37}$$

The form factors $f_T\left(q^2\right)$ and $f_+\left(q^2\right)$ can be parameterized by [122]

$$f\left(q^2\right) = \frac{r_1}{1 - q^2/m_1^2} + \frac{r_2}{1 - q^2/m_{fit}^2}, \tag{5.38}$$

using

	r_1	m_1^2	r_2	m_{fit}^2
f_+^π	0.744	5.279	-0.486	40.73
f_T^π	1.387	5.279	-1.134	32.22

. (5.39)

For the branching ratio of the exclusive semileptonic decay $B \to \pi\ell^+\ell^-$ [122] just an upper bound exists from BaBar. At 90% C.L.

$$\mathrm{BR}(B \to \pi\ell^+\ell^-) < 9.1 \cdot 10^{-8}. \tag{5.40}$$

5.1.4 Further constraints

In this section we describe further constraints not directly related to hadronic decays.
Beyond tree level the $A_{ii}^{u,d}$ (diagonal A-term entries) contribute to up and down-quark masses (Fig.5.4).

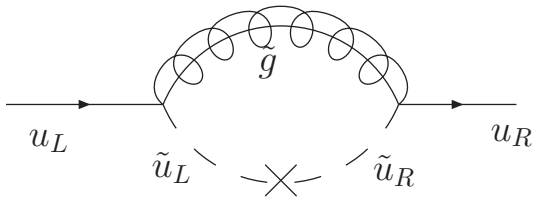

Figure 5.4: One loop squark-gluino contribution to the up-quark mass.

At one loop this contribution can be roughly estimated by

$$\delta m_{q_i} \propto \frac{\alpha_s}{4\pi} m_{\tilde{g}} \delta^q_{LR\,ii}, \qquad (q = u, d; \quad i = 1, 2, 3)\ . \tag{5.41}$$

We require the SUSY-QCD corrections to be smaller than the experimental central values of the quark masses: $\delta m_q \lesssim m_q$. The light quark masses impose serious contraints on $A_{ii}^{u,d} = \delta^{u,d}_{LR\,ii} M^2_{SUSY}/v_{u,d}$, $i = 1, 2$. However, A_{33} is just limited to large values.
General vacuum stability constraints limit the inter-generational A-terms [145]:

$$\begin{aligned} |A^d_{i3}|, |A^d_{3i}| &\leq \frac{m_b}{v_d}\sqrt{2\tilde{m}_d^2 + \tilde{m}_\ell^2} \simeq \sqrt{3}\ y_b\ M_{\mathrm{SUSY}}, \\ |A^u_{i3}|, |A^u_{3i}| &\leq \frac{m_t}{v_u}\sqrt{2\tilde{m}_u^2 + 2\tilde{m}_\ell^2} \simeq \sqrt{3}\ y_t\ M_{\mathrm{SUSY}}, \qquad (i = 1, 2). \end{aligned} \tag{5.42}$$

The masses $\tilde{m}_u, \tilde{m}_d, \tilde{m}_\ell$ are the mean squark and slepton masses defined for (4.47). Because of the smaller Yukawas the down sector is much stronger constrained than the up sector. We do not explicitly show analogous bounds for LR mixing among the first and second generations, which are strongly suppressed by the strange and charm Yukawas.

Inter-generational mixing involving the third generation always affects the lightest Higgs mass and the ρ parameter [146, 148]. The ρ parameter (the ratio of the amplitude of the neutral currents against the charged currents in the low-energy limit $q^2 = 0$) is equal to one at lowest order in the MSSM. Universal fermionic and sfermionic corrections can be written as

$$\rho = \frac{1}{1-\delta\rho}; \quad \delta\rho = \frac{\Sigma^Z(0)}{M_Z^2} - \frac{\Sigma^W(0)}{M_W^2}, \tag{5.43}$$

where Σ^V is the selfenergy of the gauge-boson V. The T parameter of Section 3.3.2 is simply the shift of the ρ parameter due to new physics. Thus, mixing in the squark sector can modify the ρ parameter. In the MSSM the corrections to M_W and $\sin^2\theta_{eff}$ can be related to $\delta\rho$ by

$$\delta M_W \simeq \frac{M_W}{2}\frac{\cos^2\theta_W}{\cos^2\theta_W - \sin^2\theta_W}\delta\rho, \tag{5.44}$$

$$\delta\sin^2\theta_{eff} \simeq -\frac{\cos^2\theta_W \sin^2\theta_W}{\cos^2\theta_W - \sin^2\theta_W}\delta\rho. \tag{5.45}$$

Experimental constraints for these quantities exist [147]: $\delta M_W < 34$ MeV and $\delta\sin^2\theta_{eff} < 15\times10^{-5}$. However, the constraints from rare decays and direct squark searches are generally stronger [148].
Further experimental constraints are from the Tevatron squark–mass bounds [149] and affect all entries in the squark mass matrix.

In principal B-meson decays into $\tau\nu$ final states might be relevant as well. This process receives contributions from a charged-Higgs exchange. Up to now B-factories suggest that the branching ratio for $B_u^- \to \tau\bar{\nu}$ is in agreement with the Standard Model but results and predictions suffer from substantial theoretical and experimental uncertainties [150]. Since for our moderate values of $\tan\beta$ the $H^\pm$-mediated amplitude cannot compete with the tree-level W-exchange, $B_u^- \to \tau\bar{\nu}$ data does not put additional constraints on the up squarks and we will neglect this decay in our numerical analysis. As mentioned in Section 4.3.2, we confine our considered parameter space to real soft terms. Hence, a possible CP-violating phase, which might give rise to electric dipole moments, is not studied.

5.1.5 Summary

In Kaon- and B-FCNCs, leading contributions by the down-squark matrices A^d and $m^2_{\tilde{D}_{L,R}}$ are mediated by gluinos which couple proportional to g_s. These are in general stronger than contributions from the up-squark matrices A^u and $m^2_{\tilde{U}_{L,R}}$, mediated by the charginos which couple proportional to the Yukawa couplings or g_w. Keeping the charged-Higgs production in mind, we can limit our analysis to up-squark mixing between different generations while neglecting down-squark mixing, as long as it is not required by (4.38). We also constrain ourselves to consider just intergenerational mixing between the first/second and third generation, parametrized by δ^u_{i3}, $(i = 1, 2)$. Mixing between first– and second–generation squarks receives much stronger

bounds from K-physics [100, 101] and by the recent measurements of $D^0\bar{D}^0$-mixing [116]. All constraints on the supersymmetric flavor sector we implement at 90% C.L.

The relevant up-sector parameters[3] A^u_{i3} and $m^2_{\tilde{U}_L\, i3}$ are constrained by data on $b \to s$ and $b \to d$ transitions, as well as by the weak isospin relation (4.38). The corresponding mass-matrix entries A^u_{3i} and $m^2_{\tilde{U}_R i3}$ are only very loosely bounded by flavor physics, the LR-chirality flip mostly by theoretical arguments (5.42). The reason is that they involve right-handed squarks $\tilde{u}_R$ and $\tilde{c}_R$. Those enter FCNC processes with external down quarks only via higgsino vertices proportional to the small up and charm Yukawa. To circumvent this Yukawa-suppression, we could combine $\tilde{t} - \tilde{u}_L(\tilde{c}_L)$ mixing with a subsequent generational-diagonal left-right mixing $\tilde{u}_R - \tilde{u}_L\ (\tilde{c}_R - \tilde{c}_L)$. However, generation-diagonal mixing is strongly constrained by the quark masses (5.41).

Collecting the results of Section 5.1, $\delta^u_{LR\,3i}$ and $\delta^u_{RR\,i3}$, $(i = 1, 2)$ are actually the least constrained flavored SUSY couplings. Kaon, charm and B-physics experiments are largely insensitive to the mixing of $\tilde{u}_R$ or $\tilde{c}_R$ with stops. In the following we investigate the potential impact of these relevant δ^u_{3i} on charged-Higgs collider searches. This involves computing all constraints in the high-dimensional parameter space. For the calculation of the constraints we do not use the mass-insertion approximation. Instead, we perform the full diagonalization of the squark-mass matrix.

5.2 Single-Charged-Higgs Production

The most promising charged-Higgs production rates for $m_{H^\pm} > m_t - m_b$, e.g. $gb \to H^\pm t$ and $gg \to tbH^\pm$, are phasespace suppressed and, due to their instable final states, receive a huge QCD background. Thus, a first step to produce a detectable charged Higgs might be the single-Higgs production from quark-antiquark scattering. This process could give a clean signal. To leading order it can be described by a general type-II two-Higgs-doublet model (Sec. 2.2). In Figure 5.5 we show the Drell-Yan-like diagram for $q\bar{q}' \to H^\pm$. In the quark mass basis the corresponding coupling is given by

$$\mathcal{L}_{H^\pm qq'} = \sqrt{2} V_{ij}\ \bar{u}_i \left(\frac{m_{d_j}}{v} P_R \tan\beta + \frac{m_{u_i}}{v} P_L \cot\beta \right) d_j H^+ \ + \ \text{h.c.} \tag{5.46}$$

with the quark fields u, d, their masses $m_{u,d}$ and the CKM matrix elements V_{ij} $(i, j = 1, .., 3)$. The Yukawa couplings are given in terms of $v = 2m_W/g = 246$ GeV, $g = e/\sin\theta_W$. Here $\tan\beta = v_2/v_1 = \langle H_2 \rangle / \langle H_1 \rangle$ denotes the ratio of vacuum expectation values of the two Higgs doublets. The physical charged Higgs scalar in terms of interaction eigenstates is $H^+ = \sin\beta (H_1^-)^* + \cos\beta H_2^+$. The chiral projectors are defined as $P_{L,R} = (1 \mp \gamma_5)/2$.

[3] We use the convention

$$A_{ij} = A_{L_i R_j} \neq A_{ji}.$$

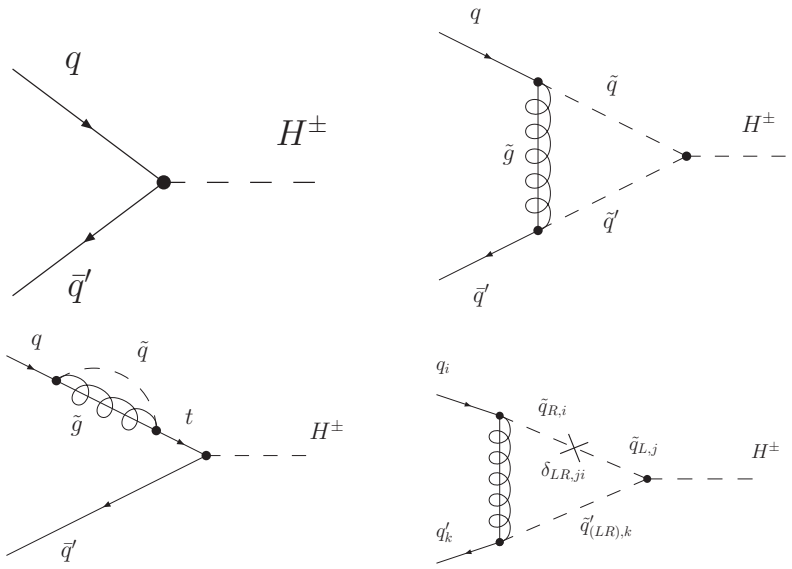

Figure 5.5: Feynman diagrams contributing to $q\bar{q}' \to H^\pm$ in the MSSM at tree level and at one-loop level in MFV and beyond.

Following (5.46) the amplitude for single-Higgs production in the type-II two-Higgs-doublet model is proportional to the quark Yukawa coupling, i.e. it is small unless third-generation quarks are involved. This chiral suppression is generic and with proper assumptions of minimal-flavor violation survives radiative corrections, like the SUSY-QCD corrections shown in Figure 5.5. Every gauge-invariant operator linking quark–antiquark–Higgs fields involves a chirality flip, hence vanishes with $m_q \to 0$ as long as the theory has a chiral limit. The renormalizable operators contributing up to dimension 4 are (modulo hermitian conjugates) [151]

$$\overline{Q} H_u^C U, \qquad \overline{Q} H_d^C D, \qquad\qquad \overline{Q} H_d U, \qquad \overline{Q} H_u D, \tag{5.47}$$

where $H^C = i\tau_2 H^*$, and Q and U, D are the $SU(2)$ weak-interaction eigenstate doublets and singlets, respectively. In general, capital letters describe interaction eigenstates, while small letters denote mass eigenstates.

While the first two operators in (5.47) are the usual tree-level Yukawa interaction, the second two operators involve the 'wrong' Higgs fields, and do not occur in the plain type-II two-Higgs-doublet model. Such 'wrong' Higgs operators are induced by SUSY breaking. They are proportional to a soft SUSY-breaking parameter like the gluino mass or an A-term and couple the Higgs to a squark loop [115]. Since after spontaneous symmetry breaking all operators in (5.47) contribute to the fermion masses, the lowest-order relation between the measured quark masses and the Yukawas is broken. This effect becomes numerically important for large $\tan\beta$. As long as we are only interested in small and moderate values of $\tan\beta$, we can safely neglect this effect. As far as the chiral limit of the MSSM is concerned, it is not spoiled as long as the soft-breaking $A^{u,d}$ terms are proportional to the respective quark Yukawa $y_{u,d}$.

In the following we will calculate the contributions by the four operators in (5.47), including necessarily some kind of chirality flip. The possiblity of circumventing the suppression from light-Yukawa couplings will be considered in Section 5.3. If we couple an external gauge boson to the process of single-Higgs production, we can build an extended set of operators containing fermions of the same chirality.

5.2.1 Tree-Level Single-Higgs Production

The top quark is too heavy for the gluon to split into a collinear $t\bar{t}$ pair at the LHC, hence the large flavor-diagonal CKM element V_{tb} does not play any role in single-Higgs production. At tree-level the charged Higgs couples to two fermions with the strength of the singlet's Yukawa coupling. Except for the top-Yukawa coupling, they are small compared to the gauge couplings. Thus, the leading order process is suppressed by small Yukawa couplings or by small entries of the CKM matrix, such as $V_{cb} \simeq 0.04$ [153]. Due to these two facts, the smallest over-all suppression receive the partonic processes $c\bar{s} \to H^+$ and $c\bar{b} \to H^+$, because $m_s V_{cs}$ and $m_b V_{cb}$ are of similar size. Using the $\overline{\text{MS}}$ quark masses given in the Appendix D at typical Higgs-mass scales the charm–bottom channel is favored. Hence, the single-charged-Higgs amplitude is proportional to $|m_b V_{cb} \tan\beta|^2$, if $\tan\beta$ is large enough.
For example, for $\tan\beta = 7$ and a charged-Higgs mass of $m_{H^\pm} = 188\ \text{GeV}$ we find LHC cross sections for H^+ production of $\sigma_{cs} = 10.1$ fb and $\sigma_{cb} = 25.3$ fb. If we neglect the theoretically poorly defined strange-quark Yukawa, the cross section decreases to $\sigma_{cs} = 0.56$ fb. Neglecting the charm Yukawa does not visibly shift σ_{cb}. The more we increase $\tan\beta$, the more the process will be dominated by the enhanced bottom Yukawa in $\bar{b}{-}c$ scattering, in spite of its strong CKM suppression.

Depending on the charged-Higgs mass the dominant decay channel is $H \to \tau\nu$ or $H \to tb$. Especially in the mass region where the latter decay is phase-space suppressed, $m_{H^\pm} \lesssim m_t + m_b$, the charged Higgs can be found in $H \to \tau\nu$ decays, which gives a clean signal without huge QCD backgrounds. While W boson decays are generation blind, the charged-Higgs decays predominantly into heavy fermions, because of the Yukawa instead of the generation-universal gauge couplings. The background to our searches is single-W production, mediated by

$$\mathcal{L}_{W^\pm qq'} = -V_{ij}\frac{g}{\sqrt{2}}\,\bar{u}_i\,\gamma^\mu P_L\,d_j\,W^+_\mu \;+\; \text{h.c.}. \tag{5.48}$$

This coupling is much bigger than the couplings in (5.46): $g/\sqrt{2} \sim \mathcal{O}(0.5) \gg y_{u,d}$. Hence, the W^+ production cross section of $90 \cdot 10^6$ fb [152] will be a serious challenge to our H^+ search in the two-Higgs-doublet model.

5.2.2 Single-Higgs Production in MFV and NMFV

From the former sections it is obvious that the Yukawa-coupling suppression of the single-charged-Higgs production is a generic feature of the existence of a chiral limit of the theory.

Assuming the quark masses to be small, i.e. $m_q \to 0$, renders the cross section to zero at any order of perturbation theory. This behavior can be circumvented if we allow non-minimal flavor violation in the squark sector, according to Section 4.3.2. Apart from the Yukawa-coupling suppression, squark loops can alleviate CKM suppression as well.
Relevant for the three-scalar couplings of squarks and Higgses are contributions from three different sources:

$$\mathcal{L}_{H^\pm \tilde{q}\tilde{q}'} = D\text{-term} + F\text{-term} + A\text{-term}. \tag{5.49}$$

The D-term couples the charged Higgs to two doublet squarks, i.e. the combination LL, proportional to the gauge coupling g:

$$\mathcal{L}_{H^\pm \tilde{q}\tilde{q}'}|_D = -\frac{V_{ij}\, g^2 v\, \sin(2\beta)}{2\sqrt{2}}\, \tilde{u}^*_{Li}\tilde{d}_{Lj}H^+ \;+\; \text{h.c.} \tag{5.50}$$

As we are interested in a cross-section enhancement for small $\tan\beta$, D-terms are interesting candidates, i.e. they are suppressed by $\sin(2\beta)$ and do not break chirality.
F terms, arising from the superpotential are Yukawa-induced and involve all four possible combinations of L and R squarks:

$$\begin{aligned}\mathcal{L}_{H^\pm \tilde{q}\tilde{q}'}|_F = \frac{gV_{ij}}{\sqrt{2}m_W} H^+ \Big[\; & \tilde{u}^*_{L,i}\tilde{d}_{L,j}\left(m^2_{d,j}\tan\beta + m^2_{u,i}\cot\beta\right) \\ & + \tilde{u}^*_{R,i}\tilde{d}_{R,j} m_{u,i} m_{d,j}\left(\cot\beta + \tan\beta\right) + \mu m_{d,j}\tilde{u}^*_{L,i}\tilde{d}_{R,j} + \mu m_{u,i}\tilde{u}^*_{R,i}\tilde{d}_{L,j}\Big].\end{aligned} \tag{5.51}$$

A-terms and soft masses are general soft SUSY-breaking parameters. A-terms occur with a chirality flipping squark combination. We keep the soft terms $A^{u,d}$ with all flavor indices i, j, k:

$$\mathcal{L}_{H^\pm \tilde{q}\tilde{q}'}|_A = \tilde{d}_{Li}V_{ki}A^u_{kj}\tilde{u}^*_{Rj}\cos\beta\, H^+ + \tilde{u}_{Li}V^*_{ik}A^d_{kj}\tilde{d}^*_{Rj}\sin\beta\, H^- \;+\; \text{h.c.} \tag{5.52}$$

While the D- and F-term contributions to the charged-Higgs–squark coupling are driven by the respective CKM element, the A-terms, induced by SUSY breaking, are not.

Giving up the assumption of a chiral limit of the theory allows us to introduce NMFV contributions to the single-charged-Higgs production, which can lift the cross section above the two-Higgs-doublet model prediction in Section 5.2.1. In this case the operators in (5.47) are not necessarily proportional to Yukawa-couplings, but to a Majorana mass, e.g. $m_{\tilde{g}}$, with a left-right mixing δ_{LR} among the squarks. The enhancement for $H^\pm$-production can be roughly approximated by the following comparison of gluino-loops versus the tree-level strange–charm $\mathcal{A}_{cs}$ and bottom–charm $\mathcal{A}_{cb}$ amplitudes:

$$\begin{aligned}\frac{\mathcal{A}_{\text{gluino-loop}}}{\mathcal{A}_{cs}} &\propto \frac{\alpha_s}{4\pi}\,\frac{m_{\tilde{g}}}{m_c}\delta^u_{LR,3i}, \\ \frac{\mathcal{A}_{\text{gluino-loop}}}{\mathcal{A}_{cb}} &\propto \frac{\alpha_s}{4\pi}\,\frac{m_{\tilde{g}}}{V_{cb}m_b}\,\frac{1}{\tan^2\beta}\,\delta^u_{LR,3i} \qquad (i=1,2).\end{aligned} \tag{5.53}$$

The diagonal CKM elements were assumed to be $V_{tb}, V_{cs} \simeq 1$. Both ratios in (5.53) exhibit an enhancement of the gluino loop that can be as large as $\mathcal{O}(10)$ for suitable SUSY masses and

$\tan\beta$. These loop contributions can be induced with a first or second-generation up quark in the initial state, whereas first-generation quark contributions are luminosity enhanced. To determine the possible numerical value of δ_{LR}, the experimental and theoretical constraints form Section 5.1.4 have to be taken into account. The dominant one-loop corrections are due to the gluino vertex and self-energy diagrams shown in Figure 5.5.
With this estimate in mind, we then calculate H^+ production from quark-antiquark fusion including the dominant squark–gluino loops. Generally, the amplitude $\mathcal{A}^{ij}$ for $u_i\bar{d}_j \to H^+$ production can be written with quark u_q and antiquark v_q spinors as

$$\mathcal{A}^{ij} = \sum_{\sigma} \mathcal{F}^{ij,\sigma}\mathcal{M}^{ij,\sigma} \tag{5.54}$$

with $\mathcal{M}^{ij,\sigma} = \bar{v}_{d_j}\, P_\sigma\, u_{u_i}$ and $\mathcal{F}^{ij,\sigma} = \mathcal{F}_0^{ij,\sigma} + \mathcal{F}_S^{ij,\sigma} + \mathcal{F}_V^{ij,\sigma},\ \ (\sigma = L, R)$.
Although we do not use the mass-insertion approximation (Sec.4.3.2) to calculate the numerical results, we use it to give the analytical expressions for the amplitude of this process. It is a convenient way to exploit parameter dependencies in this process. For the tree-level, $\mathcal{F}_0$, one-loop self-energy, $\mathcal{F}_S$, and vertex, $\mathcal{F}_V$, form factors we obtain[4]:

$$\begin{aligned}
\mathcal{F}_0^{ij,R} &= \frac{eV_{ij}^*}{\sqrt{2}m_W \sin\theta_w} m_{u_i} \cot\beta, \\
\mathcal{F}_0^{ij,L} &= \frac{eV_{ij}^*}{\sqrt{2}m_W \sin\theta_w} m_{d_j} \tan\beta, \\
\mathcal{F}_S^{ij,R} &= \frac{\sqrt{2}eV_{3j}^*}{m_W \sin\theta_w} \frac{\alpha_s}{4\pi} C_F \frac{m_{\tilde{g}}}{\tan\beta}\, \delta^u_{LR,3i}\, \tilde{m}^2\, \mathcal{I}_{12}(m_{\tilde{g}}, m_{\tilde{q}}), \\
\mathcal{F}_V^{ij,R} &= \frac{\sqrt{2}eV_{3j}^*}{m_W \sin\theta_w} \frac{\alpha_s}{4\pi} C_F \left(\frac{m_t^2}{\tan\beta} - m_W^2 \sin(2\beta) \right) m_{\tilde{g}} \delta^u_{LR,3i}\, \tilde{m}^2\, \mathcal{I}_{13}(m_{\tilde{g}}, m_{\tilde{q}}),
\end{aligned} \tag{5.55}$$

where we define

$$\mathcal{I}_{lm}(m_{\tilde{g}}, m_{\tilde{q}}) = \int \frac{d^4q}{i\pi^2} \frac{1}{(q^2 - m_{\tilde{g}}^2)^l (q^2 - m_{\tilde{q}}^2)^m}, \qquad (l + m > 2). \tag{5.56}$$

For $M_{SUSY} \sim m_{\tilde{g}} \sim m_{\tilde{q}}$ $\mathcal{I}_{lm}$ scales as $M_{SUSY}^{4-2l-2m}$. Equations 5.55 exhibit in bottom-up fusion that the gluino-loops with $\delta^u_{LR,3i}$ are proportional to $V_{tb}m_{\tilde{g}}$, avoiding the CKM and quark-mass suppression. F- and D-terms contribute with opposite sign, hence they cancel each other partly in the vertex correction $\mathcal{F}_V^{ij,R}$. Therefore, the self-energies give the dominant MSSM contribution described in in (5.53). Additionally, $\mathcal{F}_S^{ij,R}$ becomes large for small $\tan\beta$, awakening the hope to constitute an increasing total cross section in this parameter region.

To make the results from Section 5.1 and the lines above explicit, we give the whole up-squark mass matrix, defined in Section 4.3.2 , exposing the bilinear couplings which are severely con-

[4] In agreement with [153].

straint and which give the largest contributions to charged Higgs production:

$$\mathcal{M}_u^2 = \begin{pmatrix} M^2_{u,LL,11} & M^2_{u,LL,12} & M^2_{u,LL,13} & M^2_{u,LR,11} & M^2_{u,LR,12} & M^2_{u,LR,13} \\ & M^2_{u,LL,22} & M^2_{u,LL,23} & M^2_{u,LR,21} & M^2_{u,LR,22} & M^2_{u,LR,23} \\ & & M^2_{u,LL,33} & M^2_{u,LR,31} & M^2_{u,LR,32} & M^2_{u,LR,33} \\ & & & M^2_{u,RR,11} & M^2_{u,RR,12} & M^2_{u,RR,13} \\ & \text{h.c.} & & & M^2_{u,RR,22} & M^2_{u,RR,23} \\ & & & & & M^2_{u,RR,33} \end{pmatrix}. \tag{5.57}$$

The red entries are constraint by Kaon- and B-physics, as well as theoretical considerations. Remarkably, the green entries increase the charged-Higgs production most and remain almost unconstraint.

To test the effects of flavor structures on the single-Higgs cross section we choose two generic MFV SUSY parameter points which do not violate any current bounds. We then allow for flavor violation beyond MFV. Because of current experimental and theoretical constraints discussed in detail in Section 5.1, the up-squark parameters $\delta^u_{LR,3i}$ and $\delta^u_{RR,3i}$ involving 1-3 and 2-3 mixing are the least constrained and therefore expected to cause the biggest effects. The mass insertions δ^u_{LL} and $\delta^u_{LR,i3}$ are stronger bounded by flavor physics.
Because of the size of the strong coupling we are mainly interested in gluino-squark loops contributing to $u\bar{b} \to H^+$ and $c\bar{b} \to H^+$. These one-loop corrections are not CKM suppressed if we allow for the supersymmetric flavor-breaking parameters δ^u_{3i}.

For the first parameter point we assume the following values:

Parameter point A		
$\tan\beta = 7$	$m_A = 170$ GeV	$\mu = -300$ GeV
$m_{\tilde{U}_{LL,RR}\,ii} = m_{\tilde{D}_{LL,RR}\,ii} = 600$ GeV	$M_2 = 700$ GeV	$m_{\tilde{g}} = 500$ GeV
$A^{u,c} = 0$	$A^{d,s,b} = 0$	$A^t = 1460$ GeV

(5.58)

where m_A denotes the mass of the CP-odd Higgs leading to $m_{H^+} = 188$ GeV. M_2 is the SUSY-breaking wino mass. The diagonal soft-breaking entries in the squark mass matrices defined in (4.21) we choose universal. All parameters are given at a scale of order m_{H^+}. The large value of A^t (corresponding to $\delta^u_{LR,33}$) increases the light Higgs mass to 119.9 GeV at two loops [154]. For this parameter choice the tree-level H^+ production cross section at the LHC in the two-Higgs-doublet model is 41.2 fb.

To show the dependence on the diagonal squark-mass entries we take the second parameter point to be:

Parameter point B		
$\tan\beta = 5$	$m_A = 500$ GeV	$\mu = -200$ GeV
$m_{\tilde{U}_{LL,RR}\,ii} = m_{\tilde{D}_{LL,RR}\,ii} = 800$ GeV	$M_2 = 500$ GeV	$m_{\tilde{g}} = 500$ GeV
$A^{u,c} = 0$	$A^{d,s,b} = 0$	$A^t = 1260$ GeV.

(5.59)

The impact of the experimental squark bound depends crucially on the squark masses we choose. This can be illustrated if we consider the eigenvalues m_i^2 of a (2×2) mass matrix with off-diagonal mixing δ and a diagonal sfermion mass m_0:

$$M^2 = m_0^2 \begin{pmatrix} 1 & \delta \\ \delta & \Delta \end{pmatrix}, \qquad m_i^2 = \frac{1+\Delta}{2} \pm \sqrt{\frac{(1-\Delta)^2}{4} + \delta^2} \tag{5.60}$$

If we allow for non-degenerate diagonal entries Δ close to one (as possible in models beyond MFV), both δ and Δ increase the mass splitting. From an experimental limit $m_i > m_{\text{bound}}$ we obtain an analytical expression for a bound on δ:

$$\delta < \sqrt{\Delta - r^2(\Delta+1) + r^4}, \qquad r = \frac{m_{\text{bound}}}{m_0}, \tag{5.61}$$

or simply $\delta < 1 - r^2$ for degenerate diagonal matrix elements. For $\Delta < 1 (\Delta > 1)$, the constraint on the mixing δ improves (eases) with respect to the $\Delta = 1$ case. Clearly, for increasing values of the squark mass scale m_0 the bound on the off-diagonal mixing from direct search limits weakens and the flavor constraints are of most importance. We can make this explicit by slightly increasing the soft-breaking squark masses and m_A, according to parameter point B: The charged-Higgs mass is now $m_{H^+} = 507$ GeV. The tree-level cross section of 0.48 fb in the two-Higgs-doublet model is suppressed by this heavy final-state mass. The color coding for the different constraints in Figure 5.7 is the same as in Figure 5.6.
The numerical evaluation was done using the program FeynArts [155] for the generation of graphs and amplitudes and for the integrals the package FormCalc/LoopTools [156]. In the end the differential cross section was convoluted with the CTEQ6 [157] parton distribution functions, whereas we chose the renormalization and factorization scale at the charged Higgs mass.

In Figure 5.6 we show the hadronic cross sections for the single-charged Higgs production beyond minimal flavor violation. Intergenerational mixing can enhance the rates to values above 100 fb. The allowed region, which does not violate any bound is given in the rainbow colored area, while the parameter choices outside this area are ruled out by the specific bounds, indicated by its color.
The different experimental constraints impacting the parameter point A shown in Figure 5.6 include:

- Tevatron searches for mass-degenerate first- and second-generation squarks require $m_{\tilde{q}} > 200$ GeV [149]. They rule out the yellow points.
- squark searches and radiative and semileptonic decay limits rule out the green points.
- black points are forbidden by the squark–mass limits, B mixing, and radiative and semileptonic decays.
- blue points indicate a violation of the radiative and semileptonic decay bounds only.
- orange points correspond to a violation of the B mixing and radiative and semileptonic decay limits.

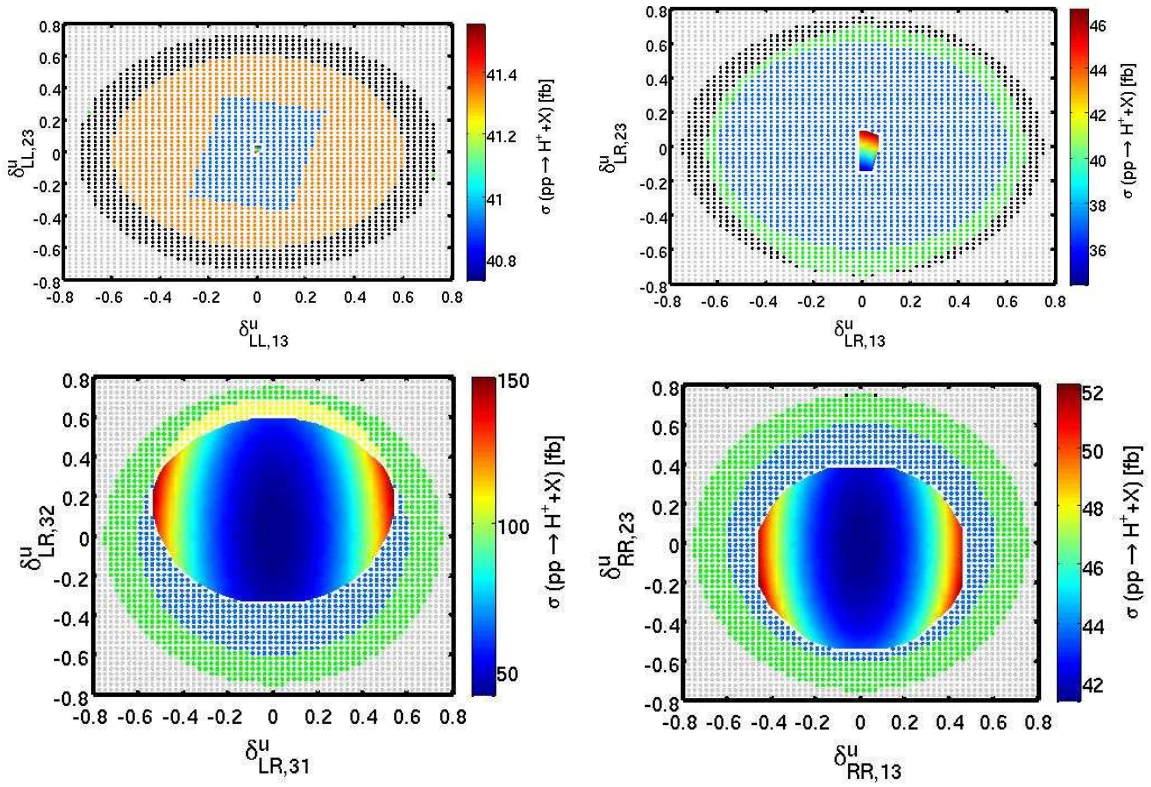

Figure 5.6: Single-charged-Higgs production cross sections including NMFV effects. For the MSSM parameters we choose parameter point A.

- red points are ruled out by B mixing alone.
- grey points on the outside of the panels indicate a negative squark mass square after diagonalizing the squark mass matrix.

In Figure 5.6 we see that the strongest bounds to the allowed parameter space come from radiative and semileptonic decays followed by the Tevatron limit on light-flavor squark masses. As expected, varying δ^u_{LL} and $\delta^u_{LR,i3}$ just allows for a very narrow viable region, whereas the region for $\delta_{LR,3i}$ and δ_{RR} is quite large. $\delta^u_{LL,i3} \neq 0$ induces SUSY-QCD contributions to the flavor constraints, according to (4.38). The entry $\delta^u_{LR,31}$ has the strongest impact on the rate. It allows mixing between a right-handed up-squark and a left-handed top-squark. Hence, the processes profits from the large parton luminosity of the up-quark in the initial state, as well as the large D- term coupling (5.58) without CKM suppression. The maximal single-Higgs cross section is obtained at $|\delta^u_{LR,31}| \sim 0.6$ in association with $\delta^u_{LR,23}$ (third panel). In the fourth panel we show the variation of δ^u_{RR}, which gives just moderately enhanced rates compared to the tree-level cross section, although just weakly constrained. This is due to the fact, that δ^u_{RR} cannot induce a D-term coupling. For this purpose an additional LR mixing is needed. Since A^u_{33} is typically large, the relevant combination $\delta^u_{RR,13}\delta^u_{LR,33}$ is numerically sizeable, as is the F-term contribution $\propto m_t \mu \delta^u_{RR,13}$.

The calculation should not be done in the mass-insertion approximation, which is not valid where $\delta^u \lesssim 1$. Current experimental limits, for example from squark searches generally imply $\delta^u < 1$, but not necessarily $\delta^u \ll 1$.

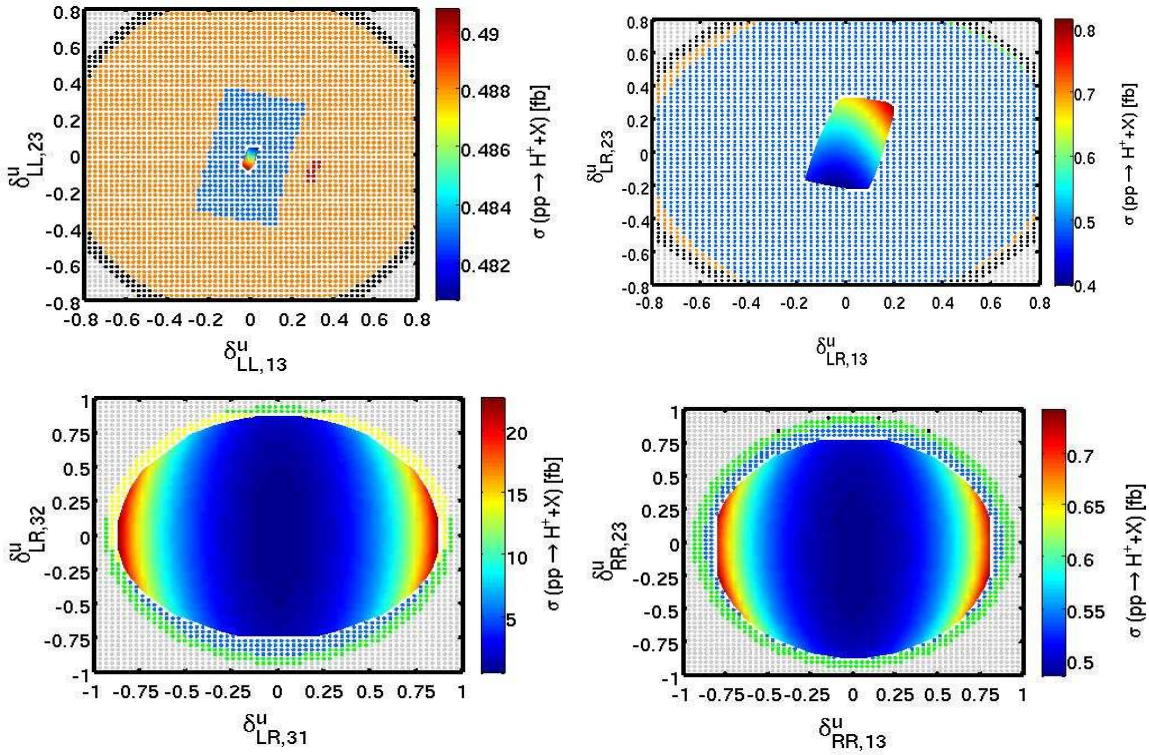

Figure 5.7: Single charged Higgs production cross sections including NMFV effects. The MSSM parameters are governed by parameter point B.

In parameter point B we increased the soft-breaking squark masses and m_A. The observations about which δ^u are stronger or weaker constrained remain the same. But the allowed region in parameter space is larger for all parameters. Increasing the SUSY masses reduces the impact of SUSY corrections to the flavor observables. This is a common feature, ending in the decoupling limit [158]. For the allowed region with LR mixing we obtain a radius $\delta^u_{LR,3i} \lesssim 1.0$ and for RR mixing $\delta^u_{RR,i3} \lesssim 0.8$. The hadronic-cross-section results are smaller than for parameter point A, mainly because of the heavier Higgs mass.

Still the question is, if there is an enhancement for small $\tan\beta$ and how large this enhancement might be? Figure 5.8 shows the $\tan\beta$ dependence of the hadronic cross section $pp \to H^+$. $\tan\beta = 7$, as in parameter point A, determines the minimum of the curve. We obtain an enhancement for large values due to the enhanced bottom-quark coupling to the charged Higgs and for very small $\tan\beta$ due to the D- and F-term couplings of the top and stop. The region of very low values is governed by (5.55). For the large $\tan\beta$ region they are not applicable because they just describe the limit of neglectable light fermion masses, $m_f \to 0$ if $m_f \leq m_b$.

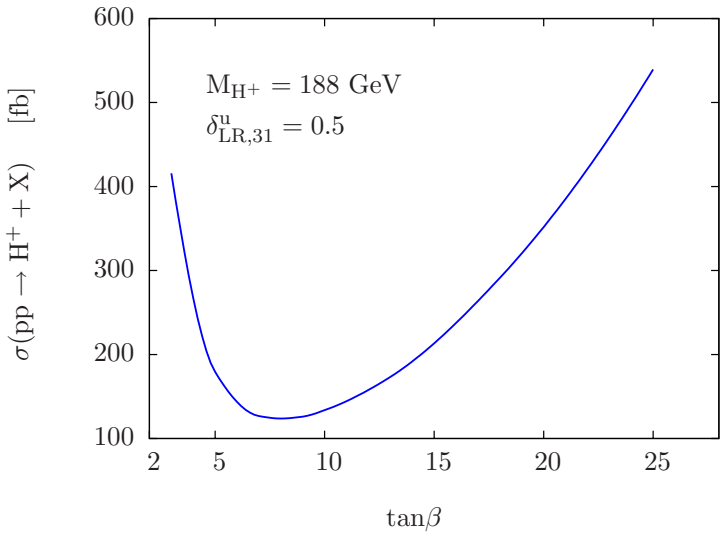

Figure 5.8: Hadronic cross section allowing NMFV effects in parameter point A.

In Figure 5.9 we show the ratio of the cross section including beyond-MFV diagrams over the leading-order two-Higgs-doublet-model cross section. At tree level we include all Standard-Model Yukawa couplings. We choose parameter point A and just vary the charged Higgs mass between 188 and 500 GeV. To show the typical size of the observed effect, we vary the dominant beyond-MFV parameter $\delta^u_{LR,31}$ within its allowed range, with all other beyond-MFV parameters zero. In general supersymmetric one-loop corrections in MFV are of higher order and cannot enhance the total cross section compared to the tree-level cross section by a factor of 4. Here, beyond-MFV it is different. From (5.53) we can read off, that the large effect we observe are expression of an additional source of fermionic mass insertion. Hence, it does not mean that perturbation theory becomes instable.

5.3 Charged-Higgs Production with a hard Jet

Between the single-Higgs production and the one in association with a jet exists a fundamental difference. While the former is strictly zero in MFV in the limit of neglectable small fermion masses, the latter is not. It does not posses this generic chiral suppression according to the F- and A-terms, which are proportional to the Yukawa couplings, as described in Section 5.2.2. Instead, the D-term couplings shown in (5.50) are gauge couplings, thus they could be considerably larger than light-flavor Yukawa couplings. Effectively, operators of the form

$$i\,\overline{Q}\gamma_\mu Q\, H_u \overleftrightarrow{D^\mu} H_u^C \tag{5.62}$$

lead to higher dimensional $q\bar{q}' H g$ operators after electroweak symmetry breaking [151]. To induce these operators no 'chiral flip' caused by fermion masses is needed. Even in a non-supersymmetric two-Higgs-doublet model this limit is zero. Contributions to non-chiral operators arise at two loops, when the charged Higgs couples to neutral Higgses and gauge bosons

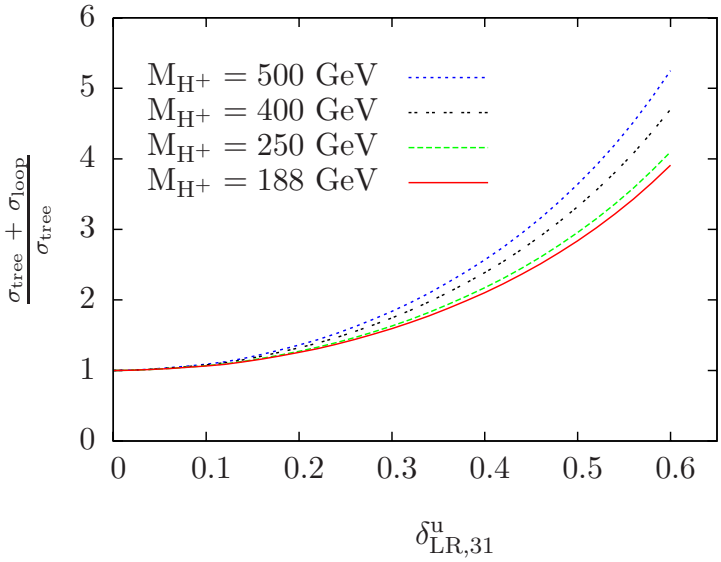

Figure 5.9: Ratio of single-charged-Higgs rates in NMFV vs. two-Higgs-doublet model. All supersymmetric parameters are given in parmeter point A

and not directly to fermions[5] . This circumstance gives rise to hope, that the main contributions to this process can be calculated in the limit of $m_f \to 0$, if $m_f \leq m_b$. This would simplify the numerical evaluation tremendously and could make its integration into Monte-Carlo programs like Sfitter [159], an analysis tool to determine supersymmetric model parameters, applicable. Diagrams for this process can be derived by radiating a gluon from the single-Higgs production diagrams. Requiring a hard jet, e.g. $p_{T,j} > 100$ GeV, cuts the collinear divergences. In principal, to compare the loop corrections to the tree-level rates we have calculate all contributions to order g_s^3. But according to the single charged Higgs production in NMFV we assume to obtain flavor effects which can be much larger than next-to-leading order QCD effects. Therefore, we limit our analysis to tree-level rates and SUSY-QCD corrections with MFV assumption and beyond. However, we include further decays of the charged Higgs. If the Higgs mass is small, $m_{H^+} \lesssim 200$ GeV, the Higgs decay into a hadronic τ lepton is the most promising [108, 109]. For parameter point A we find $\mathrm{BR}(H^- \to \tau\bar{\nu}) = 71\%$, with a taggable hadronic tau branching ratio of around roughly two thirds [123]. The dominant background to this signature is clearly W+jet production, again with the W decaying to a hadronic τ. For the cross section of this process we obtain $\sigma(W + \mathrm{jet}) \approx 1$ nb.

5.3.1 MFV and Decoupling

In the limit $m_f \to 0$ tree-level diagrams are absent and in MFV just 5 diagrams do contribute at one loop (Fig.5.10). The Higgs just couples to left-handed squarks with gauge-interaction strength. The amplitude is finite, hence a renormalization procedure is not needed. We just

[5] Numerically these two-loop contributions are tiny. They are suppressed by $(g^2/(16\pi^2))^2 \sim 10^{-5}$

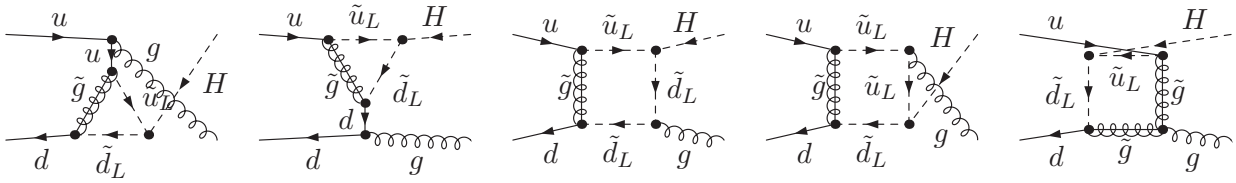

Figure 5.10: Lowest order SUSY QCD diagrams for $u\bar{d} \to gH^{\pm}$ with MFV and massless quarks.

consider QCD corrections. Chargino and neutralino loops are sub-leading due to their smaller gauge coupling. A mixed quark-gluon initial state, e.g. up quark and gluon, yields the largest cross section at the LHC, taking advantage from the high-x valence quark parton densities and the large gluon luminosity at lower x.

The general amplitude for the partonic subprocess $u_i + \bar{d}_j \to H^+ + g$ is given in terms of form factors as

$$\mathcal{A}^{ij} = \sum_{\sigma} \sum_{k=1}^{6} \mathcal{F}_k^{ij,\sigma} \mathcal{M}_k^{ij,\sigma} \ , \quad \sigma = L, R \tag{5.63}$$

with 12 standard matrix elements [161]

$$\begin{aligned}
\mathcal{M}_1^{ij,\sigma} &= \bar{v}_j(p_2) \not{\varepsilon} P_\sigma u_i(p_1) \ , & \mathcal{M}_4^{ij,\sigma} &= \bar{v}_j(p_2) \not{k}_2 \not{\varepsilon} P_\sigma u_i(p_1) \ , \\
\mathcal{M}_2^{ij,\sigma} &= \bar{v}_j(p_2) \not{k}_2 P_\sigma u_i(p_1) \ (\varepsilon \cdot p_1) \ , & \mathcal{M}_5^{ij,\sigma} &= \bar{v}_j(p_2) P_\sigma u_i(p_1) \ (\varepsilon \cdot p_1) \ , \\
\mathcal{M}_3^{ij,\sigma} &= \bar{v}_j(p_2) \not{k}_2 P_\sigma u_i(p_1) \ (\varepsilon \cdot p_2) \ , & \mathcal{M}_6^{ij,\sigma} &= \bar{v}_j(p_2) P_\sigma u_i(p_1) \ (\varepsilon \cdot p_2) \ .
\end{aligned} \tag{5.64}$$

We assign the momenta p_1 and p_2 to the quarks $u_i(p_1)$ and $\bar{d}_j(p_2)$ in the initial state and the momenta k_1 and k_2 to the charged Higgs $H^+(k_1)$ and gluon $g(k_2)$ in the final state. The corresponding Mandelstam variables are $s = (p_1 + p_2)^2$, $t = (p_1 - k_1)^2$, $u = (p_1 - k_2)^2$, and ε is the polarization vector of the gluon. Ward identities follow from the global or gauged symmetries of a theory [160]. Here, the $SU(3)$-gauge invariance implies a Ward identity, which means that the amplitude has to vanish, if we replace the external gluon polarization vector by the gluon momentum. This relates the different form factors to each other:

$$\mathcal{F}_1^{ij,\sigma} + \mathcal{F}_2^{ij,\sigma} \, (p_1 \cdot k_2) + \mathcal{F}_3^{ij,\sigma} \, (p_2 \cdot k_2) = 0 \ , \ \ \mathcal{F}_5^{ij,\sigma} \, (p_1 \cdot k_2) + \mathcal{F}_6^{ij,\sigma} \, (p_2 \cdot k_2) = 0 \tag{5.65}$$

We compute the form factors for H^+ plus jet production in the limit $m_f \to 0$ assuming MFV. For massless light quarks the form factors $\mathcal{F}_{4,5,6}^{ij,\sigma}$ vanish and the one including right-handed squarks, $\mathcal{F}_{1\ldots6}^{ij,R}$, are zero because couplings to a charged Higgs are always Yukawa-like. Only two of the 24 form factors are independent and can be written as

$$\begin{aligned}
\mathcal{F}_1^{ij,L} &= eg_s^3\frac{m_W}{\pi^2}\,\frac{V_{ij}^*\sin 2\beta}{12\sqrt{2}\sin\theta_w}\left\{-C_1(c_1)-C_1(c_2)+\frac{D_{00}(d_1)}{4}+\frac{D_{00}(d_2)}{4}\right.\\
&\quad+\frac{9}{8}\left[D_0(d_3)m_{\tilde{g}}^2-D_1(d_3)m_{H^+}^2-D_2(d_3)u-2D_{00}(d_3)-D_{11}(d_3)m_{H^+}^2\right.\\
&\quad\left.\left.-D_{12}(d_3)\left(m_{H^+}^2+u\right)-D_{13}(d_3)\left(s+u\right)-D_{22}(d_3)u-D_{23}(d_3)u\right]\right\} \qquad (5.66)\\
\mathcal{F}_2^{ij,L} &= eg_s^3\frac{m_W}{\pi^2}\,\frac{V_{ij}^*\sin 2\beta}{48\sqrt{2}\sin\theta_w}\left\{D_{23}(d_1)-D_2(d_2)-D_{22}(d_2)-D_{23}(d_2)\right.\\
&\quad\left.-9\left[D_1(d_3)+D_2(d_3)+D_{11}(d_3)+2D_{12}(d_3)+D_{13}(d_3)+D_{22}(d_3)+D_{23}(d_3)\right]\right\}
\end{aligned}$$

where the tensor coefficients $C_{i\ldots}$, $D_{i\ldots}$ are defined as in [162]. We use the following abbreviations to specify the arguments of the three-point and four-point integrals:

$$\begin{aligned}
c_1 &= \left(m_{H^+}^2, t, 0, m_{\tilde{u}_j}, m_{\tilde{d}_i}, m_{\tilde{g}}\right)\ ,\\
c_2 &= \left(m_{H^+}^2, u, 0, m_{\tilde{d}_j}, m_{\tilde{u}_i}, m_{\tilde{g}}\right)\ ,\\
d_1 &= \left(0, 0, m_{H^+}^2, 0, s, t, m_{\tilde{g}}, m_{\tilde{d}_j}, m_{\tilde{d}_j}, m_{\tilde{u}_i}\right)\ ,\\
d_2 &= \left(0, m_{H^+}^2, 0, 0, s, u, m_{\tilde{g}}, m_{\tilde{d}_j}, m_{\tilde{u}_i}, m_{\tilde{u}_i}\right)\ ,\\
d_3 &= \left(m_{H^+}^2, 0, 0, 0, t, u, m_{\tilde{u}_i}, m_{\tilde{d}_j}, m_{\tilde{g}}, m_{\tilde{g}}\right), \qquad (5.67)
\end{aligned}$$

They are connected to the ordering scheme for the arguments of the loop functions defined in [162] as

$$\begin{aligned}
c &= \left(p_1^2, (p_1-p_2)^2, p_2^2, m_1, m_2, m_3\right) \equiv (p_1, p_2, m_1, m_2, m_3)\,,\\
d &= \left(p_1^2, p_2^2, p_3^2, p_4^2, (p_2-p_3)^2, (p_1-p_2)^2, m_1, m_2, m_3, m_4\right) \equiv (p_1, p_2, p_3, m_1, m_2, m_3, m_4)\,.
\end{aligned} \qquad (5.68)$$

In Table 5.1 we show the numerical results in the fifth column, indicated by MFV and $m_f = 0$. The hadronic cross section appear to be extremely small, at the order of $\mathcal{O}(10^{-4})$ fb. We give the numbers for parameter point A and vary $\tan\beta$ and m_{H^+}. Although we observe the relative enhancement for small $\tan\beta$, the absolute rate for H^++jet is small compared to the MFV results including all Yukawa couplings in column three. The reason for this difference is subtle. The purely D-term induced cross sections in the limit $m_f \to 0$ suffer from an additional mass suppression $1/M_{\rm SUSY}^4$ in the decoupling limit, i.e. $m_{H^+}^2, m_W^2, u, s, t \ll M_{\rm SUSY}^2$, where $M_{\rm SUSY}$ denotes a common squark and gluino mass. This behavior can be understood after a closer look at (5.66). The only sources of non-SUSY masses in the amplitude's denominators are the 1P-reducible vertex diagrams in Figure 5.10, which can be shown to contribute only to the form factor $\mathcal{F}_1^{ij,\sigma}$. Hence, just $\mathcal{F}_1^{ij,\sigma}$ scales with $\propto 1/M_{SUSY}^2$. According to (5.65), after applying the Ward Identity these contributions have to be compensated by contributions to other form factors. However, the other form factors just receive contributions $\propto 1/M_{SUSY}^4$ and cannot compensate for the $\propto 1/M_{SUSY}^2$ scaling. It follows, that all contributions in $\mathcal{F}_1^{ij,\sigma}$ proportional to $1/M_{SUSY}^2$

m_{H^+}	$\tan\beta$	$\sigma_{\rm 2HDM}$	$\sigma_{\rm 2HDM}^{(m_s=0)}$	$\sigma_{\rm MFV}$	$\sigma_{\rm MFV}^{(m_s=0)}$	$\sigma_{\rm MFV}^{(m_f=0)}$
188 GeV	3	$2.5 \cdot 10^{-1}$	$1.9 \cdot 10^{-1}$	$2.6 \cdot 10^{-1}$	$2.0 \cdot 10^{-1}$	$6.7 \cdot 10^{-4}$
188 GeV	7	$9.9 \cdot 10^{-1}$	$6.0 \cdot 10^{-1}$	$1.1 \cdot 10^{0}$	$6.5 \cdot 10^{-1}$	$1.5 \cdot 10^{-4}$
400 GeV	3	$4.0 \cdot 10^{-2}$	$3.0 \cdot 10^{-2}$	$4.2 \cdot 10^{-2}$	$3.2 \cdot 10^{-2}$	$4.2 \cdot 10^{-4}$
400 GeV	7	$1.6 \cdot 10^{-1}$	$1.0 \cdot 10^{-1}$	$1.7 \cdot 10^{-1}$	$1.1 \cdot 10^{-1}$	$9.1 \cdot 10^{-5}$
500 GeV	3	$2.0 \cdot 10^{-2}$	$1.44 \cdot 10^{-2}$	$2.1 \cdot 10^{-2}$	$1.5 \cdot 10^{-2}$	$3.5 \cdot 10^{-4}$
500 GeV	5	$4.2 \cdot 10^{-2}$	$2.7 \cdot 10^{-2}$	$4.4 \cdot 10^{-2}$	$2.9 \cdot 10^{-2}$	$1.4 \cdot 10^{-4}$
500 GeV	7	$7.9 \cdot 10^{-2}$	$5.1 \cdot 10^{-2}$	$8.4 \cdot 10^{-2}$	$5.4 \cdot 10^{-2}$	$7.6 \cdot 10^{-5}$

Table 5.1: Production rates (in fb) for the associated production of a charged Higgs with a hard jet: $p_{T,j} > 100\ \mathrm{GeV}$. The label 2HDM denotes a two-Higgs-doublet of type II, while MFV refers to the SUSY-QCD corrected contributions, assuming MFV. For the SUSY parameters we choose parameter point A. The label $(m_s = 0)$ means a zero strange Yukawa, $(m_f = 0)$ indicates that all quark (except top) Yukawa couplings are neglected. In this case only D-term couplings contribute within MFV.

have to cancel. Numerically we confirmed this observation and found that the amplitude has the following decoupling behavior:

$$\mathcal{A}^{\tilde{q}\tilde{g}}_{\rm D-term} \propto g_s \frac{\alpha_s \alpha}{M^4_{\rm SUSY}} \sin(2\beta)\ . \tag{5.69}$$

Unfortunately, this means that the production cross section for a charged-Higgs plus a hard jet via D terms decouples as $\sigma \propto 1/M^8_{\rm SUSY}$, four powers of $M_{\rm SUSY}$ faster than the leading supersymmetric cross section.

The calculation of the full MFV SUSY-QCD corrections is much more involved. One of the 18 partonic processes consists of 17 diagrams (Fig.5.11). For the renormalization of the amplitude we use the on-shell scheme according to Appendix B. As general all SUSY-QCD-corrected diagrams share the loop-suppression factors and thus are not expected to dominate over the leading-order result numerically. The columns $1-4$ in Table 5.1 show the results for the hadronic cross section of a Higgs boson with a hard jet $(p_{T,j} > 100\ \mathrm{GeV})$ at tree level and in MFV with SUSY-QCD corrections. The cross sections tend to be small yielding sub-femtobarn values. Due to $V_{cb}m_b \approx V_{cs}m_s$ the strange-quark mass cannot be neglected. We vary $m_{H^\pm}$ and $\tan\beta$, again for parameter point A. In the opposite to the D-term contributions, the enhancement for small $\tan\beta$ is absent at tree-level and in MFV. More explicit this is shown in Figures 5.12.

The upper panel in Figure 5.12 shows the contributions from D terms only, while the lower panel include all supersymmetric MFV contributions. We consider the Higgs decay into a hadronic tau where indicated. The difference in the $\tan\beta$ dependence, shown in the figures on the right, is striking. While the D-term contributions are enhanced for low $\tan\beta$, it is the opposite in MFV. But for parameter point A the total rate in MFV is $4-5$ orders of magnitude larger, pointing out that chiral couplings are numerically dominant. The cross sections drop quite fast with an increasing Higgs mass. Even more so if the decay $H^+ \to \tau_{hadr}\nu_\tau$ is included. The

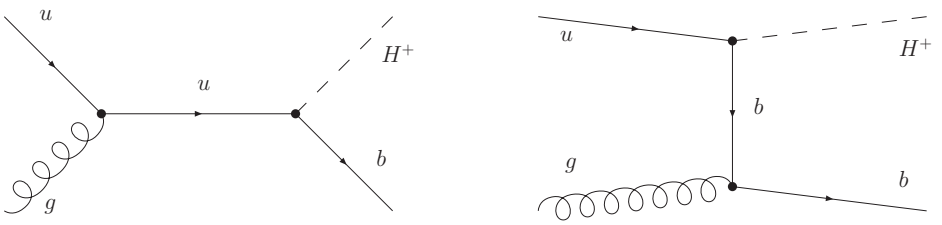

(a) Tree-level diagrams for the partonic process $ug \to H^+b$.

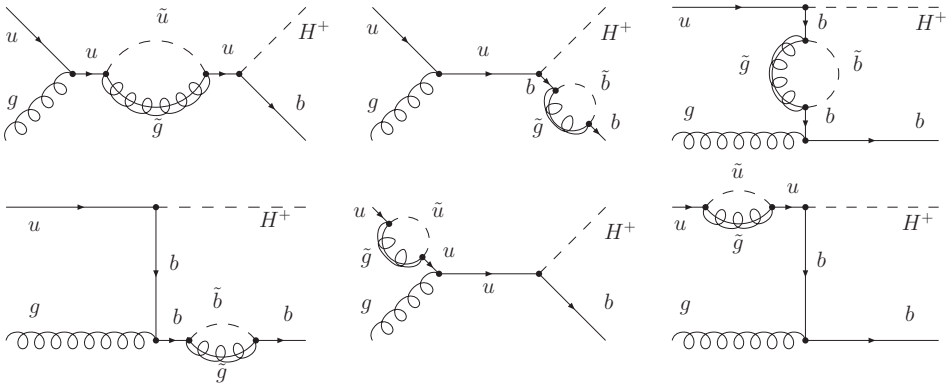

(b) Tree-level diagrams for the partonic process $ug \to H^+b$.

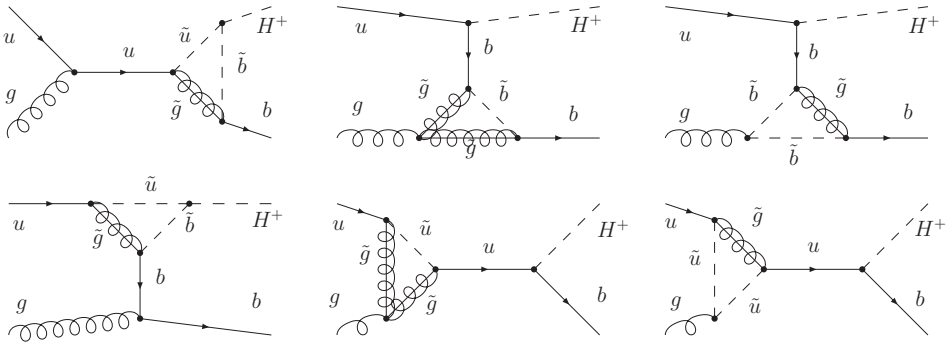

(c) Tree-level diagrams for the partonic process $ug \to H^+b$.

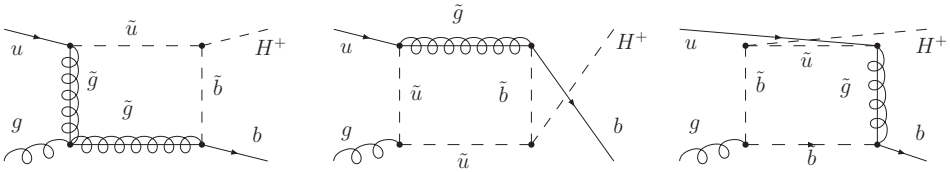

(d) Tree-level diagrams for the partonic process $ug \to H^+b$.

Figure 5.11: $ug \to H^+b$ is one of 18 partonic processes entering the hadronic $pp \to H^+ + jet$.

branching ratio of this decay becomes smaller for larger values of the Higgs mass. Especially in the region around $m_{H^+} \approx 190\,\mathrm{GeV}$ where the decay $H^+ \to t\bar{b}$ is allowed the branching ratio drops fast.

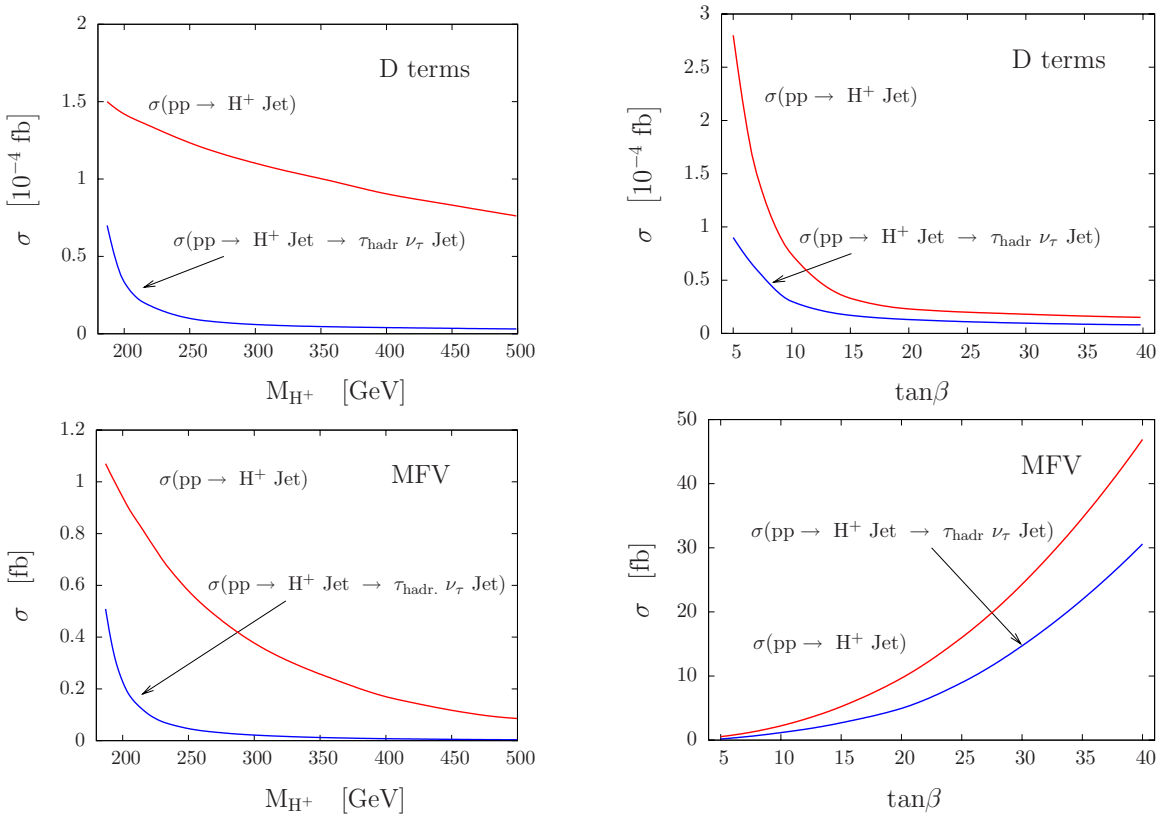

Figure 5.12: Dependence of the hadronic cross section from M_{H^+} and $\tan\beta$. The upper plots show just D-term contributions in $m_f \to 0$, while the lower show the full cross sections in MFV.

Anyway, compared to the large background cross section $\sigma(W + \mathrm{jet}) \approx 1\,\mathrm{nb}$ it is very unlikely to be able to detect a charged Higgs for small $\tan\beta$ at the LHC. Inspired by NMFV effects of the single-Higgs production discussed in Section 5.2.2, we consider the impact of the mixing parameter $\delta^u_{LR,31}$ in charged Higgs + jet production.

5.3.2 $H^+ + \mathrm{jet}$ in NMFV

After allowing for NMFV effects, in contrast to single-charged-Higgs production, the operator basis for a jet-associated production does not get significantly extended. But anyway, if we allow for sizeable $\delta^u_{AB,ij}$ the effective vertices which enhance the production of a single Higgs tremendously contribute here as well. Two kinds of mixings are largely unconstraint: $\delta^u_{RR,3i}$ and $\delta^u_{LL,i3}$. We found in Section 5.2.2 that squark mixing between the first and third generation,

m_{H^+}	$\tan\beta$	$\sigma_{\rm SUSY}$	$\sigma_{\rm SUSY}^{(m_s=0)}$	$\sigma_{\rm SUSY}^{(m_f=0)}$
188 GeV	3	$14.3 \cdot 10^0$	$14.2 \cdot 10^0$	$13.9 \cdot 10^0$
188 GeV	7	$4.6 \cdot 10^0$	$4.4 \cdot 10^0$	$3.0 \cdot 10^0$
400 GeV	3	$2.4 \cdot 10^0$	$2.4 \cdot 10^0$	$2.3 \cdot 10^0$
400 GeV	7	$7.9 \cdot 10^{-1}$	$7.3 \cdot 10^{-1}$	$5.4 \cdot 10^{-1}$
500 GeV	3	$1.3 \cdot 10^0$	$1.3 \cdot 10^0$	$1.2 \cdot 10^0$
500 GeV	5	$5.5 \cdot 10^{-1}$	$5.4 \cdot 10^{-1}$	$5.0 \cdot 10^{-1}$
500 GeV	7	$4.0 \cdot 10^{-1}$	$3.7 \cdot 10^{-1}$	$2.8 \cdot 10^{-1}$

Table 5.2: Production rates (in fb) for the associated production of a charged Higgs with a hard jet: $p_{T,j} > 100$ GeV. SUSY refers to the complete set of supersymmetric diagrams, assuming NMFV. Imposed are the same assumptions as in Figure 5.1.

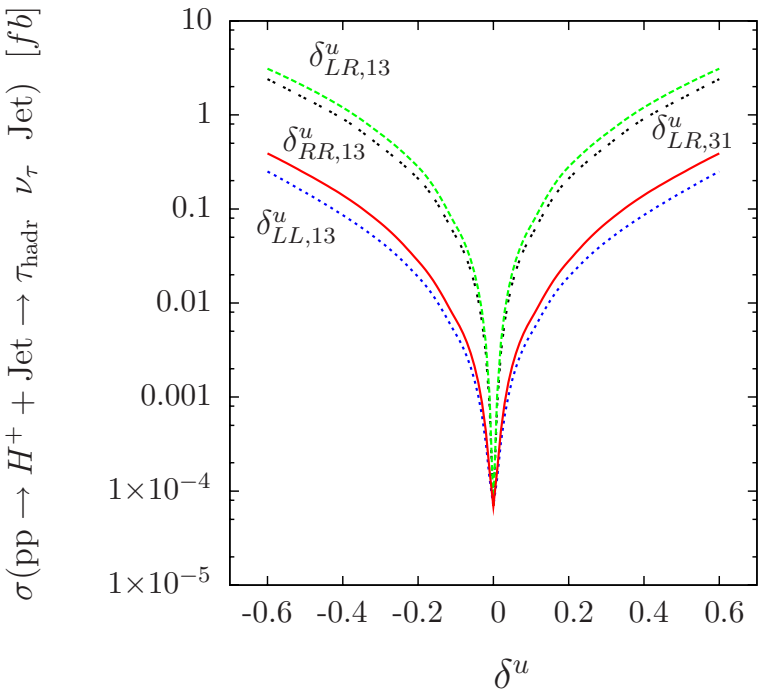

Figure 5.13: Hadronic charged-Higgs-boson production cross section in association with a hard jet, including decays into a hadronic τ. We vary the four δ^u which lead to the largest enhancement of the cross section. No constraints from Section 5.1 are considered.

i.e. $\delta^u_{LR,31}$, cause the largest enhancement. According to Section 5.1 mixing between the second and third generation is equally less constrained but anyway disfavored due to the slightly reduced charm parton density.
In Table 5.2 we show the numerical results for three different charged-Higgs masses (188, 400, 500) GeV and for each two low values of $\tan\beta$ $(3, 7)$. Again, as in Table 5.1, we distinguish between results where we pick up all Yukawa couplings, no bottom-Yukawa and smaller couplings $(m_s = 0)$ and no strange-Yukawa and smaller couplings $(m_b = 0)$. These numbers have to be compard with the MFV results and finally with the W + jet background. The differences between MFV and NMFV are obvious. Where MFV contributions were not enhanced for small $\tan\beta$ the NMFV ones are strongly enhanced. For $m_H^+ = 188$ GeV and $\tan\beta = 3$ the NMFV cross section is roughly 50 times larger than the cross section in MFV, whereas the enhancement factor for $\tan\beta = 7$ is only a factor $\mathcal{O}(5)$. The results are almost insensitive to the contributions of the Yukawa couplings. Even for $(m_f = 0)$ the cross sections remain large, without being proportional to a D-term coupling only; i.e. A-term couplings cause a chiral flip and compensate for the missing Yukawa couplings. Thus, they do not suffer from the fast decoupling of $1/M^8_{SUSY}$. The same effect we see in the left panel of Figure 5.13, where we show the variation of the Higgs cross section times branching ratio to a hadronic tau as a function of the δ^u, each of them varied independently. For example $|\delta^u_{LR,31}| > 0.2$ outgrows the tree-level results for the SUSY parameters listed in (5.58). $|\delta^u_{LR,13}|$ gives the largest contributions due to the additionally induced top-Yukawa coupling to the charged Higgs. But although we very $|\delta^u_{LR,13}|$ and $|\delta^u_{LL,13}|$ up to 0.6 these values are excluded by flavor physics (Sec. 5.1). We nevertheless show the curves, because there might be cancellations of different deltas in the rare-decay observables. The four curves illustrate that the contribution of the different parameters beyond MFV are generically of similar size.
However, all cross sections in MFV and NMFV without considering further decays are small compared to the W + jet background. Strategies to reduce the background are necessary. One possibility is to use the large difference in the distributions of the invariant masses:

$$m^2_{T,H} = (|p_{T,\text{hadr}}| + |p_{T,\text{miss}}|)^2 - (\vec{p}_{T,\text{hadr}} + \vec{p}_{T,\text{miss}})^2 \tag{5.70}$$

For sufficiently large Higgs masses and modulo detector-resolution effect mostly on the missing transverse momentum vector, we could use such a distribution to enhance the signal over the backgrounds (Fig.5.14).
In Figure 5.15 we show the distributions of the transverse momentum of the jets, which are equivalent to the transverse momentum of the bosons. The left plot shows D-term contributions only (Fig.5.10), whereas the right one includes beyond-MFV effects ($\delta_{LR,31} = 0.5$) (Fig.5.11). For small transverse momenta the cross section with D-term couplings is finite, because the loops have no counterpart in single-Higgs production and the $2 \to 2$ process is not an IR-sensitive real-emission correction. Moreover, the heavy particles in the box define the typical energy scale of the process and show a threshold behavior around $p_T \sim 500$ GeV. On contrast, in the right panel we see that the p_T distributions for the charged Higgs and the W boson are infrared divergent for small values p_T. This infrared (soft and collinear) divergences will of course be canceled by virtual corrections and factorization contributions to the single-Higgs or single-W processes. A proper description of the p_T spectrum in the small-p_T domain would require soft-gluon resummation.

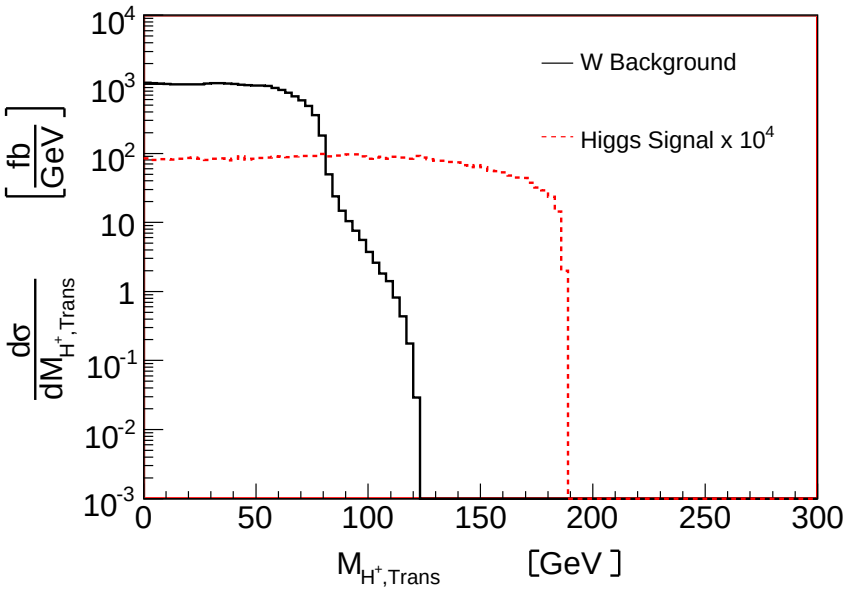

Figure 5.14: Transverse mass distribution for a W boson and a charged Higgs with a hard jet.

5.4 Summary

The results of this chapter are published in [166]. The detection of a charged Higgs is a difficult task for small values of $\tan\beta$ according to present analyses at CMS and Atlas. We studied two types of loop-induced production mechanisms which can significantly increase the production cross section in this parameter region.

The dominant source of genuine supersymmetric flavor enhancement in the charged-Higgs production rate is the soft-breaking A term for up-type squarks A^u_{i3}. It mixes the doublet-stop with light-generation singlets. Stop mixing with $\tilde{u}_R$ or $\tilde{c}_R$ is invisible to Kaon, charm and B-experiments, which are mostly sensitive to the chirality-flipped A^u_{3i}.
Single-charged Higgs production in pp collisions in a general two-Higgs-doublet model is suppressed by either light-generation quark Yukawa couplings or by small CKM mixing. For models with minimal flavor violation, this chiral suppression is generic and cannot be lifted by supersymmetric loops. Without imposing minimal flavor violation supersymmetric loop-contributions can induce left-right chiral flips which enhance the single-charged-Higgs production cross section by an order of magnitude - even after including all current bounds on squark-flavor mixing.
Charged-Higgs production in association with a hard jet does not suffer from a generic chiral suppression. The cross section is even in the limit of neglectable fermion masses finite, due to D-term couplings. Because of the strong SUSY-mass suppression of the D-term contributions they are just a small fraction of the whole amplitude. After allowing for NMFV effects this sup-

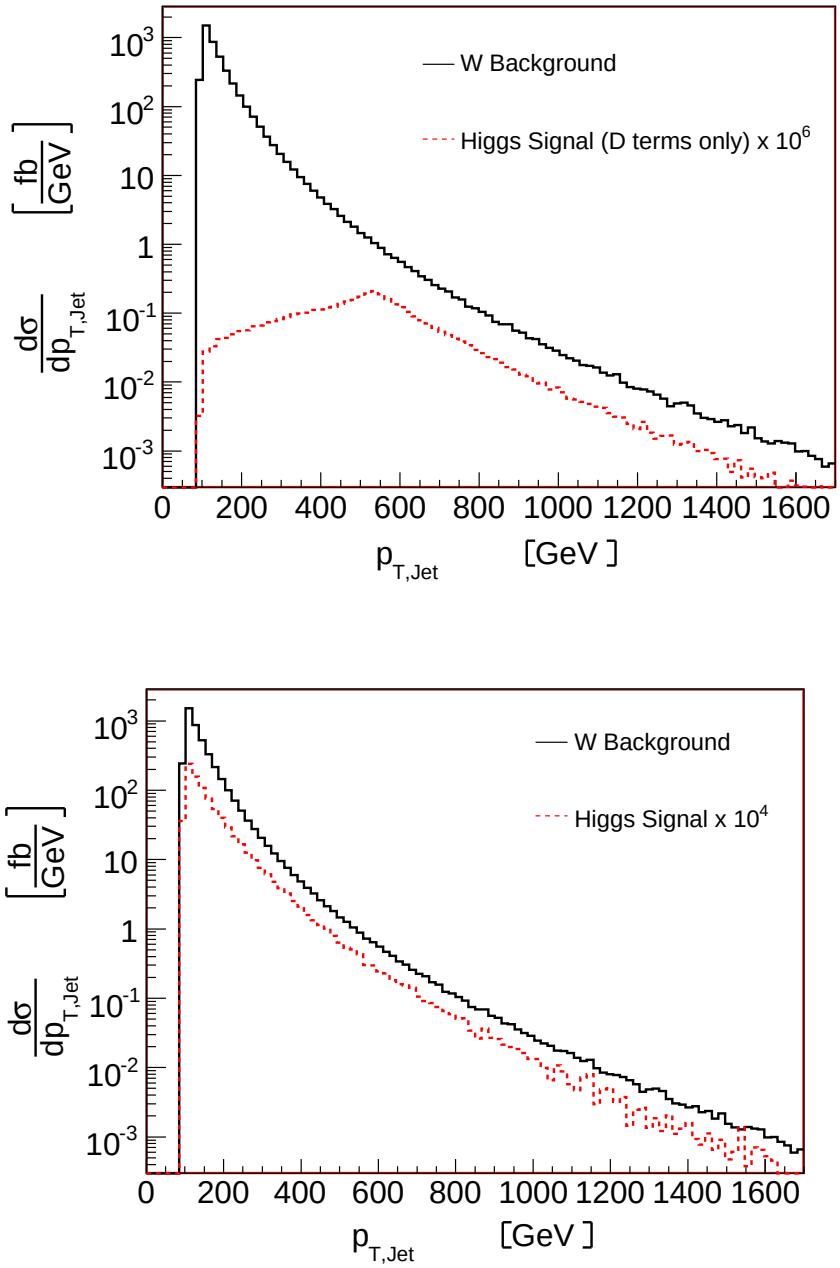

Figure 5.15: Transverse momentum distributions for charged-Higgs production with a jet including the decay to a hadronic tau. We also show the scaled background distributions from W+jet production. The left panel shows MFV and D terms only, The right panel includes beyond-MFV effects ($\delta^u_{LR,31} = 0.5$). All other parameters given in parameter point A.

pression can be compensated by off-diagonal A terms. In contrast to the MFV case in NMFV we observe an enhancement for small $\tan\beta$ and an overall enhancement of the production cross section of one to two orders of magnitude.
For a final decision if a flavor-enhanced charged-Higgs production is detectable at the LHC a detailed signal-to-background analysis is necessary. But the expenditure would be worthwhile itself. Beside a breakdown of the Standard Model, the assumption of minimal-flavor-violation could be excluded. Further, measuring the charged Higgs precisely could give bounds to the free parameters in the soft-susy Lagrangian, $A^u_{LR,3i}$. This is an extraordinary feature for high-energy processes in collider physics.

Chapter 6

Results and Outlook

In this thesis we discussed the discovery potential of a Higgs particle at the LHC within popular extensions of the SM. After giving a very brief review about the most promising production processes and decays of a SM Higgs, we collected results for a Higgs without couplings to fermions. A fermiophobic Higgs, despite the absence of the dominant SM Higgs production process $gg \to H$, appears to be no severe test for the LHC. There are processes over the whole theoretically and experimentally allowed Higgs-mass region ($105\ \mathrm{GeV} \leq m_H \leq 700\ \mathrm{GeV}$).

We reestablished the Standard-Model-extension of a fourth generation. Due to electroweak precision measurements it was excluded by PDG [39]. We showed, that this is not necessarily true. Assuming a proper mass splitting between the particles of the fourth generation, the model is in perfect agreement with all present bounds. The question if the neutrinos are Majorana or Dirac particles does not affect the possible existence of a fourth generation. The Higgs particle would reveal a completely different decay pattern which makes it possible to discriminate this model from other common extensions of the SM, like MSSM or 2HDM. Whereas the enhancement of the effective Higgs-gluon-gluon coupling opens the process $gg \to H \to ZZ$ for the entire Higgs-mass region, making it possible to detect or exclude a Higgs particle at a very early stage after data acquisition.

The most popular extension of the SM is supersymmetry. The assumption of a symmetry between fermions and bosons gives rise to the MSSM, motivated mainly by the hierarchy problem and dark matter. Good agreement between measurements of flavor-physics observables and their SM predictions encourage the assumption of minimal-flavor violation, which is not stipulated from theoretical considerations. We investigated the production of a single-charged Higgs and in association with a hard jet in MFV and NMFV, which is - especially for small $\tan\beta$ - a tedious task. Yukawa-coupling suppression in single-Higgs production, always present in MFV, could be circumvented in NMFV. These additional contributions can enhance the production cross section by one-to-two orders of magnitude. But flavor-violating parameters, induced from the supersymmetry-breaking sector, do contribute to flavor-changing neutral currents as well. Respecting all relevant theoretical and experimental bounds, we determined their allowed numerical values. We found, that the SSB-parameters, which enhance the production of a charged Higgs, are hardly constrained by flavor physics. Hence, we can turn around the argumentation

and state, that if a charged Higgs is detected with a certain production cross section at the LHC this process can be used to constrain the SSB-parameters. This is a rare example where the fields of flavor and collider physics profit from each other mutually. For the production of a charged Higgs in association with a jet we considered the most favorably mixing $\tilde{u}_R$-$\tilde{t}_L$. Although we found a sizeable enhancement in the region of small $\tan\beta$, both processes suffer from a large W-boson background.

The LHC, which has the main task to detect the Higgs particle, will show, if we have to modify our present understanding of the Standard Model and - maybe - will be able to point into the direction of the necessary modifications. In this work we discussed new aspects of Higgs physics in connection with two very popular extensions and gained results relevant for experiments at the LHC. With the improvement of the flavor-physics measurements, demanding for more precise theoretical predictions, constraints to new physics become increasingly severe. Even apart from the two models we presented here, the intersectional field of flavor and collider physics is an interesting ground for further analyses.

Appendix A

CKM matrix

The CKM matrix [130] connects the weak eigenstates (d', s', b') and the mass eigenstates (d, s, b). Its unitarity ensures the absence of elementary FCNC vertices but on the other hand, due to the fact that the matrix coefficients can be complex numbers, it allows CP violation in the Standard Model. This quark-mixing matrix V_{CKM} is defined by

$$\begin{pmatrix} d' \\ s' \\ b' \end{pmatrix} = \underbrace{\begin{pmatrix} V_{ud} & V_{us} & V_{ub} \\ V_{cd} & V_{cs} & V_{cb} \\ V_{td} & V_{ts} & V_{tb} \end{pmatrix}}_{V_{CKM}} \begin{pmatrix} d \\ s \\ b \end{pmatrix} . \tag{A.1}$$

Because of the masslessness of the neutrinos in the Standard Model and the MSSM the analogous mixing matrix is a unit matrix. While many parametrizations of the CKM matrix have been proposed, two of them are very common: the standard parametrization [128] and the Wolfenstein parametrization [167].

Standard Parametrization

The quark-mixing matrix V_{CKM} can be parametrized by three angles and a complex phase. With $c_{ij} = \cos\theta_{ij}$ and $s_{ij} = \sin\theta_{ij}$ $(i, j = 1, 2, 3)$, the standard parametrization is given by:

$$V_{CKM} = \begin{pmatrix} c_{12}c_{13} & s_{12}c_{13} & s_{13}e^{-i\delta} \\ -s_{12}c_{23} - c_{12}s_{23}s_{13}e^{i\delta} & c_{12}c_{23} - s_{12}s_{23}s_{13}e^{i\delta} & s_{23}c_{13} \\ s_{12}s_{23} - c_{12}c_{23}s_{13}e^{i\delta} & -s_{23}c_{12} - s_{12}c_{23}s_{13}e^{i\delta} & c_{23}c_{13} \end{pmatrix} .$$

The complex phase, necessary for CP violation, varies in the range $0 \leq \delta \leq 2\pi$ and the c_{ij} and s_{ij} can be chosen to be positive. Measurements of CP violation in K decays force δ to be in the range $0 < \delta < \pi$. We know from the experiment, that s_{13} and s_{23} are small numbers, hence $c_{13} \approx c_{23} \approx 1$ and the four independent parameters are given by

$$s_{12} = |V_{us}| , \quad s_{13} = |V_{ub}| , \quad s_{23} = |V_{cb}| , \quad \delta.$$

Obviously, the CP violating phase is alwasy multiplied by the very small quantity s_{13}, which shows the suppression of CP violation in SM and MSSM.

Wolfenstein Parametrization

The Wolfenstein parametrization is no exact, but an approximative parametrization of the CKM matrix, where each element is expanded as a power series in the small parameter $\lambda = |V_{us}| = 0.22$,

$$V = \begin{pmatrix} 1 - \frac{\lambda^2}{2} & \lambda & A\lambda^3 (\rho - i\eta) \\ -\lambda & 1 - \frac{\lambda^2}{2} & A\lambda^2 \\ A\lambda^3 (1 - \rho - i\eta) & -A\lambda^2 & 1 \end{pmatrix} + O\left(\lambda^4\right).$$

The four independent parameters in this case are

$$\lambda, \quad A, \quad \rho, \quad \eta.$$

In general, the fits [168] to determine the free parameters of the CKM matrix are not model independent. For calculations in extensions of the Standard Model values which are determined from tree-level processes have to be used. Hence, in these models the CKM matrix introduces large uncertainties to the calculation.

Appendix B

Regularization and Renormalization

In perturbative Quantum Field Theory, beyond tree-level calculations, divergent loop integrals may occur. Physical observables remain finite quantities. Thus, to give these divergent expressions a meaning, one first has to regularize the divergence. For this purpose several regularization schemes have been developed. The two most popular are dimensional regularization (DRED) and dimensional reduction (DREG). In any case the singularities are parameterized by a regularization parameter, from which then the resulting integrals depend.
Dimensional regularization exploits the fact that the divergent behavior of the integrals depends on the space-time dimension in which they are performed [169]. Shifting from 4 to $D = 4 - 2\varepsilon$ dimensions the divergences appear as poles in the infinitesimal parameter ε. This method respects Lorentz and gauge invariance but introduces peculiarities in the treatment of the matrix $\gamma_5 \equiv i\gamma^0\gamma^1\gamma^2\gamma^3 = -i/4\varepsilon^{\mu\nu\rho\sigma}$ which is obviously a four-dimensional object, anti-commuting with the matrices γ^μ in four dimensions. In the technically elaborate HV scheme [170] γ^5 can be treated consistently, even in d dimensions. For supersymmetric theories a further disadvantage of DREG comes from the fact that supersymmetry is not preserved. After shifting to D dimensions the numbers of fermionic and bosonic degrees of freedom do not coincide anymore. Hence, DRED, a modification of DREG, was introduced, also modifying the dimensionality of spacetime, but maintains four-vectors as four-component objects. Just recently a mathematically consistent formulations could be established [171]. DRED thus preserves supersymmetry, at least up to two-loop calculations.
Calculations using DRED versus DREG differ only in the finite parts of one-loop amplitudes, but differ even in the divergent part of two-loop amplitudes. Thus, the renormalization group equation (RGE) calculated via DREG or via DRED will be equivalent to one-loop order.

Next, the renormalization procedure takes care of eliminating the unphysical parameters in the theory, introduced via regularization. For a predictive theory it must be ensured that the renormalization process does not induce new couplings in any new order of perturbation theory. This would lead to a non-renormalizable theory with infinitely many undetermined parameters. If all the couplings of the Lagrangian have non-negative dimension the theory is renormalizable, e.g. SM, MSSM. In effective field theories couplings with negative dimension may occur. Here the parameters of this theory is fixed by a matching procedure, in which the effective

theory Green's functions are related to Standard Model Green's functions, so that the theory is predictive.

Multiplicative renormalization is frequently used, where bare parameters g_0 of the Lagrangian are replaced by renormalized parameters g and renormalization constants Z_g according to the relation

$$g_0 = Z_g g = \left(1 + \delta Z_g^{(1)} + \delta Z_g^{(2)} + ...\right) g, \tag{B.1}$$

where on the right-hand side the renormalization constant has been expanded in orders of perturbation theory. The $\delta Z_g^{(i)}$ absorb the divergences which appear in the loop integrals. Thus they remove the depdce on unphysical regularization parameter. For a finite theoretical description all Green functions have to be finite. For this reason field renormalization has to be performed. Therefore the bare fields Φ_0 are replaced by the renormalized ones Φ and the field renormalization constant Z_Φ

$$\Phi_0 = \sqrt{Z_\Phi}\Phi = \left(1 + \frac{1}{2}\delta Z_\Phi^{(1)} - \frac{1}{8}\delta Z_\Phi^{(1)^2} + \frac{1}{2}\delta Z_\Phi^{(2)} + ...\right)\Phi. \tag{B.2}$$

After applying this redefinition of fields and free parameters, the Lagrangian can be split into a renormalized part and a couter term part:

$$\mathcal{L}\left(g_0, \Phi_0\right) = \mathcal{L}\left(Z_g g, \sqrt{Z_\Phi}\Phi\right) = \mathcal{L}\left(g, \Phi\right) + \mathcal{L}_{CT}\left(g, \Phi, \delta Z_g, \delta Z_\Phi\right). \tag{B.3}$$

The renormalized Lagrangian is finite, free of unphysical regularization parameters and thus suitable for theoretical predictions. The counter term part can be expressed as perturbation series in terms of the loop order

$$\begin{aligned}\mathcal{L}_{CT}\left(g, \Phi, Z_g, Z_\Phi\right) &= \mathcal{L}_{CT}^{(1)}\left(g, \Phi, \delta Z_g^{(1)}, \delta Z_\Phi^{(1)}\right) + \\ &\quad \mathcal{L}_{CT}^{(2)}\left(g, \Phi, \delta Z_g^{(1)}, \delta Z_\Phi^{(1)}, \delta Z_g^{(2)}, \delta Z_\Phi^{(2)}\right) + ...\end{aligned} \tag{B.4}$$

The definition of the finite parts of the renormalization constants is not unambiguously. Instead, their definition, relating the parameters of the theory to observables, comprise a renormalization scheme. Although practically not realizable, the result of a calculation up to infinite order in perturbation theory is renormalization scheme independent. The resulting dependence on the renormalization scheme in preformed calculations reflects the theoretical uncertainty due to missing higher-order terms.
The minimal subtraction scheme [172] (MS-scheme) is the simplest renormalization scheme. Only the divergent terms in the higher order contributions are absorbed into the counter term part of Lagrangian, but no finite contributions. The mass parameter μ introduced by the regularization to keep couplings dimensionless is now transformed to a renormalization scale parameter μ_R. A modification of the MS-scheme is the $\overline{MS}$-scheme [173]. In this scheme not only the $1/\varepsilon$ poles are subtracted but a quantity Δ^n, where n is the loop order. At one loop it reads

$$\Delta = \frac{1}{\varepsilon} - \gamma_E + \ln 4\pi. \tag{B.5}$$

γ_E is the Euler-Mascheroni constant. The $\overline{MS}$ scale is redefined as

$$\mu_R^{2\overline{MS}} \equiv \mu_R^2 e^{\ln 4\pi - \gamma_E}. \tag{B.6}$$

While the $\overline{MS}$-scheme is based on DREG the $\overline{DR}$-schem is based on DRED. Apart from that, at one-loop level, the procedure is identical and the counterterms are the same.
Another possibility is the on-shell scheme (OS scheme) [161]. On-shell means that the renormalization conditions are set for particles on their mass shell. To obey the on-shell conditions, not only divergent parts but also finite contributions are contained in the couter terms. It implies that the mass of a particle is given as real part of the pole of the propagator and thus can be interpreted as the physical mass. Additionally it is assumed that all couplings are renormalized by demanding that the coupling constants stay unchanged if all particles coupling of the vertex are on-shell. The fields are determined to be on-shell by a consistent normalization, i.e. the residua of the propagators have to be equal to unity.
Complete expressions for the OS renormalization scheme within the SM and MSSM are given in [161] and [174] respectively. For the SUSY-QCD corrections in Sections 5.2.2 and 5.3.2 we use DRED and OS scheme.

Renormalization conditions for the charged Higgs production

Here we briefly give the renormalization conditions imposed for the processes described in Sections 5.3.2 and 5.2.2. We just consider SUSY-QCD corrections.

Quarks

According to (B.2) the bare parameters in the Lagrangian are replaced by the renormalized quantities.

$$\begin{aligned} P_{L,R}\Psi_{f,i} &\rightarrow \left(1 + \frac{1}{2}\left[\delta Z_f^{L,R}\right]_{ij}\right)\Psi_{f,j}, \\ m_{f,i} &\rightarrow m_{f,i} + \delta m_i^f, \end{aligned} \tag{B.7}$$

where $\Psi_{L,R}$ are the left- and right-handed components fo the quark fields. Renormalized self-energies $\hat{\Sigma}$ can be parametrized by unrenormalized self-energies Σ and the corresponding counter terms:

$$\begin{aligned} \left[\hat{\Sigma}_f^L\left(p^2\right)\right]_{ij} &= \left[\Sigma_f^L\left(p^2\right)\right]_{ij} + \frac{1}{2}\left(\delta Z_f^L + \delta Z_f^{L\dagger}\right)_{ij}, \\ \left[\hat{\Sigma}_f^R\left(p^2\right)\right]_{ij} &= \left[\Sigma_f^R\left(p^2\right)\right]_{ij} + \frac{1}{2}\left(\delta Z_f^R + \delta Z_f^{R\dagger}\right)_{ij}, \\ \left[\hat{\Sigma}_f^{SL}\left(p^2\right)\right]_{ij} &= \left[\Sigma_f^{SL}\left(p^2\right)\right]_{ij} - \left[\frac{1}{2}\left(m_{f,i}\delta Z_f^L + m_{f,j}\delta Z_f^{R\dagger}\right) + \delta m_i^f\ \mathbf{1}\right]_{ij}, \\ \left[\hat{\Sigma}_f^{SR}\left(p^2\right)\right]_{ij} &= \left[\Sigma_f^{SR}\left(p^2\right)\right]_{ij} - \left[\frac{1}{2}\left(m_{f,i}\delta Z_f^R + m_{f,j}\delta Z_f^{L\dagger}\right) + \delta m_i^f\ \mathbf{1}\right]_{ij}, \end{aligned} \tag{B.8}$$

using the decomposition

$$\Sigma_{ab}(p) = \not{p} P_L \Sigma^L_{ab}\left(p^2\right) + \not{p} P_R \Sigma^R_{ab}\left(p^2\right) + P_L \Sigma^{SL}_{ab}\left(p^2\right) + P_R \Sigma^{SR}_{ab}\left(p^2\right). \tag{B.9}$$

The renormalization conditions for the renormalized self-energies can be chosen to be:

$$\begin{aligned}
m_j \operatorname{Re}\hat{\Sigma}^R_{ij}\left(m_j^2\right) + \operatorname{Re}\hat{\Sigma}^{SL}_{ij}\left(m_j^2\right) &= 0,\\
m_j \operatorname{Re}\hat{\Sigma}^L_{ij}\left(m_j^2\right) + \operatorname{Re}\hat{\Sigma}^{SR}_{ij}\left(m_j^2\right) &= 0,\\
m_i \operatorname{Re}\hat{\Sigma}^L_{ij}\left(m_i^2\right) + \operatorname{Re}\hat{\Sigma}^{SL}_{ij}\left(m_i^2\right) &= 0,\\
m_i \operatorname{Re}\hat{\Sigma}^R_{ij}\left(m_i^2\right) + \operatorname{Re}\hat{\Sigma}^{SR}_{ij}\left(m_i^2\right) &= 0,\\
\operatorname{Re}\hat{\Sigma}^L_{ii}\left(m_i^2\right) + m_i^2\left[\operatorname{Re}\hat{\Sigma}^{L\prime}_{ii}\left(m_i^2\right) + \operatorname{Re}\hat{\Sigma}^{R\prime}_{ii}\left(m_i^2\right)\right] &\\
+ m_i\left(\operatorname{Re}\hat{\Sigma}^{SL\prime}_{ii}\left(m_i^2\right) + \hat{\Sigma}^{SR\prime}_{ii}\left(m_i^2\right)\right) &= 0,
\end{aligned} \tag{B.10}$$

with $\hat{\Sigma}^{X\prime}_{ij}\left(m^2\right) \equiv \frac{d}{dp^2}\hat{\Sigma}^X_{ij}\left(p^2\right)\Big|_{p^2=m^2}$.

After inserting (B.8) in (B.10) we can fix the renormalization constants, δm_i^f and $\delta Z_f^{L/R}$, in terms of the unrenormalized self-energies:

$$\begin{aligned}
\delta m_i^f &= \frac{1}{2}\operatorname{Re}\left[m_{f,i}\left[\Sigma^L_f\left(m^2_{f,i}\right) + \Sigma^R_f\left(m^2_{f,i}\right)\right] + \Sigma^{SL}_f\left(m^2_{f,i}\right) + \Sigma^{SR}_f\left(m^2_{f,i}\right)\right]_{ii}\\
\left[\delta Z_f^{L/R}\right]_{ii} &= -\operatorname{Re}\left[\Sigma^{L/R}_f\left(m^2_{f,i}\right) + m^2_{f,i}\left[\Sigma^{L\prime}_f\left(m^2_{f,i}\right) + \Sigma^{R\prime}_f\left(m^2_{f,i}\right)\right]\right.\\
&\quad \left. + m_{f,i}\left[\Sigma^{SL\prime}_f\left(m^2_{f,i}\right) + \Sigma^{SR\prime}_f\left(m^2_{f,i}\right)\right]\right]_{ii}\\
&\quad + \frac{1}{2m_{f,i}}\operatorname{Re}\left[\Sigma^{SL}_f\left(m^2_{f,i}\right) - \Sigma^{SR}_f\left(m^2_{f,i}\right)\right]_{ii}\\
\left[\delta Z_f^{L/R}\right]_{ij} &= \frac{2}{m^2_{f,i} - m^2_{f,j}}\operatorname{Re}\left[m^2_{f,j}\Sigma^{L/R}_f\left(m^2_{f,j}\right) + m_{f,i}m_{f,j}\Sigma^{R/L}_f\left(m^2_{f,j}\right)\right.\\
&\quad \left. + m_{f,i}\Sigma^{SL/SR}_f\left(m^2_{f,j}\right) + m_{f,j}\Sigma^{SR/SL}_f\left(m^2_{f,j}\right)\right]_{ij}
\end{aligned}$$

Charged Higgs

Apart from the quarks the relevant parameters for the charged Higgs have to be renormalized. The renormalized self-energy is

$$\begin{aligned}
\hat{\Sigma}^{cH}_{ij}\left(p^2\right) &= \Sigma^{cH}_{ij}\left(p^2\right) + \left[\frac{1}{2}\left(\delta Z^\dagger_{H^-G^-} + \delta Z_{H^-G^-}\right)p^2\right.\\
&\quad \left. - \frac{1}{2}\left(\delta Z^\dagger_{H^-G^-}M^{HG} + M^{HG}\delta Z_{H^-G^-}\right) - \delta M^{H^-G^-}\right]_{ij}.
\end{aligned}$$

Again, the renormalization constants can be fixed in terms of the unrenormalized self-energies and mass parameters:

$$\begin{aligned}
\left[\delta Z_{H^-G^-}\right]_{ii} &= -\frac{d}{dp^2}\operatorname{Re}\left[\Sigma^{cH}\left(p^2\right)\right]\Big|_{p^2=m^2},\\
\left[\delta Z_{H^-G^-}\right]_{ij} &= \frac{2}{m_i^2 - m_j^2}\left[\operatorname{Re}\Sigma^{cH}\left(m_j^2\right) - \delta M^{hH}_{AG}\right]_{ij},
\end{aligned}$$

with $m_1 \equiv m_{H^\pm}$, $m_2 \equiv m_{G^\pm} = 0$. Algebraic expressions for δM^{hH}_{AG} and $\delta M^{H^- G^-}$ are given in [174].

Appendix C

Hadronic cross sections

Quantum Chromodynamics [39, 175], based on the $SU(3)_C$ gauge group, describes the strong interactions in the SM and MSSM. Its peculiarities stem from two special properties: Asymptotic freedom and confinement.
Due to asymptotic freedom for short-distances the interaction strength becomes weaker, which enables the strongly interacting particles, i.e. quarks and gluons, to behave almost like free particles. For large distances it is the opposite. The interaction strength rises with distance and binds the particles tightly together. Thus, quarks and gluons cannot be observed as free particles, but only as constituents of hadrons, i.e. mesons (quark-anti-quark pairs) and hadrons (three quarks or anti-quarks). Due to confinement, perturbation theory might not be justified at the hadronic level. Therefore, it is necessary to establish a connection between the short-distance interactions of quarks and gluons which can be described by means of perturbation theory and the experimentally observable interactions of hadrons. This is provided by the parton model [176] and the factorization theorem [177].
The Parton Model is a legacy of the preQCD era ($<$1972)[1]. It was motivated by experimental results from deep inelastic electron-proton scattering (DIS) [178], assuming, that every observable consists of constituents, the so-called partons, which can be identified as quarks and gluons. A further succes the explanation of Bjorken scaling [179], which states, that the structure functions in the deep inelastic region do not depend on the momentum transfer squared q^2 *and* the energy transfer ν but merely from the ratio $x = q^2/2M\nu$. This implies that the constituents of the nucleon look almost free and point-like when observed with high resolution. Hence, the process of electron-proton scattering can be approximated as an incoherent sum of elastic lepton-parton scattering, which can be described by perturbation theory.
Due to Lorentz time dilation the hadron can be treated as a static object during the scattering process. Time scales related to the movement of the hadron and to the non-perturbative process of hadronization are much larger than the time scale of the hard scattering. A parton which participates in the hard scattering carries a momentum xP^μ with $x \in [0, 1]$.
This concept can be extended to interactions of hadrons, e.g. protons, relevant for the LHC. Two colliding hadrons interact at the partonic level via a hard interaction of two partons which

[1] Later it was justified by taking QCD into account (QCD improved parton model).

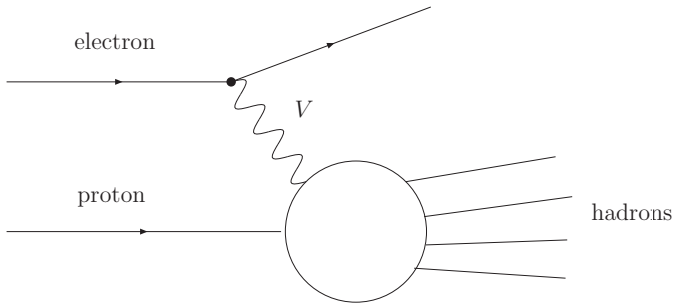

Figure C.1: Deep inelastic scattering

both carry certain fractions of hadron momenta. The hadronic cross section can be cast in the form:

$$\sigma_{had}\left(P_A, P_B\right) = \sum_{i,j} \int_0^1 \int_0^1 dx_a dx_b \hat{\sigma}_{i,j}\left(x_a P_A, x_b P_B, \mu_R\right) \Phi_{i|A}\left(x_a, \mu_f\right) \Phi_{j|B}\left(x_b, \mu_f\right). \quad \text{(C.1)}$$

$\hat{\sigma}_{i,j}$ is the partonic cross section and $\Phi_{i|A}\left(x_a, \mu_f\right)$ and $\Phi_{j|B}\left(x_b, \mu_f\right)$ are parton distribution functions (PDFs). The PDFs represent the probability to find a parton $i\,(j)$ with momentum fraction $x_a\,(x_b)$ in a hadron $A\,(B)$. Here the factorization theorem states that it is possible to separate the perturbative partonic cross section from the non-perturbative parton distribution functions. At this order of approximation the parton distribution functions are just momentum fraction dependend. The parton densities have to be determined from experiment. They are universal and hence can be used for the calculation of any hadronic process. μ_f and μ_R are factorization and renormalization scales respectively which are introduced to distinguish between long- and short-distance interactions. A consistent computation of hadronic cross sections necessitates that the short-distance partonic cross section is infrared-safe and the mass singularities have to be subtracted and absorbed into the parton distributions.

Appendix D

Quark masses

We use the running quark masses at next-to-leading order

$$m(\mu) = m(\mu_0) \left[\frac{\alpha_s(\mu)}{\alpha_s(\mu_0)}\right]^{\gamma_m^{(0)}/(2\beta_0)} \left[1 + \left(\frac{\gamma_m^{(1)}}{2\beta_0} - \frac{\beta_1\gamma_m^{(0)}}{2\beta_0^2}\right)\frac{\alpha_s(\mu) - \alpha_s(\mu_0)}{4\pi}\right]. \qquad \text{(D.1)}$$

Here, $\beta_0 = 11{-}2/3\, N_f$, $\beta_1 = 102{-}38/3\, N_f$, $\gamma_m^{(0)} = 6C_F$ and $\gamma_m^{(1)} = C_F\ (3C_F + 97 - 10/3N_f)$, where N_f denotes the number of quarks with $m_f \leq \mu$.

For our numerical analysis we use the numerical values for the quark masses [180]:

$m_u\,(2\text{ GeV})$ 2.8 ± 0.6 MeV	$m_d\,(2\text{ GeV})$ 5.0 ± 1.0 MeV	$m_s\,(2\text{ GeV})$ 95 ± 15 MeV
$m_c\,(m_c)$ 1.28 ± 0.05 GeV	$m_b\,(m_b)$ 4.22 ± 0.05 GeV	$m_t\,(m_t)$ 163 ± 3 GeV
$m_u\,(m_Z)$ 1.7 ± 0.4 MeV	$m_d\,(m_Z)$ 3.0 ± 0.6 MeV	$m_s\,(m_Z)$ 54 ± 8 MeV
$m_c\,(m_Z)$ 0.62 ± 0.03 GeV	$m_b\,(m_Z)$ 2.87 ± 0.03 GeV	$m_t\,(m_Z)$ 171 ± 3 GeV

(D.2)

Bibliography

[1] Y. Fukuda *et al.* [Super-Kamiokande Collaboration], Phys. Rev. Lett. **81**, 1562 (1998).

[2] D. Clowe, M. Bradac, A. H. Gonzalez, M. Markevitch, S. W. Randall, C. Jones and D. Zaritsky, arXiv:astro-ph/0608407; G. W. Angus, H. Shan, H. Zhao and B. Famaey, Astrophys. J. **654**, L13 (2007) [arXiv:astro-ph/0609125].

[3] G. Bertone, D. Hooper and J. Silk, Phys. Rept. **405**, 279 (2005).

[4] S. R. Coleman and J. Mandula, Phys. Rev. **159**, 1251 (1967).

[5] S. L. Glashow, Nucl. Phys. **22**, 579 (1961); A. Salam, "Weak And Electromagnetic Interactions," *Elementary Particle Theory, Proceedings Of The Nobel Symposium Held 1968 At Lerum, Sweden*, Stockholm 1968, 367-377*; S. Weinberg, Phys. Rev. Lett. **19**, 1264 (1967).

[6] G. Arnison *et al.* [UA1 Collaboration], Phys. Lett. B **122**, 103 (1983).

[7] H. Fritzsch and M. Spannowsky, Europhys. Lett. **75**, 882 (2006).

[8] Y. Nambu, Phys. Rev. Lett. **4**, 380 (1960); J. Goldstone, Nuovo Cim. **19**, 154 (1961).

[9] G. Abbiendi *et al.* [OPAL Collaboration], Eur. Phys. J. C **45**, 307 (2006); P. Achard *et al.* [L3 Collaboration], Eur. Phys. J. C **45**, 569 (2006); S. Schael *et al.* [ALEPH Collaboration], Eur. Phys. J. C **47**, 309 (2006).

[10] G. Abbiendi *et al.* [OPAL Collaboration], Eur. Phys. J. C **19**, 587 (2001); P. Abreu *et al.* [DELPHI Collaboration], Eur. Phys. J. C **16**, 371 (2000); M. Acciarri *et al.* [L3 Collaboration], Eur. Phys. J. C **16**, 1 (2000); R. Barate *et al.* [ALEPH Collaboration], Eur. Phys. J. C **14**, 1 (2000).

[11] J. Alcaraz *et al.* [ALEPH Collaboration], arXiv:hep-ex/0612034.

[12] [ALEPH Collaboration], Phys. Rept. **427**, 257 (2006).

[13] C. F. Kolda and H. Murayama, JHEP **0007**, 035 (2000).

[14] J. Gunion, H. Haber, G. Kane and S. Dawson, *The Higgs Hunter's Guide*, Addison-Wesley, 1990.

[15] W. J. Marciano, G. Valencia and S. Willenbrock, Phys. Rev. D **40**, 1725 (1989).

[16] H. Arason, D. J. Castano, B. Keszthelyi, S. Mikaelian, E. J. Piard, P. Ramond and B. D. Wright, Phys. Rev. D **46**, 3945 (1992).

[17] M. Gockeler, H. A. Kastrup, T. Neuhaus and F. Zimmermann, Nucl. Phys. B **404**, 517 (1993).

[18] M. Sher, Phys. Rept. **179**, 273 (1989).

[19] A. Djouadi, "The anatomy of electro-weak symmetry breaking. I: The Higgs boson in the standard model," (2005).

[20] G. Isidori, G. Ridolfi and A. Strumia, Nucl. Phys. B **609**, 387 (2001).

[21] D. Graudenz, M. Spira and P. M. Zerwas, Phys. Rev. Lett. **70**, 1372 (1993).

[22] R. N. Cahn and S. Dawson, Phys. Lett. B **136**, 196 (1984) [Erratum-ibid. B **138**, 464 (1984)]; D. A. Dicus and S. S. D. Willenbrock, Phys. Rev. D **32**, 1642 (1985).

[23] T. Han, G. Valencia and S. Willenbrock, Phys. Rev. Lett. **69**, 3274 (1992).

[24] R. Raitio and W. W. Wada, Phys. Rev. D **19**, 941 (1979); W. Beenakker, S. Dittmaier, M. Kramer, B. Plumper, M. Spira and P. M. Zerwas, Phys. Rev. Lett. **87**, 201805 (2001).

[25] M. Spira, http://people.web.psi.ch/spira/proglist.html

[26] A. Djouadi, J. Kalinowski and M. Spira, Comput. Phys. Commun. **108**, 56 (1998) [arXiv:hep-ph/9704448].

[27] J. R. Ellis, M. K. Gaillard and D. V. Nanopoulos, Nucl. Phys. B **106**, 292 (1976); M. A. Shifman, A. I. Vainshtein, M. B. Voloshin and V. I. Zakharov, Sov. J. Nucl. Phys. **30**, 711 (1979) [Yad. Fiz. **30**, 1368 (1979)]; B. A. Kniehl and M. Spira, Z. Phys. C **69**, 77 (1995).

[28] V. Buscher and K. Jakobs, Int. J. Mod. Phys. A **20**, 2523 (2005).

[29] CMS Collaboration, Nucl. Part. Phys. **34**,995 (2007)

[30] H. Georgi, Hadronic J. **1**, 155 (1978).

[31] J. A. Grifols and A. Mendez, Phys. Rev. D **22**, 1725 (1980).

[32] L. Brucher and R. Santos, Eur. Phys. J. C **12**, 87 (2000); A. Barroso, L. Brucher and R. Santos, Phys. Rev. D **60**, 035005 (1999); A. G. Akeroyd and M. A. Diaz, Phys. Rev. D **67**, 095007 (2003);

[33] P. Achard *et al.* [L3 Collaboration], Phys. Lett. B **568**, 191 (2003). A. Sopczak, Phys. Part. Nucl. **36**, 65 (2005) [Fiz. Elem. Chast. Atom. Yadra **36**, 127 (2005)].

[34] A. Stange, W. J. Marciano and S. Willenbrock, Phys. Rev. D **49**, 1354 (1994).

[35] R. Kinnunen, H.D. Yildiz, M.T. Zeyrek, CMS-Note-2001/050; D. Dittmar and A.S. Nicollerat, CMS-Note-2001/036; S. Asai *et al.*, Eur. Phys. J. C **32S2**, 19 (2004); D. Acosta, M. Stoutimore, S.M. Wang, CMS-Note-2001/033.

[36] G. L. Landsberg and K. T. Matchev, Phys. Rev. D **62**, 035004 (2000).

[37] X. Calmet and H. Fritzsch, Phys. Lett. B **496**, 190 (2000).

[38] C. T. Hill, Phys. Lett. B **345**, 483 (1995).

[39] W. M. Yao *et al.* [Particle Data Group], J. Phys. G **33**, 1 (2006).

[40] P. H. Frampton, P. Q. Hung and M. Sher, Phys. Rept. **330**, 263 (2000).

[41] M. E. Peskin and T. Takeuchi, Phys. Rev. D **46**, 381 (1992).

[42] H. J. He, N. Polonsky and S. f. Su, Phys. Rev. D **64**, 053004 (2001).

[43] V. A. Novikov, L. B. Okun, A. N. Rozanov and M. I. Vysotsky, Phys. Lett. B **529**, 111 (2002).

[44] V. A. Novikov, L. B. Okun, A. N. Rozanov and M. I. Vysotsky, JETP Lett. **76**, 127 (2002) [Pisma Zh. Eksp. Teor. Fiz. **76**, 158 (2002)].

[45] M. Maltoni, V. A. Novikov, L. B. Okun, A. N. Rozanov and M. I. Vysotsky, Phys. Lett. B **476**, 107 (2000).

[46] E. Arik, M. Arik, S. A. Cetin, T. Conka, A. Mailov and S. Sultansoy, Eur. Phys. J. C **26**, 9 (2002).

[47] E. Arik, O. Cakir, S. A. Cetin and S. Sultansoy, Phys. Rev. D **66**, 033003 (2002).

[48] J. M. Frere, A. N. Rozanov and M. I. Vysotsky, Phys. Atom. Nucl. **69**, 355 (2006).

[49] E. Arik, O. Cakir, S. A. Cetin and S. Sultansoy, Acta Phys. Polon. B **37**, 2839 (2006).

[50] B. Holdom, JHEP **0608**, 076 (2006); B. Holdom, JHEP **0703**, 063 (2007); B. Holdom, arXiv:0705.1736 [hep-ph].

[51] W. Skiba and D. Tucker-Smith, Phys. Rev. D **75**, 115010 (2007).

[52] P. Achard *et al.* [L3 Collaboration], Phys. Lett. B **587**, 16 (2004).

[53] B. W. Lynn, M. E. Peskin and R. G. Stuart, in Physics at LEP, CERN Report 86-02.

[54] M. Golden and L. Randall, Nucl. Phys. B **361**, 3 (1991); D. C. Kennedy and P. Langacker, Phys. Rev. Lett. **65**, 2967 (1990) [Erratum-ibid. **66**, 395 (1991)]; C. P. Burgess, Pramana **45**, S47 (1995).

[55] B. A. Kniehl, Nucl. Phys. B **352**, 1 (1991).

[56] J. Alcaraz *et al.* [ALEPH Collaboration], arXiv:hep-ex/0612034.

[57] [CDF Collaboration], arXiv:hep-ex/0703034.

[58] E. Gates and J. Terning, Phys. Rev. Lett. **67**, 1840 (1991).

[59] B. A. Kniehl and H. G. Kohrs, Phys. Rev. D **48**, 225 (1993).

[60] E. Golowich, J. Hewett, S. Pakvasa and A. A. Petrov, arXiv:0705.3650 [hep-ph].

[61] W. S. Hou, R. S. Willey and A. Soni, Phys. Rev. Lett. **58**, 1608 (1987) [Erratum-ibid. **60**, 2337 (1988)]; W. S. Hou, A. Soni and H. Steger, Phys. Lett. B **192**, 441 (1987).

[62] J. L. Hewett, Phys. Lett. B **193**, 327 (1987); G. Eilam, J. L. Hewett and T. G. Rizzo, Phys. Lett. B **193**, 533 (1987); J. L. Hewett and T. G. Rizzo, Mod. Phys. Lett. **3A**, 975 (1988).

[63] V. M. Abazov *et al.* [D0 Collaboration], arXiv:hep-ex/0612052.

[64] T. P. Cheng and L. F. Li, *Oxford, Uk: Clarendon (1984) 536 P. (Oxford Science Publications)*

[65] P. Bamert, C. P. Burgess and R. N. Mohapatra, Nucl. Phys. B **438**, 3 (1995).

[66] P. Achard *et al.* [L3 Collaboration], Phys. Lett. B **517**, 75 (2001).

[67] J. Conway et *al.*,
http://www-cdf.fnal.gov/physics/new/top/2005/ljets/tprime/gen6/public.html

[68] S. M. Oliveira and R. Santos, Phys. Rev. D **68**, 093012 (2003).

[69] M. Sher, Phys. Rev. D **61**, 057303 (2000).

[70] A. Arhrib and W. S. Hou, Phys. Rev. D **64**, 073016 (2001).

[71] CDF Collaboration, arXiv:0706.3264 [hep-ph].

[72] J. F. Gunion, D. W. McKay and H. Pois, Phys. Lett. B **334**, 339 (1994); J. F. Gunion, D. W. McKay and H. Pois, Phys. Rev. D **53**, 1616 (1996).

[73] S. C. Hsu [CDF Collaboration], arXiv:0706.2200 [hep-ex].

[74] D0 collaboration, http://www-d0.fnal.gov/Run2Physics/WWW/results/prelim/HIGGS/H21/H21F0_supplement.eps

[75] D. L. Rainwater and D. Zeppenfeld, Phys. Rev. D **60**, 113004 (1999) [Erratum-ibid. D **61**, 099901 (2000)]; N. Kauer, T. Plehn, D. L. Rainwater and D. Zeppenfeld, Phys. Lett. B **503**, 113 (2001).

[76] M. Dittmar and H. K. Dreiner, Phys. Rev. D **55**, 167 (1997).

[77] T. Plehn, D. L. Rainwater and D. Zeppenfeld, Phys. Lett. B **454**, 297 (1999); A. Alves, O. Eboli, T. Plehn and D. L. Rainwater, Phys. Rev. D **69**, 075005 (2004).

[78] O. J. P. Eboli and D. Zeppenfeld, Phys. Lett. B **495**, 147 (2000).

[79] T. Plehn, D. L. Rainwater and D. Zeppenfeld, Phys. Rev. Lett. **88**, 051801 (2002); V. Hankele, G. Klamke, D. Zeppenfeld and T. Figy, Phys. Rev. D **74**, 095001 (2006).

[80] J. Alwall *et al.*, arXiv:0706.2334 [hep-ph].

[81] G. D. Kribs, T. Plehn, M. Spannowsky and T. M. P. Tait, "Four Generations and Higgs Physics," arXiv:0706.3718 [hep-ph].

[82] E. Gildener and S. Weinberg, Phys. Rev. D **13**, 3333 (1976); E. Gildener, Phys. Rev. D **14**, 1667 (1976).

[83] R. Haag, J.T. Lopuszanski and M.F. Sohnius Nucl.Phys.B **88** 257 (1975)

[84] G.R. Farrar and P. Fayet, Phys. Lett. B **76**, 575 (1978)

[85] P. Fayet and J. Iliopoulos, Phys. Lett. B **51**, 461 (1974); L. O'Raifeartaigh, Nucl. Phys. B **96**, 331 (1975).

[86] A. H. Chamseddine, R. Arnowitt and P. Nath, Phys. Rev. Lett. **49**, 970 (1982); R. Barbieri, S. Ferrara and C. A. Savoy, Phys. Lett. B **119**, 343 (1982); L. J. Hall, J. D. Lykken and S. Weinberg, Phys. Rev. D **27** (1983) 2359.

[87] M. Dine and A. E. Nelson, Phys. Rev. D **48**, 1277 (1993); G. F. Giudice and R. Rattazzi, Phys. Rept. **322**, 419 (1999).

[88] L.Girardello and M. T. Grisaru, Nucl. Phys. B **194**, 65 (1982).

[89] H.P. Nilles, Phys. Rept. **110** 1 (1984); J. Wess and J. Bagger, Supersymmetry and Supergravity (Princeton Univ. Press, Princeton, NJ, 1983); H.E. Haber and G.L. Kane, Phys. Rep. **117** 75 (1985)

[90] A. Salam and J. Strathdee, Fortschritte der Physik **26**, 57 (1978)

[91] A. Dabelstein, Z.Phys. C **67**, 495-512 (1995); H. E. Haber, R. Hempfling and A. H. Hoang, Z. Phys. C **75**, 539 (1997); R. Hempfling and A. H. Hoang, Phys. Lett. B **331**, 99 (1994).

[92] S. Heinemeyer, W. Hollik and G. Weiglein, Eur.Phys.J.C **9** 343-366 (1999)

[93] M. Misiak, S. Pokorski and J. Rosiek, Adv. Ser. Direct. High Energy Phys. **15**, 795 (1998).

[94] E. Barberio *et al.* [Heavy Flavor Averaging Group (HFAG) Collaboration], arXiv:0704.3575 [hep-ex].

[95] R. S. Chivukula and H. Georgi, Phys. Lett. B **188**, 99 (1987).

[96] L. J. Hall and L. Randall, Phys. Rev. Lett. **65**, 2939 (1990).

[97] G. D'Ambrosio, G. F. Giudice, G. Isidori and A. Strumia, Nucl. Phys. B **645**, 155 (2002).

[98] W. Altmannshofer, A. J. Buras and D. Guadagnoli, arXiv:hep-ph/0703200.

[99] L. J. Hall, V. A. Kostelecky and S. Raby, Nucl. Phys. B **267**, 415 (1986).

[100] J. S. Hagelin, S. Kelley and T. Tanaka, Nucl. Phys. B **415**, 293 (1994); F. Gabbiani, E. Gabrielli, A. Masiero and L. Silvestrini, Nucl. Phys. B **477**, 321 (1996).

[101] G. Colangelo and G. Isidori, JHEP **9809**, 009 (1998).

[102] M. Dührssen, S. Heinemeyer, H. Logan, D. Rainwater, G. Weiglein and D. Zeppenfeld, Phys. Rev. D **70**, 113009 (2004)

[103] R. M. Barnett, H. E. Haber and D. E. Soper, Nucl. Phys. B **306**, 697 (1988). A. C. Bawa, C. S. Kim and A. D. Martin, Z. Phys. C **47**, 75 (1990); V. D. Barger, R. J. Phillips and D. P. Roy, Phys. Lett. B **324**, 236 (1994) S. Moretti and K. Odagiri, Phys. Rev. D **55**, 5627 (1997).

[104] S. H. Zhu, Phys. Rev. D **67**, 075006 (2003); J. Alwall and J. Rathsman, JHEP **0412**, 050 (2004); N. Kidonakis, JHEP **0505**, 011 (2005).

[105] T. Plehn, Phys. Rev. D **67**, 014018 (2003).

[106] E. L. Berger, T. Han, J. Jiang and T. Plehn, Phys. Rev. D **71**, 115012 (2005).

[107] J. C. Collins and W. K. Tung, Nucl. Phys. B **278**, 934 (1986); M. A. G. Aivazis, J. C. Collins, F. I. Olness and W. K. Tung, Phys. Rev. D **50**, 3102 (1994); F. I. Olness and W. K. Tung, Nucl. Phys. B **308**, 813 (1988); M. Krämer, F. I. Olness and D. E. Soper, Phys. Rev. D **62**, 096007 (2000); E. Boos and T. Plehn, Phys. Rev. D **69**, 094005 (2004).

[108] D. P. Roy, Phys. Lett. B **459**, 607 (1999).

[109] K. A. Assamagan and Y. Coadou, Acta Phys. Polon. B **33**, 707 (2002); Y. Coadou, FERMILAB-THESIS-2003-31.

[110] J. F. Gunion, Phys. Lett. B **322**, 125 (1994); J. A. Coarasa, D. Garcia, J. Guasch, R. A. Jimenez and J. Sola, Phys. Lett. B **425**, 329 (1998); S. Moretti and D. P. Roy, Phys. Lett. B **470**, 209 (1999).

[111] K. A. Assamagan, Y. Coadou and A. Deandrea, report ATL-COM-PHYS-2002-002, arXiv:hep-ph/0203121; K. A. Assamagan and N. Gollub, Eur. Phys. J. C **39S2**, 25 (2005); P. Salmi, R. Kinnunen and N. Stepanov, arXiv:hep-ph/0301166. S. Lowette, J. D'Hondt and P. Vanlaer, CERN-CMS-NOTE-2006-109; also see S. Lowette, Ph.D thesis http://web.iihe.ac.be/ slowette

[112] T. Plehn, M. Spira and P. M. Zerwas, Nucl. Phys. B **479**, 46 (1996) [Erratum-ibid. B **531**, 655 (1998)]; S. Dawson, S. Dittmaier and M. Spira, Phys. Rev. D **58**, 115012 (1998); A. Djouadi, W. Kilian, M. Mühlleitner and P. M. Zerwas, Eur. Phys. J. C **10**, 45 (1999); A. A. Barrientos Bendezu and B. A. Kniehl, Phys. Rev. D **64**, 035006 (2001); U. Baur, T. Plehn and D. L. Rainwater, Phys. Rev. D **69**, 053004 (2004).

[113] D. A. Dicus, J. L. Hewett, C. Kao and T. G. Rizzo, Phys. Rev. D **40**, 787 (1989); A. A. Barrientos Bendezu and B. A. Kniehl, Phys. Rev. D **59**, 015009 (1998); and Phys. Rev. D **63**, 015009 (2001); O. Brein, W. Hollik and S. Kanemura, Phys. Rev. D **63**, 095001 (2001); Z. Fei, M. Wen-Gan, J. Yi, H. Liang and W. Lang-Hui, Phys. Rev. D **63**, 015002 (2000); W. Hollik and S. H. Zhu, Phys. Rev. D **65**, 075015 (2002).

[114] J. F. Gunion, H. E. Haber, F. E. Paige, W. K. Tung and S. S. Willenbrock, Nucl. Phys. B **294**, 621 (1987); S. S. D. Willenbrock, Phys. Rev. D **35**, 173 (1987); A. Krause, T. Plehn, M. Spira and P. M. Zerwas, Nucl. Phys. B **519**, 85 (1998); A. A. Barrientos Bendezu and B. A. Kniehl, Nucl. Phys. B **568**, 305 (2000); O. Brein and W. Hollik, Eur. Phys. J. C **13**, 175 (2000); E. Eichten, I. Hinchliffe, K. D. Lane and C. Quigg, Rev. Mod. Phys. **56**, 579 (1984) [Addendum-ibid. **58**, 1065 (1986)]; N. G. Deshpande, X. Tata and D. A. Dicus, Phys. Rev. D **29**, 1527 (1984); for a recent update and overview, see *e.g.* : A. Alves and T. Plehn, Phys. Rev. D **71**, 115014 (2005).

[115] L. J. Hall, R. Rattazzi and U. Sarid, Phys. Rev. D **50**, 7048 (1994); M. Carena, M. Olechowski, S. Pokorski and C. E. Wagner, Nucl. Phys. B **426**, 269 (1994); M. Carena, D. Garcia, U. Nierste and C. E. Wagner, Nucl. Phys. B **577**, 88 (2000); A. Belyaev, D. Garcia, J. Guasch and J. Sola, Phys. Rev. D **65**, 031701(R) (2002); J. Guasch, P. Häfliger and M. Spira, Phys. Rev. D **68**, 115001 (2003).

[116] *see, e.g.* Y. Nir, arXiv:hep-ph/0703235; *and references therein.*

[117] B. Aubert *et al.* [BABAR Collaboration], Phys. Rev. D **72**, 052004 (2005); P. Koppenburg *et al.* [Belle Collaboration], Phys. Rev. Lett. **93**, 061803 (2004); S. Chen *et al.* [CLEO Collaboration], Phys. Rev. Lett. **87**, 251807 (2001); W.-M. Yao *et al.*, J. Phys. Lett. G **33**, 1 (2006); R. Barate *et al.* [ALEPH Collaboration], Phys. Lett. B **429**, 169 (1998); H. F. A. Group(HFAG), arXiv:hep-ex/0505100.

[118] P. L. Cho, M. Misiak and D. Wyler, Phys. Rev. D **54**, 3329 (1996); J. L. Hewett and J. D. Wells, Phys. Rev. D **55**, 5549 (1997); F. M. Borzumati and C. Greub, Phys. Rev. D **58**, 074004 (1998) and Phys. Rev. D **59**, 057501 (1999); G. Hiller and F. Krüger, Phys. Rev. D **69**, 074020 (2004).

[119] K. Abe *et al.*, Phys. Rev. Lett. **96**, 221601 (2006); B. Aubert *et al.* [BABAR Collaboration], arXiv:hep-ex/0612017;

[120] B. Aubert *et al.* [BABAR Collaboration], Phys. Rev. Lett. **93**, 081802 (2004). K. Abe *et al.* [Belle Collaboration], arXiv:hep-ex/0408119; A. Ali, E. Lunghi, C. Greub and G. Hiller, Phys. Rev. D **66**, 034002 (2002); B. Grinstein, M. J. Savage and M. B. Wise, Nucl. Phys. B **319**, 271 (1989); D. Guetta and E. Nardi, Phys. Rev. D **58**, 012001 (1998).

[121] E. Lunghi, A. Masiero, I. Scimemi and L. Silvestrini, Nucl. Phys. B **568**, 120 (2000); G. Buchalla, G. Hiller and G. Isidori, Phys. Rev. D **63**, 014015 (2001); G. Hiller, Phys. Rev. D **66**, 071502 (2002).

[122] [BABAR Collaboration], arXiv:hep-ex/0703018; A. Ali, P. Ball, L. T. Handoko and G. Hiller, Phys. Rev. D **61**, 074024 (2000); P. Ball and R. Zwicky, Phys. Rev. D **71**, 014015 (2005).

[123] W. M. Yao *et al.* [Particle Data Group], J. Phys. G **33** (2006) 1; E. Barberio *et al.* [Heavy Flavor Averaging Group (HFAG)], http://www.slac.stanford.edu/xorg/hfag.

[124] V. M. Abazov *et al.* [D0 Collaboration], Phys. Rev. Lett. **97**, 021802 (2006); A. Abulencia *et al.* [CDF Collaboration], Phys. Rev. Lett. **97**, 242003 (2006).

[125] S. Bertolini, F. Borzumati, A. Masiero and G. Ridolfi, Nucl. Phys. B **353**, 591 (1991); G. C. Branco, G. C. Cho, Y. Kizukuri and N. Oshimo, Phys. Lett. B **337**, 316 (1994).

[126] A. Bartl, T. Gajdosik, E. Lunghi, A. Masiero, W. Porod, H. Stremnitzer and O. Vives, Phys. Rev. D **64**, 076009 (2001); M. Blanke, A. J. Buras, D. Guadagnoli and C. Tarantino, JHEP **0610**, 003 (2006); T. Goto, T. Nihei and Y. Okada, Phys. Rev. D **53**, 5233 (1996) [Erratum-ibid. D **54**, 5904 (1996)].

[127] E. C. G. Stueckelberg and A. Petermann, Helv. Phys. Acta **26**, 499 (1953); M. Gell-Mann and F. E. Low, Phys. Rev. **95**, 1300 (1954).

[128] G. Buchalla, A.J. Buras and M.E. Leutenbacher, Rev. Mod. Phys. **68** (1996); A. Ali and C. Greub, Z. Phys. C **49** 431 (1991); A.J. Buras et al., Nucl. Phys. B **424** 374 (1994).

[129] K.G. Wilson, Phys. Rev. **179** 1499 (1969); K.G. Wilson and W. Zimmermann, Comm. Math. Phys. **24** 87 (1972)

[130] N. Cabibbo, Phys. Rev. Lett. **10** 531 (1963); M. Kobayashi and K. Maskawa, Prog. Thoer. Phys. **49** 652 (1973).

[131] J.H. Christenson, J.W. Cronin, V.L. Fitch and R. Turlay, Phys. Rev. Lett. **13** 128 (1964)

[132] M.K. Gaillard and B.W. Lee, Phys. Rev. **D10** 897 (1974)

[133] H. Albrecht et al. (ARGUS), Phys. Lett. **B192** 245 (1987); M. Artuso et al. (CLEO) Phys. Rev. Lett. **62** 2233 (1989)

[134] D. Becirevic *et al.*, Nucl. Phys. B **634**, 105 (2002).

[135] F. Gabbiani, E. Gabrielli, A. Masiero, L. Silvestrini, Nucl. Phys. **B477**, 321 (1996)

[136] M. Misiak, S. Pokorski, J. Rosiek, Adv. Ser. Direct. High Energy Phys. **15**, 795 (1998)

[137] A. Ali and C. Greub, Z. Phys. C **49**, 431 (1991); A. J. Buras, M. Misiak, M. Munz and S. Pokorski, Nucl. Phys. B **424**, 374 (1994).

[138] K. Chertyrkin, M. Misiak and M. Münz, Phys. Lett. B **400**, (1997) 206; A.L. Kagan and M. Neubert, Eur. Phys. J. C **7** (1999) 5-27

[139] B. Aubert, *et al.* (BABAR) Phys. Rev. Lett. **93** (2004) 011803

[140] M. Ciuchini *et al.*, Phys. Lett. B **316** (1993) 127.

[141] S. Heinemeyer, W. Hollik, G. Weiglein, Comput.Phys.Commun. **124** 76-89 (2000)

[142] S.W. Bosch, G. Buchalla JHEP 0501:035 (2005)

[143] F. Kruger and L. M. Sehgal, Phys. Rev. D **55**, 2799 (1997).

[144] D. M. Pierce, J. A. Bagger, K. T. Matchev and R. j. Zhang, Nucl. Phys. B **491**, 3 (1997).

[145] J. A. Casas and S. Dimopoulos, Phys. Lett. B **387**, 107 (1996).

[146] S. Heinemeyer, W. Hollik, F. Merz and S. Penaranda, Eur. Phys. J. C **37**, 481 (2004).

[147] [ALEPH Collaboration], Phys. Rept. **427**, 257 (2006).

[148] J. Cao, G. Eilam, K. i. Hikasa and J. M. Yang, Phys. Rev. D **74**, 031701 (2006).

[149] Recent limits: http://www-cdf.fnal.gov/physics/exotic/exotic.html; V. M. Abazov *et al.* [D0 Collaboration], Phys. Lett. B **638**, 119 (2006).

[150] K. Ikado *et al.*, Phys. Rev. Lett. **97**, 251802 (2006); B. Aubert *et al.* [BABAR Collaboration]; arXiv:hep-ex/0608019; A. G. Akeroyd and S. Recksiegel, J. Phys. G **29**, 2311 (2003).

[151] C. N. Leung, S. T. Love and S. Rao, Z. Phys. C **31**, 433 (1986); W. Buchmüller and D. Wyler, Nucl. Phys. B **268**, 621 (1986).

[152] A. Kulesza and W. J. Stirling, Phys. Lett. B **475**, 168 (2000).

[153] J. L. Diaz-Cruz, H. J. He and C. P. Yuan, Phys. Lett. B **530**, 179 (2002); H. J. He and C. P. Yuan, Phys. Rev. Lett. **83**, 28 (1999); C. Balazs, H. J. He and C. P. Yuan, Phys. Rev. D **60**, 114001 (1999); S. R. Slabospitsky.

[154] H. E. Haber, R. Hempfling and A. H. Hoang, Z. Phys. C **75**, 539 (1997); M. Frank, T. Hahn, S. Heinemeyer, W. Hollik, H. Rzehak and G. Weiglein.

[155] T. Hahn, Comput. Phys. Commun. **140** (2001) 418; T. Hahn and C. Schappacher, Comput. Phys. Commun. **143** (2002) 54.

[156] T. Hahn and M. Perez-Victoria, Comput. Phys. Commun. **118** (1999) 153.

[157] J. Pumplin, D. R. Stump, J. Huston, H. L. Lai, P. Nadolsky and W. K. Tung, JHEP **0207** (2002) 012.

[158] H. E. Haber, arXiv:hep-ph/9305248.

[159] R. Lafaye, T. Plehn and D. Zerwas, "SFITTER: SUSY parameter analysis at LHC and LC," arXiv:hep-ph/0404282.

[160] J. C. Ward, Phys. Rev. **78**, 182 (1950).

[161] A. Denner, Fortschr. Phys. **41** (1993).

[162] A. Denner and S. Dittmaier, Nucl. Phys. B **734**, 62 (2006).

[163] V. A. Smirnov, Phys. Lett. B **394** (1997) 205.

[164] T. Stelzer and W. F. Long, Comput. Phys. Commun. **81**, 357 (1994); F. Maltoni and T. Stelzer, JHEP **0302**, 027 (2003); http://madgraph.phys.ucl.ac.be

[165] Y. Nir and N. Seiberg, Phys. Lett. B **309**, 337 (1993).

[166] S. Dittmaier, G. Hiller, T. Plehn and M. Spannowsky, "Charged-Higgs Collider Signals with or without Flavor," arXiv:0708.0940 [hep-ph].

[167] L. Wolfenstein, Phys. Rev. Lett. **51**, 1945 (1983).

[168] A. Hocker, H. Lacker, S. Laplace and F. Le Diberder, Eur. Phys. J. C **21**, 225 (2001).

[169] J.C. Collins, Renormalization, (Cambridge University Press, Cambridge, 1984)

[170] G. 't Hooft and M. J. G. Veltman, Nucl. Phys. B **44**, 189 (1972).

[171] D. Stockinger, JHEP **0503**, 076 (2005).

[172] G. 't Hooft, Nucl. Phys. B **61**, 455 (1973).

[173] W.A. Bardeen, A.J. Buras, D.W. Duke and T.Muta, Phys. Rev. D **18**, 3998 (1978).

[174] T. Fritzsche, PhD thesis, Cuvillier, Göttingen, 2005, ISBN 3-86537-577-4

[175] H. Fritzsch, M. Gell-Mann and H. Leutwyler, Phys. Lett. B **47**, 365 (1973).

[176] J. D. Bjorken and E. A. Paschos, Phys. Rev. **185**, 1975 (1969); R. P. Feynman, Phys. Rev. Lett. **23**, 1415 (1969).

[177] J. C. Collins, D. E. Soper and G. Sterman, Adv. Ser. Direct. High Energy Phys. **5**, 1 (1988).

[178] E. D. Bloom *et al.*, Phys. Rev. Lett. **23**, 930 (1969); M. Breidenbach *et al.*, Phys. Rev. Lett. **23**, 935 (1969); J. I. Friedman and H. W. Kendall, Ann. Rev. Nucl. Part. Sci. **22** (1972) 203.

[179] J. D. Bjorken, Phys. Rev. **179**, 1547 (1969).

[180] M. Jamin, Talk - given at the University of Granada, March 2006

Acknowledgements

I would like to thank Prof. Fritzsch for giving me the possibility to write a PhD thesis in this interesting branch of physics and for supporting me during the last three years.

I am especially grateful to Tilman Plehn, Gudrun Hiller and Stefan Dittmaier. Without their answers to all of my questions, enduring encouragement and permanent support, this work would not have been possible.

Furthermore, I would like to thank all the people at the Chair of Prof. Fritzsch, who I had the pleasure to get to know during my stay in Munich, for creating an enjoyable atmosphere in- and outside the University: Gerhard Buchalla, Volker Pilipp, Matthäus Bartsch, Guido Bell, Sebastian Jäger, Dao-Neng Gao, Gamal Eldahoumi, Abdul Aziz Bhatti, Valentina Aquila, Michaela Albrecht, Marc Lietzow, Alp Denis Ozer, Salim Safir and Alexander Kubelsky.

For friendly and uncomplicated hospitality I want to thank all members of the „Max-Planck Institute for Physics in Munich“. Especially Michael Rauch was a huge help by answering lots of computing and HadCalc related questions.

Last but not least, many thanks go to the Graduiertenkolleg „Teilchenphysik im Energiebereich neuer Phänomene“ and its organizers for financial support over the whole period of my thesis and stimulating working conditions.